Institute of Geosciences, UiT, The Arctic University of Norway

Distribution, deposition and impact of tailing disposal on the seafloor in Ranfjorden, northern Norway

—

Anders Eirik Haugen

Master's thesis in Geosciences… July 2018

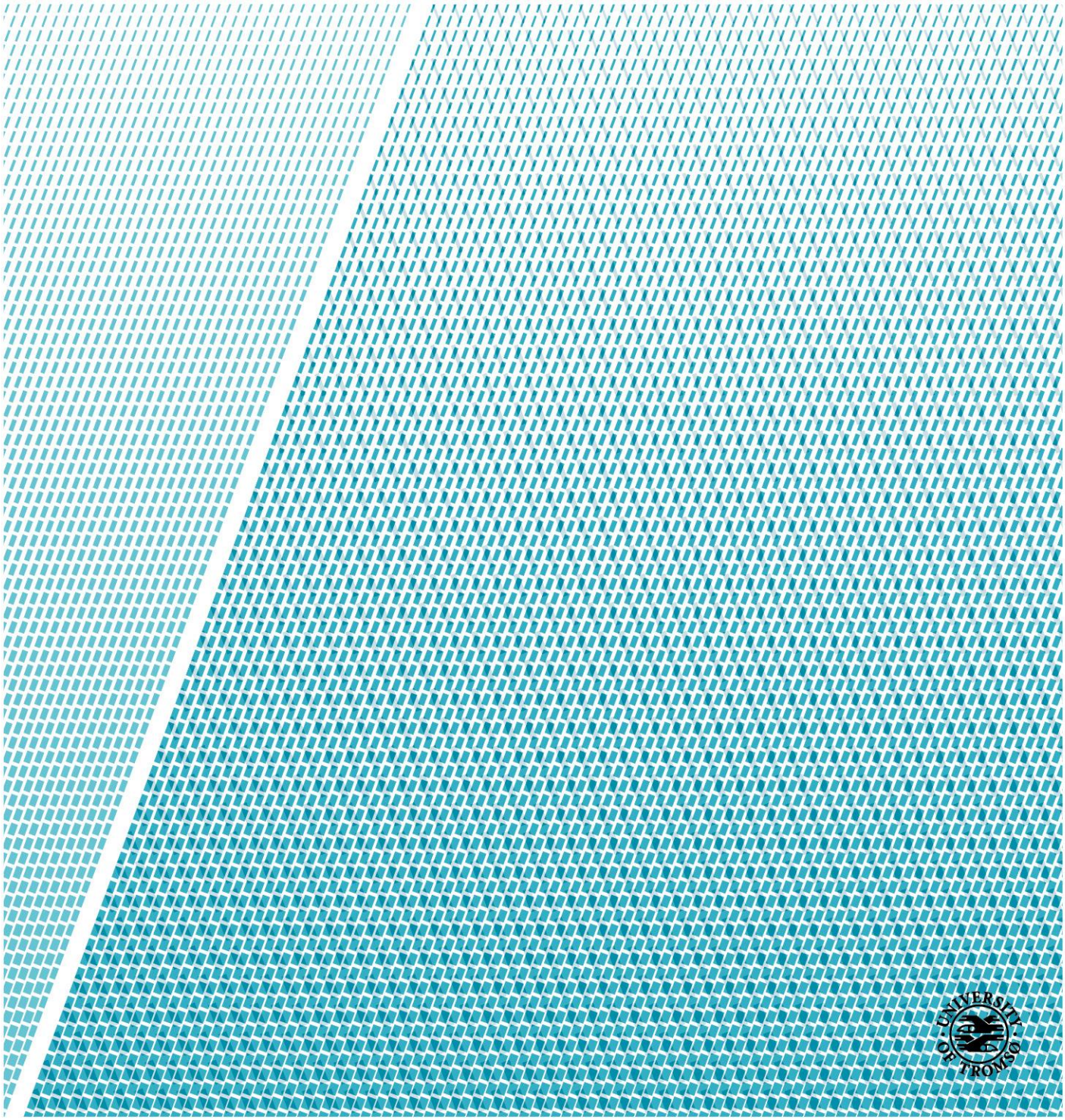

Table of Contents

List of Tables

List of Figures

Abstract

This study is conducted in Ranfjorden in northern Norway with the goal of gaining a better understanding of the interaction between natural and anthropologic sediments within the fjord. Ranfjorden is of interest due to the fact that it has experienced extensive anthropologic impacts over the last 100 years with the submarine tailings placement (STP) of mine tailings ongoing. The analysis of this study uses the combination of 6 Niemistö sediment cores, 10 sediment grabs, swath bathymetry and high resolution seismic data to identify natural and anthropologic sediments and determine how their distribution has impacted the fjord.

The sediment cores were analyzed to determine their physical properties including magnetic susceptibility, geochemical element measurements, grainsize analysis and lithological analysis. The resulting data showed mine tailings sediments to be characterized by a darker red color, higher magnetic susceptibility and Fe/Sum values with low fluctuations in Fe/Sum values. The more natural fjord sediments are characterized by gray colors, lower magnetic susceptibility and Fe/Sum values with higher fluctuations in Fe/Sum values. Using these identifying traits it was shown that the majority of the inner fjord has experience varied levels of impact from the mine tailings, with all the sediment cores showing traces of mine tailings. The mean grainsize of the sampled mine tailings was shown to vary from fine sand to very fine silt.

The fjord slopes surrounding the mine tailings discharge points at the head of the fjord appeared in the swath bathymetry to have experienced extensive erosion in the form of mass movement and gravity flows. This is attributed to the accumulation of finer mine tailings along these slopes due to back flowing estuarine circulation currents. These currents accompanied by the river-induced halocline appear to capture rising sediment plumes in the water column and concentrate them in those areas. The eroded sediments from those slopes combined with coarser mine tailings are carried further out into the fjord by turbidity currents within a larger submarine channel seen on the swath bathymetry and TOPAS seismic profiles. Samples from the channel show sandy tailing deposits consistent with turbidity currents while areas outside the channels show massive layers of finer tailing sediments consistent with sediment plume fallout. Sandy mine tailing sediments transported by turbidity currents were found 17 km from the discharge point. Shallower samples in the same vicinity showed potential evidence of fine tailing sediments from suspension plume settling.

The discharge of large amounts of tailings at shallower depths combined with the hydrological characteristics of the fjord has allowed for the submarine tailing placement (STP) sediments to have spread throughout the inner fjord basin by turbidity currents and suspension plumes.

Acknowledgements

I would first and foremost like to thank my supervisor Matthias Forwick for his continued willingness to provide invaluable insight even with his constantly busy work schedule. His depth of knowledge in the field of marine geology was a huge asset. Without his assistance, I would have been extremely lost. A huge thank you also goes out to my co-supervisors Nicole Jeanne Baeten, Juho Junttila and Aivo Lepland for providing support in areas ranging from geotechnical to geochemical to GIS. They all made this experience much more enjoyable. Another huge shout out goes to the wonderful ladies of the lab, Trine Dahl, Ingvild Hald and Karina Monsen. Their keen direction in the IG lab made daunting tasks surmountable.

I would also like to thank NYKOS and all the research partners involved for allowing me to partake in this interesting and exciting project and for sharing their data. Furthermore, I would also like to thank NGU for hosting me at their Trondheim office and showing me their facilities.

Finally, I would like to thank my family and friends for providing mental, social, gastronomic and grammatical support through this incredibly educational experience.

1 Introduction

This study investigates the impact and spreading of submarine deposited mine tailings on the seafloor of Ranfjorden, in Nordland County, Northern Norway. Ranfjorden is located between 66°08'-66°20'N and 12°5'-14°8'E (Figure 1) and is approximately 70km long and ranging from 2-4 km wide. It extends towards the Norwegian Sea in a WSW direction with a maximum depth of 530m. (Lysså, Seirup et al. 2004) The main study area is located at the inner Ranfjorden (Figure 1) near the city of Mo I Rana. The focus of this study extends from the mouth of the Ranaelva river out to the southwest (Figure 1).

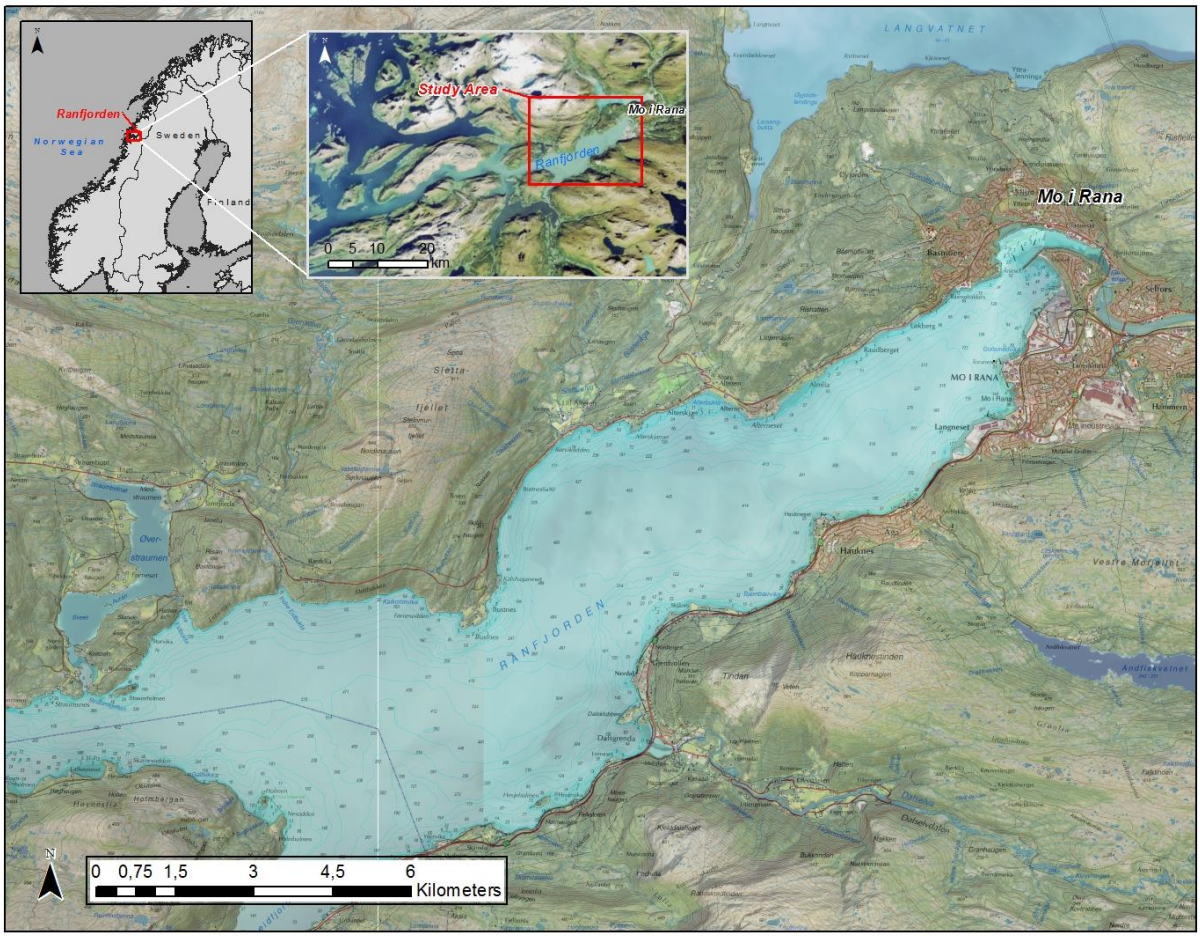

Figure 1. Ranfjorden Study Area

1.1 Aim of Study

This thesis is part of the NYKOS (New Knowledge on Sea Disposal) research project that is a joint competence-building project between the Research Council of Norway (RCN) (BIA-Program) and the mineral industry in Norway. The main research partners that make up the project are SINTEF (project lead), the Norwegian University of Science and Technology (NTNU), The Norwegian Institute for Water Research (NIVA), University of Tromsø (UiT) – The Arctic University of Norway and the Geological Survey of Norway (NGU). Participating companies are Nussir ASA, Sibelco Nordic, Rana Gruber, Omya Hustadmarmor, Nordic Mining and Titania.

The aim of this project is to gain a better understanding of the effects of submarine deposition of fine-grained mining tailings on Norwegian marine environments and to help develop more sustainable methods for the Norwegian mining industry.

This thesis specifically aims to investigate the distribution, deposition and impact of tailing disposals on the seafloor in Ranfjorden in northern Norway by using:

1. Niemistö cores
2. Sediment grabs
3. TOPAS Seismic data
4. Swath bathymetry data

The specific aims of this study are:

1. Distinguish natural and anthropogenic deposits in the fjord
2. Identify the spreading of submarine tailings placements
3. Identify the impact of submarine tailings on the fjord seafloor
4. Analyze the interaction of a large river on the placement and spreading of submarine tailings.

The overall NYKOS project is divided into 6 closely related work packages with this thesis being part of Work Package 3 (WP3):

- WP1: Project Management
- WP2: Tailings Improvement and Characteristics. Exploiting the pre-depositioning potential
- **WP3: Study of three comparable fjords**
- WP4: Effects from mine tailings and associated chemicals on marine, benthic ecosystems
- WP5: Modelling, Impact acceptance criteria and Risk aspects
- WP6: Best Available Techniques (BAT) for STPs

The aim of WP3 is to gain a better understanding of the impact of submarine tailings placements (STPs) on fjord seafloors and their natural sediments.

1.2 Background

As the world's demand for mineral resources continues to grow (Figure 2), alongside it grows a need to find more environmental and economical ways to responsibly dispose of the waste that is created from these practices (Ramirez-Llodra, Trannum et al. 2015). Mine tailings are the most common waste produced and have traditionally been stored on land. Due to their toxicity and large volumes other alternatives have begun to be utilized, including submarine tailings placement (Vogt 2013, Ramirez-Llodra, Trannum et al. 2015).

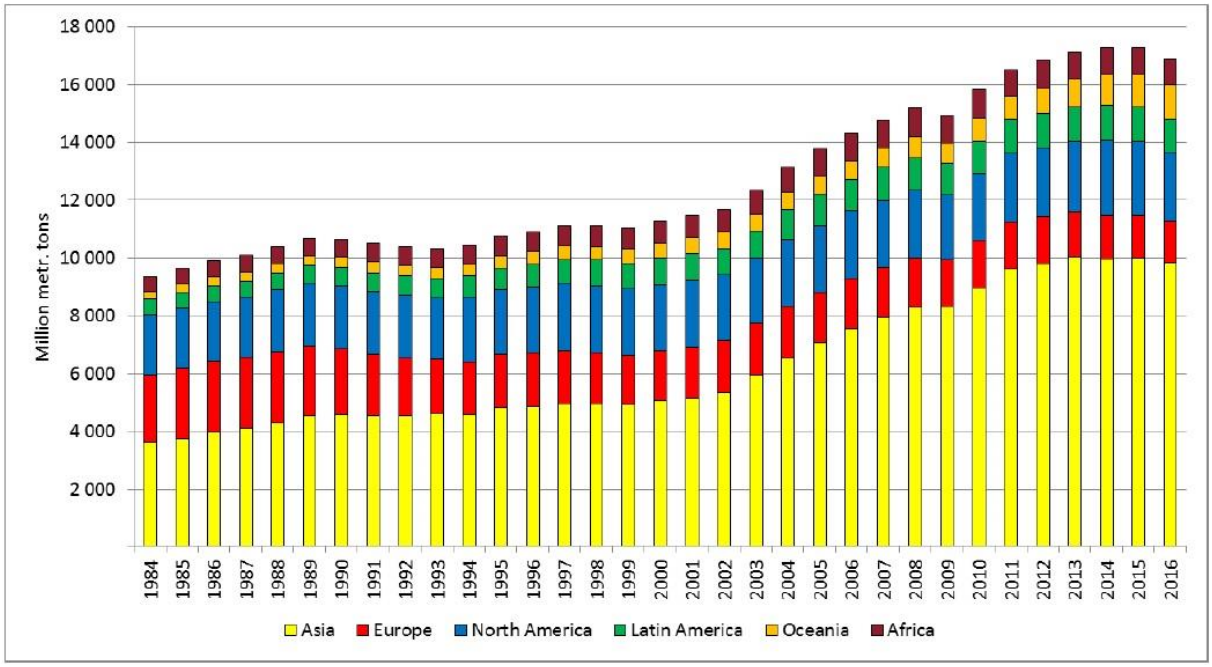

Figure 2. World mining production 1984-2016 by continents (without construction minerals, in Million metric tons)

1.2.1 Mine tailings

Mining is the process of extracting minerals and metals from the earth's crust and mine tailings are one of the two main waste materials left over after the final separation of the desired ores is completed. The other waste product is the overburden rock and soil removed to gain access to the ore (Vogt 2013). Mine tailings will be the focus of this study due to their relevance to the study area.

Mine tailings are most often a finer-grained slurry of the left over materials from the ore, and depending on the ores being extracted can contain chemical reagents used in the separation process (Vogt 2013). This separation process consists of multiple cycles of crushing, grinding and separation in order to concentrate the desired ore(s) (Figure 3). The percentage of the total ore mined that becomes tailings can often account for over 99% with gold, up to 99% for copper and about 60% for iron (Vogt 2013, Ramirez-Llodra, Trannum et al. 2015). Since the separation process does not recover all of the minerals, the slurry often has a high potential to be toxic and with its large volumes is the main environmental concern of any mining activity (Vogt 2013). For them to be disposed of safely they must be made physically stable, chemically inert and completely isolated from the environment in all ways (Franks, Boger et al. 2011).

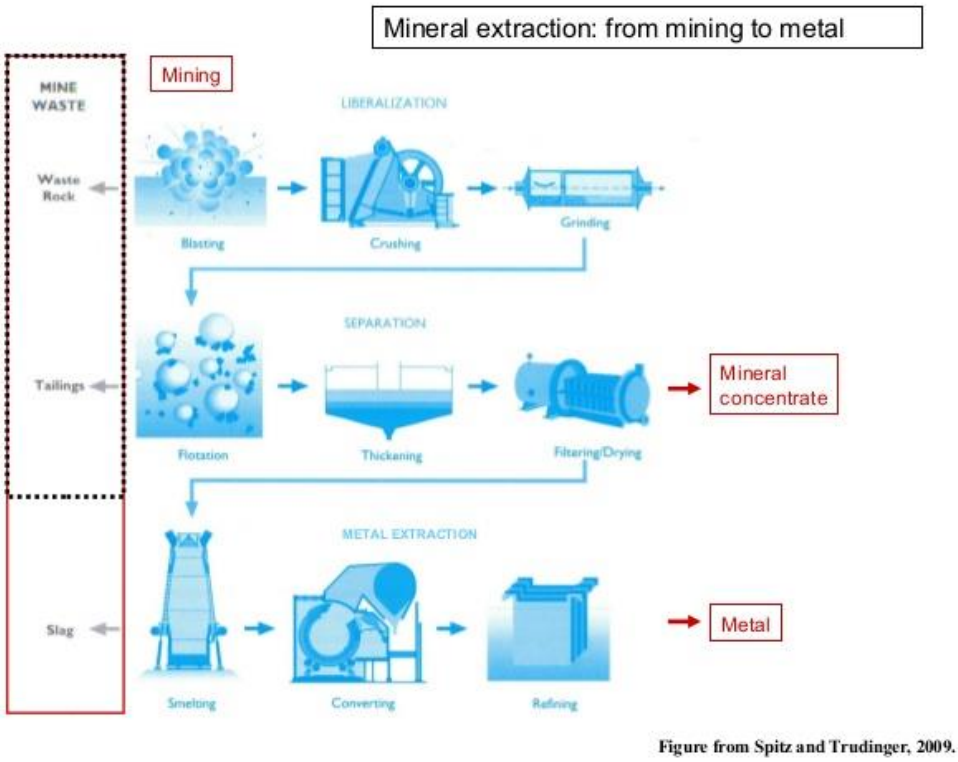

Figure 3. Mining Process (Spitz and Trudinger, 2009)

At present, approximately 99% of the industrial sized mines operating worldwide dispose of their mine tailings on land. The tailings are placed either under water in impoundments/dams or backfilled into open-pits or underground mines. The total number of mine tailing dams/impoundments that exist today is at least 3,500 (Vogt 2013). This type of tailings storage requires large areas of land that can affect up to one half of the total area affected by the mining activity (Cornwall 2013, Ramirez-Llodra, Trannum et al. 2015). These storage areas can have significant impact on the local surrounding environment and public safety. There is the threat of loss of habitat due to the land being used for tailings storage and the continuing specter of contamination to surface and ground water. The leaching of toxic chemicals and metals into surrounding waters along with the acidification of waters from sulfide mineral oxidation carry lasting consequences (Arnesen, Bjerkeng et al. 1997, Ramirez-Llodra, Trannum et al. 2015). The facilities designed and built to contain the mine tailings have a significant support industry that must continue to monitor and maintain the storage areas even long after the mines have closed. For many mines this monitoring must continue in perpetuity, increasing costs and extending the potential impact to the local area (Vogt 2013). But these facilities are quite often unreliable due to poor waste management (Ramirez-Llodra, Trannum et al. 2015) and can cause major environmental and societal damage when they fail. There have been 138 significant recorded mine tailing dam failures from when they were first used and up until 2013 (Vogt 2013). These failures have the potential to continue harming the local environment long after the event, with some failures causing irreparable damage (Ramirez-Llodra, Trannum et al. 2015).

The issues associated with the storage of mine tailings on land has driven a search for alternative storage/disposal options with “Submarine Tailings Placement” (STP) being a method occasionally used (Ramirez-Llodra, Trannum et al. 2015).

1.2.2 Submarine Tailings Placement

Since humans first began mining, the practice of depositing mining waste into riverine and marine environments has been common (Davis, Welty et al. 2000). In the past, riverine discharge has been utilized extensively for tailings disposal worldwide but has fallen out of favor due to its high environmental and societal impact. Increased environmental awareness and legislation has reduced this practice to only a handful of industrial sized mines (Vogt 2013). The marine disposal of mine tailings is a more popular alternative but due to uncertainties about its environmental effects, the practice is not often used. Of 2,500 industrial sized mines worldwide only approximately 14 (0.6%) use marine disposal (Vogt 2013, Ramirez-Llodra, Trannum et al. 2015) There are 3 different classifications of marine disposal of mine tailings with STP/DSTP being the focus of this study (Figure 4):

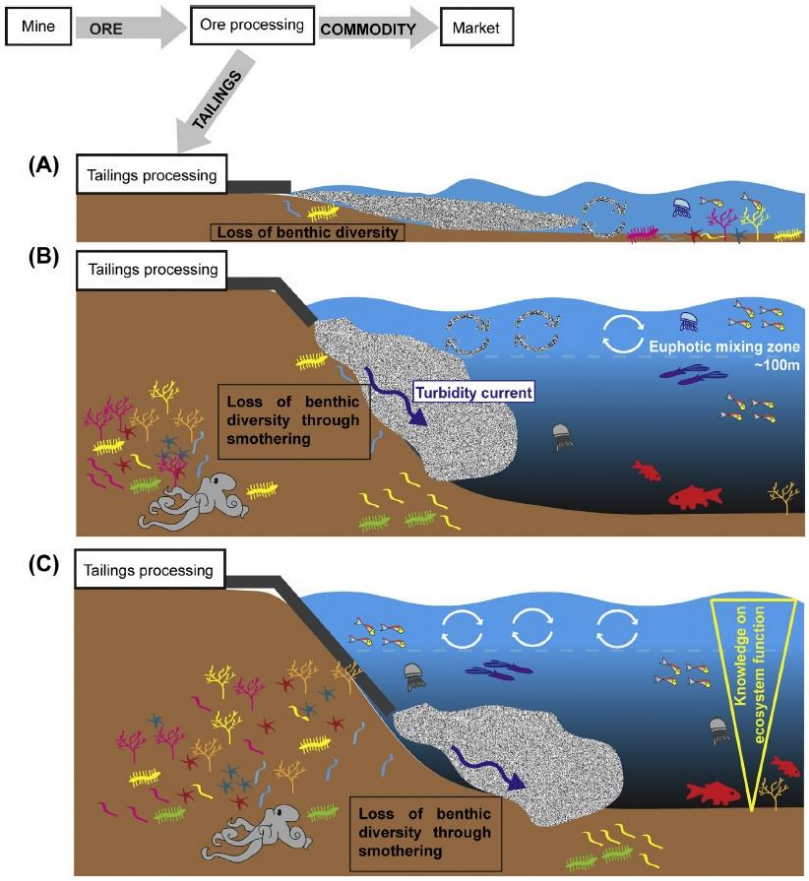

Figure 4. Schematic of three representative marine disposal processes (Ramirez-Llodra, Trannum et al. 2015)

- Coastal shallow water placement (CTP) (Figure 4A): where tailings are disposed of at the surface in shallow coastal waters in the euphotic mixing zone (Franks, Boger et al. 2011). This practice is also used under the label “land reclamation” in some coastal nations when using inert tailings.
- Submarine tailing placement (STP) (Figure 4B): where tailings are disposed of underwater using an underwater pipeline at depths of less than 100m in the euphotic mixing zone (Vogt 2013, Skei 2014). The deposited tailings often create a gravity flow that transports the tailings into deeper waters below the euphotic zone.
- Deep-sea tailing placement (DSTP) (Figure 4C): where tailings are deposited using an underwater pipeline in deeper waters of greater than 100m, below the euphotic mixing zone and near a drop-off (Franks, Boger et al. 2011, Skei 2014).

Due to perceived environmental and reputational risk along with more stringent regulatory conditions, STP use has decreased greatly in most developed nations. The exception to this trend is Norway (Figure 5) (Cornwall 2013). The main reason for this is the combination of Norway’s rugged terrain and abundance of fjords. The terrain makes storage on land difficult and the close proximity of fjords provides an attractive alternative (Cornwall 2013, Vogt 2013, Ramirez-Llodra, Trannum et al. 2015).

Figure 5. Recently active and proposed STP Norwegian STP operations (Cornwall 2013)

1.2.2.1 Tailings Deposition Techniques

The argument for the marine disposal of tailings has always been that the material will be much more stable on the sea floor when compared to onshore storage methods. The thought being that there will be a lower chance of the tailings being disturbed and a greater chance of them residing in chemically inert conditions. This method is also much cheaper and easier to use than on land storage facilities with virtually no maintenance costs after deposition (Vogt 2013, Ramirez-Llodra, Trannum et al. 2015).

Much of the concepts concerning STP are theoretical and dependent on location and condition. To ensure minimal spreading and impact of the tailings once they are deposited, containment to a specific area is needed (Franks, Boger et al. 2011). This containment is dependent greatly on the stratification of the water column and the depth at which the tailings are deposited. With STP and DSTP, the tailings are in theory deposited below the euphotic mixing zone and have a lower chance of mixing vertically and horizontally (Cornwall 2013). The density of both the water layers at the deposition site and the tailings themselves greatly influences this potential for spreading. STPs rely on turbidity flows carrying the tailings into deeper waters where conditions are thought to be more stable and where the thermocline of the upper water layers will act as a barrier preventing upward diffusion. The issue with this is that conditions can change that affect the depth of the mixing layer and the density of the tailings themselves influence their ability to travel. If their density is less than that of the surrounding water then an upwardly mobile plume can occur (Ramirez-Llodra, Trannum et al. 2015).

To reduce the tailing's ability to disperse once deposited, several measures prior to deposition such as thickening, de-aeration and particle flocculation are often used (Vogt 2013). A tailing slurry mixture's density can be increased by increasing the solid material quotient and/or by the addition of colder seawater. This will greatly assist in reducing the upward mobility of the tailing mixture especially when the seawater used mimics the conditions at the location where the tailings will be deposited. The removal of air from a slurry mixture can greatly reduce the buoyance of the tailings, especially when DSTP is involved (Skei 2014). The use of flocculation chemicals with seawater can also help increase the rate of settlement (Ramirez-Llodra, Trannum et al. 2015).

How and where the tailings are deposited also plays a large factor in how the tailings behave once they are deposited. Since a turbidity current is desired, the discharge point should be at a location where the current can flow uninhibited. Research has shown that the release point of the pipeline should be on a slope of 12° and that the tailings should be released as a high-velocity jet (Vogt 2013). These two factors combine to reduce the chance of build-up of sediment at the discharge pipe.

1.2.2.2 Environmental Effects

One of the greatest threats to the benthic environment from marine deposited tailings is hyper-sedimentation (Ramirez-Llodra, Trannum et al. 2015). Most tailings deposits will encompass huge amounts of material that will be discharged at potentially high rates over an extended period. This material can quickly bury and smother any benthic

organisms that reside in the area. Even if the tailing are non-toxic, whole ecosystems can be smothered (Vogt 2013). The rate of deposition has shown to have a huge effect on the survival rate of organisms. Studies have shown that on the community level sedimentation rates of 4-5cm of tailings per year can result in changes in faunal composition, but at a rate of 1mm per year no changes are seen (Olsgard and Hasle 1993). Other studies have shown that up to 50% of benthic species would die when exposed to 5.4cm of instantaneous burying while 5% would die if covered more gradually by 6.3mm of sediment (Smit, Halthaus et al. 2008). Each ecosystem will react differently to different types of sediment but it has been shown that it is expected to see the creation of a barren area close to the zone of discharge. The changes in the community composition and biomass will improve in a gradient with increased distance from the source back to the original environment (Ramirez-Llodra, Trannum et al. 2015).

Metals and processing chemicals are factors that can greatly increase the toxicity of mine tailings. Not all metals are toxic to fauna and for them to be toxic they must be in a bioavailable form (Lyndersen, Stefan et al. 2002). The general changes seen in macrobenthos communities due to copper toxicity are extensive with a complete change in the species representation; reduced diversity, altered lifestyles, biomass, density and body size ((Neira, Mendoza et al. 2011) as cited by Ramirez-Llodra *et al.*2015). The processing chemicals used to help concentrate the ore during the early stages of processing can also effect benthic communities. At present, not enough investigative studies have been conducted on the toxic effects of these chemicals to fully know their long-term impact on the environment (Ramirez-Llodra, Trannum et al. 2015).

The size and shape of the mine tailing particles will vary greatly with respect to the type of minerals being extracted. This factor plays an important role with respect to the benthic fauna if the grain size of the tailings is greatly different then the original sediment (Ramirez-Llodra, Trannum et al. 2015). Mine tailings are low in organic contents and are usually a ground rock with a fine sand-silt fraction, which can greatly reduce the amount of nutritional value available to benthic organisms. The change in porosity and permeability of the sea floor sediment will also have an effect on the benthic environment (Ramirez-Llodra, Trannum et al. 2015).

The method in which the tailings are deposited into the ocean can maximize or minimize the area in which the sediments can affect the local environment. If the sediment plume does not settle but instead experiences upwelling through the water column then the area impacted by the tailings can be an order of magnitude larger. Slope failure is another process that can occur at the location of deposition and result in the resuspension of sediment into the water column. These events can greatly affect previously non-affected environments (Vogt 2013, Ramirez-Llodra, Trannum et al. 2015).

1.3 Previous Work

Ranfjorden has been the subject of numerous assessments looking to investigate the environmental impact of the industrial activities that have been present there for over a century (Berg 1996). In addition to the mining activities in the area, a coking plant and an iron works have previously discharged into the fjord resulting in elevated levels of potentially toxic pollutants in the fjord sediments (Syvitski, Burrell et al. 1987). Monitoring has been occurring since the 1970's, building a collection of data that has been used to better understand the dynamics at play in the fjord (Skei 2014).

Impact assessments from the 1970's began to look into the interaction and impact of industrial discharge on the fjord and found extensive spreading of polycyclic aromatic hydrocarbons (PAHs) and heavy metals. Other fine particle contaminants were also found to have broadly spread out through the fjord basin (Kirkerud 1977).

Research during the 1980s showed continued high levels of PAHs and heavy metals that had large negative impacts over large portions of the fjord. Their presence proved to have resulted in a significant reduction in the inner fjord's ecological diversity vs. the less affected outer areas. Much of this loss of diversity was attributed to hyper-sedimentation (Kirkerud, Haakstad et al. 1985). During the period of 1986-93 several larger polluting industries in the area shut down, including the coking plant, iron works and some mining industry (Johnsen, Golmen et al. 2004). The results of these closures began to show up in later studies during the 1990s, which showed a continued impact from industry discharge but with PAH levels lower than measured in the 1980s. Smothering from hyper-sedimentation was still a factor (Green, Pedersen et al. 1995). Further studies in the 1990s showed that though the biodiversity of the inner fjord continued to be affected negatively by high levels of sedimentation, these effects were greatly reduced with increasing distance from the point of mine tailings discharge (Helland, Rygg et al. 1994).

Studies in the hydrodynamics of the fjord have also been performed showing mine tailings particles being present in the water column several kilometres from the point of discharge (Tesaker 1978, Johnsen, Golmen et al. 2004, Golmen and Norli 2013).

Seismic geotechnical studies performed in the inner Ranfjorden in relation to slope stability have shown a dynamic depositional environment. A study in 1983 by GEOTEAM A/S, in relation to the potential development of a new deep-water dock, showed significant accumulation of finer sediments close to shore on the slopes of the southern portion of the inner-fjord. Areas with steeper slope showed considerably less accumulation (GEOTEAM 1983). A seismic report completed by NOTEBY A/S in 1994 covered the innermost portion of the fjord surrounding the discharge points of Rana Gruber's mine tailings. It showed significant mass movement events with large amounts of sediments having been transported downslope to deeper portions of the fjord (Røe 1994). A study into the sedimentary environment of Ranfjorden since the last deglaciation shows clear evidence of anthropological sediments. When compared to outer fjord samples, samples taken from the inner fjord showed considerably higher sedimentation rates over the last 100 years (Lysså, Seirup et al. 2004).

2 Study Area

Ranfjorden is located between approximately 66°08'-66°20'N and 12°5'-14°8'E in northern Norway and is oriented in a WSW-ENE direction. It is almost 70 km long, 2-4 km wide and with depths of up to 530 m. The length of the fjord is divided into 4 main basins separated by glacial sills or bedrock (Lysså, Seirup et al. 2004), with the inner fjord basin being the deepest. The fjord gradually narrows and becomes shallower westward as it approaches the Norwegian Sea with an outer basin depth of approximately 300 m. The inner fjord is the primary basin of interest in this study and is the widest and the deepest with a length of approximately 26km. The study area stretches out approximately 18 km from the Mo i Rana harbor at the mouth of the Ranaelva to near Hemnesberget (Figure 6).

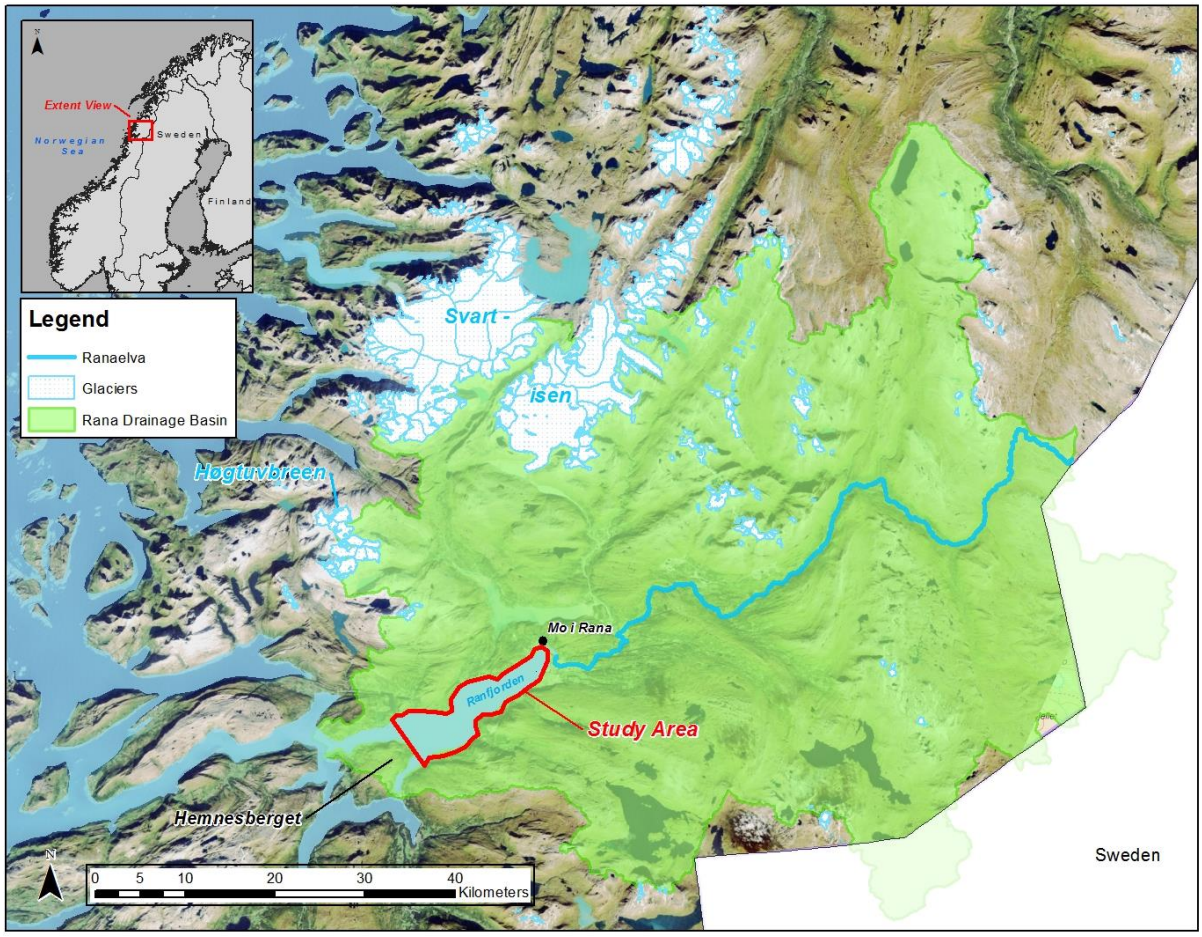

Figure 6. Ranfjorden study area and features

2.1 Physiographic setting

Ranfjorden is in the catchment area of three glaciers, with Høgtuvbreen and Svartisen located in the drainage area of the Ranaelva (Figure 6). Ranaelva drains the majority of the area and enters at the head of Ranfjorden and is the primary natural sediment source to the fjord (Lysså, Seirup et al. 2004). The fjord is flanked by mountains of up to 800 m in elevation and with other mountains in the surrounding catchment area reaching close to 1600 m. The inner fjord bathymetry has steep slopes rising up from the inner

basin towards each shoreline and the head of the fjord. Several submarine valleys and channels run from the fjord head down into the fjord basin and will be discussed in more detail later Section 5. The tide has a range of ~3 m in the fjord (Green, Pedersen et al. 1995).

2.2 Regional Geology

The predominant geologic units underlying the Ranfjorden area are the Rødingsfjell Nappe Complex to the north and east and the Helgeland Nappe Complex to the south and west. Older Paleozoic gneisses, mica schists and marbles dominate each of the nappe complex's lithology (Figure 7) (Gustavson and Gjelle 1991). Sjona and Høgtuva are the tectonic basement windows to the north of the fjord and consist of granitic gneisses. To the south is the Bindalen Batholith made up of young Caledonian granites. All the rocks in the area have experienced deformation and metamorphism during the Caledonian orogeny (Olesen, Gjelle et al. 1994). The metamorphosed rocks in the region contain large amounts of high Fe-grade iron ores in the form of hematite and magnetite (Ramberg, Bryhni et al. 2013).

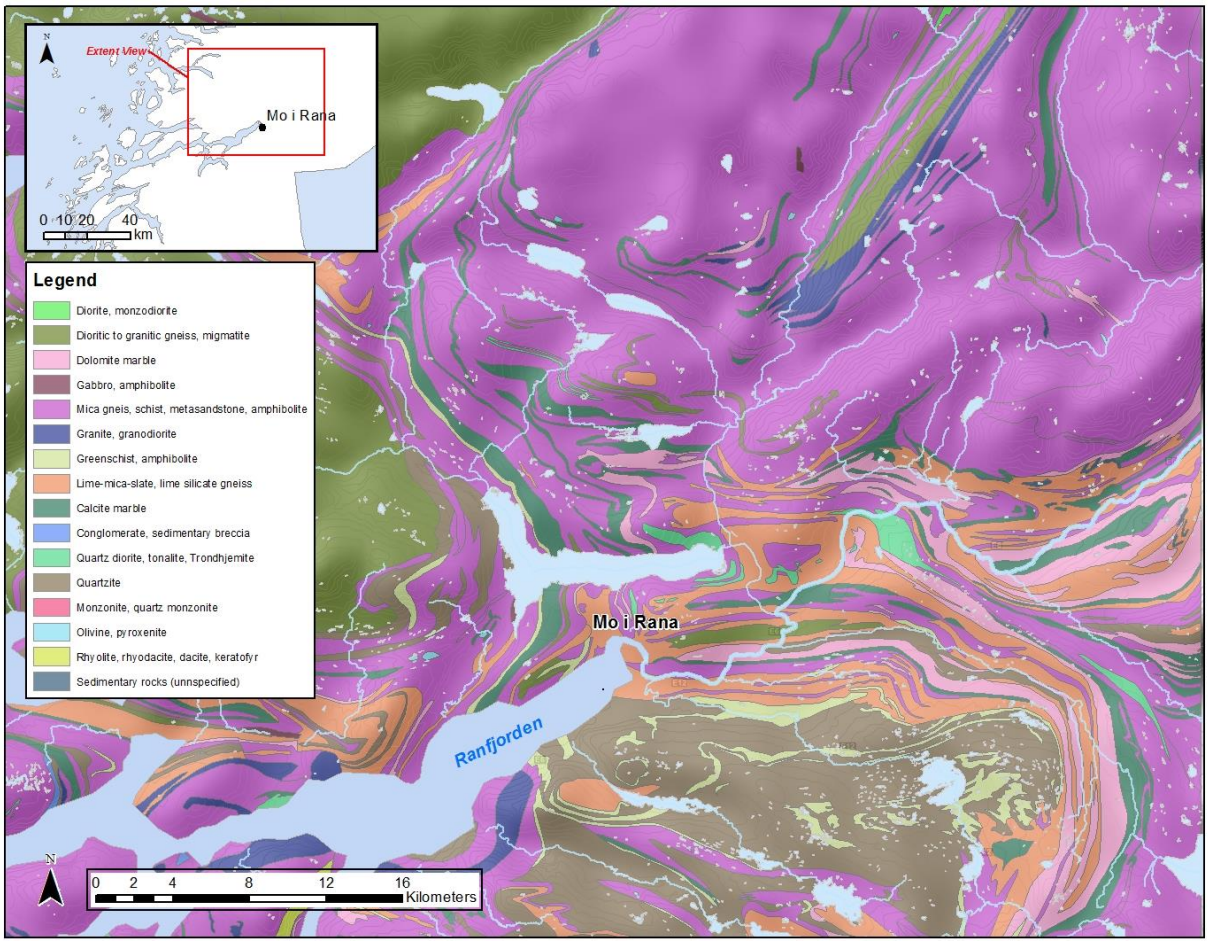

Figure 7. Regional Geology (Created using NGU datasets)

The Ranfjorden area has experienced extensive glaciation and deglaciation periods through the Quaternary period up until the present. This area is also known as the most seismotectonically active region in Norway, which has been been attributed to rapid post-

glacial crustal up-lift since the last deglaciation (Hicks, Bungum et al. 2000). As the ice-sheets retreated, the present day surrounding glaciers formed approximately 9.5 ka BP with the area around Ranfjorden becoming ice free around 9.31 ka BP (Hicks, Bungum et al. 2000). The remaining glaciers all now feed primarily into Ranfjorden.

2.3 Climate

The Ranfjorden region is located in a subarctic climate zone with normally longer, colder winters and shorter, cool to mild summers. The yearly total precipitation for the area is 1455 mm with precipitation occurring even during the driest months of April, May and June (Figure 8). The months with the most precipitation occur during the fall with October having the highest average amount of approximately 185mm.

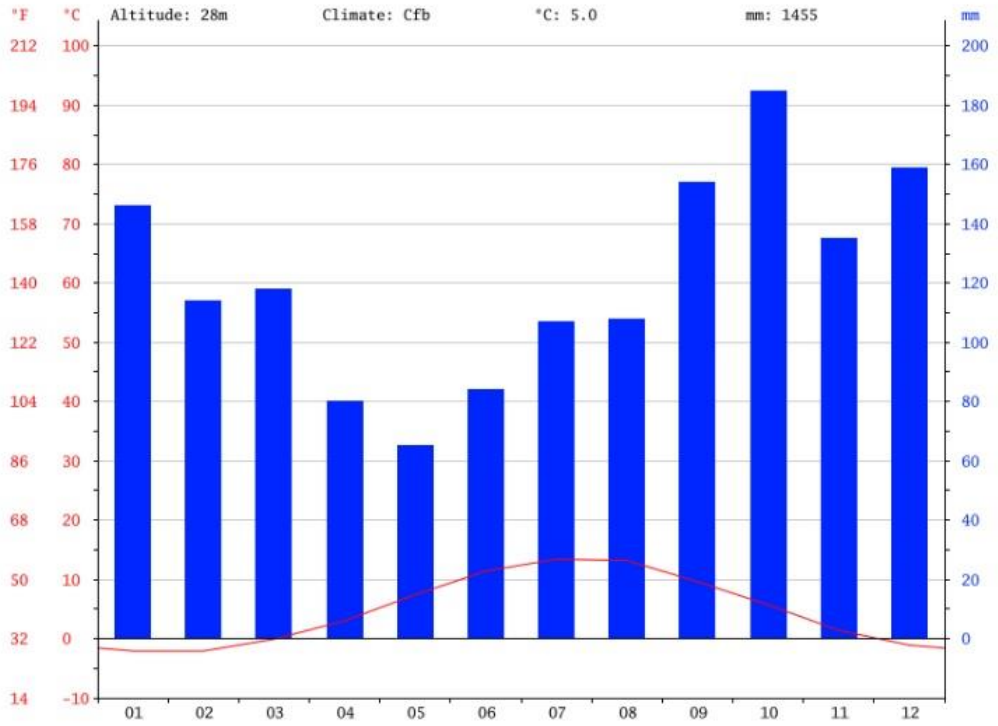

Figure 8. Average monthly precipitation for Mo i Rana (https://no.climate-data.org/)

Temperatures are relatively mild during the winters and summers with the highest temperatures occurring in July and August. The historical average water temperature of the inner fjord ranges from a low of 5°C (January – April) to a high of 12°C (August) (Table 1).

Table 1.Mo i Rana average monthly temperatures (https://no.climate-data.org/)

Monthly Temperature for Mo I Rana					
Month	Maxs Temp	Minimum Temp	Water Temp	Hours of Sunlight	Days with Precipitation
January	0.7	-4.8	5	0	24
February	0.7	-4.8	5	1	22
March	3	-3.1	5	3	21
April	6.3	-0.2	5	5	18
May	11.1	3.8	6	7	16
June	15	7.8	9	8	17
July	16.8	10.1	11	6	21
August	16.4	10	12	5	21
September	12.6	6.6	11	3	24
October	8.2	3.2	9	2	25
November	3.8	-0.9	8	1	23
December	1.6	-3.8	6	0	25

2.4 Ranaelva River

Ranaelva is a 130km long river that had its origin on the Saltfjellet plateau in the interior of Nordland County. The drainage area for the fjord is approximately 4500 km^2 and includes 3 glaciers with the Svartisen glacier (~369 km^2) being the largest (Figure 6) (Lysså, Seirup et al. 2004). The river is fed from a combination of precipitation and snow/glacier melt year-round with the latter increasing greatly during spring and summer. This increase from glacial melt also brings an increase in the fine sediment load to the fjord (Golmen and Norli 2013). Ranaelva has an estimated annual input range of ~27,000-35,000 tons of inorganic sediments that are derived from both natural erosional processes and from waste from mines located in the river's catchment area (Syvitski, Burrell et al. 1987, Johnsen, Golmen et al. 2004). These mine waste derived sediments have a high Fe content and have been estimated to total ~1,800 tons/yr in 1994-95 (Johnsen, Golmen et al. 2004).

2.5 Rana Gruber Mines

Rana Gruber A/S and its earlier parent companies have been mining and processing iron ore near Ranfjorden for over 100 years (Berg 1996). Their ore processing plant has been in operation at its present location at Gullsmedvika in Mo i Rana harbour since 1965 (Johnsen, Golmen et al. 2004) and has been discharging mine tailings into Ranfjorden since. As of 2014, ~3.7 million tons of iron ore were produced annually from the mines in the Dunderland Valley, 35 km inland from Mo i Rana. The final iron ore concentrate produced totalled close to ~1.5 million tons with the majority being hematite (over 1 million tons) and the remainder being magnetite. A small portion was used for specialty products (Skei 2014). The remaining tailings waste produced was reported to be ~3 million tons with 40 kg of flotation agent Lilaflot D817M. All of this waste is discharged into Ranfjorden (Skei 2014). The mine tailings themselves consist of 40-50% quartz, 15-20% Fe-Al-Mg silicates, mica, garnet, amphibole and epidote (Skei 2014). Some additional calcite, dolomite and 6-14% hematite is also present. No elevated levels of trace metals have been found (Skei 2014). Elutriate testing of the tailings in seawater hasn't resulted in any readings above detection limits, implying the contents of the tailings can be considered relatively inert (Skei 2014).

2.5.1 Submarine Tailing Placement

From 1965 to 2014 the submarine tailings placement (STP) of the mine tailings was divided into a coarser and a finer fraction before being transported through pipelines into the fjord. The areas of discharge have been shown to be at the edges of steep slopes of bare rock (Røe 1994). The coarser-grained fraction consisted of particles of up to 800 µm and the finer fraction consisted of particles where 20% were less than 45 µm (Johnsen, Golmen et al. 2004) and less than 2% were smaller than 10 µm (Skei 2014). Each tailings fraction was deaerated and mixed with freshwater before being discharged into the fjord at a rate of ~1100 m^3/hr for the coarser fraction and 2200 m^3/hr for the finer fraction (Golmen and Norli 2013). The final slurries contained ~10% solids and had a bulk density of 1.07 g/l (Skei 2014).

The coarse-grained tailings were originally deposited at a depth of 30 m close to the mouth of the Ranaelva near the harbour breakwater. The finer tailings were deposited more to the south at a depth of 45 m (Figure 9) (Johnsen, Golmen et al. 2004). Both discharge points were near steep submarine slopes (Syvitski, Burrell et al. 1987). Figure 9 includes an overlay of a map from the NOTEBY A/S study from 1994 (Røe 1994) showing the discharge locations and the surrounding channels/slopes. The only variation to these discharge points was for the coarse-grained tailings during the period between 1988-1992 when half of its total content was used as coastal infill for a harbour/dock complex (Johnsen, Golmen et al. 2004). This variation and drop in discharge is seen in Figure 10. A drop in total discharge from 1980 to the late 1990's also reflects a drop in total production during that period. More recent production increases are reflected in the total discharge amounts varying from 2 to 3 million tons (Vogt 2013, Skei 2014). Since May of 2014 the mine tailings have been combined and discharged through a single pipeline at a depth of 125 m at an unspecified location.

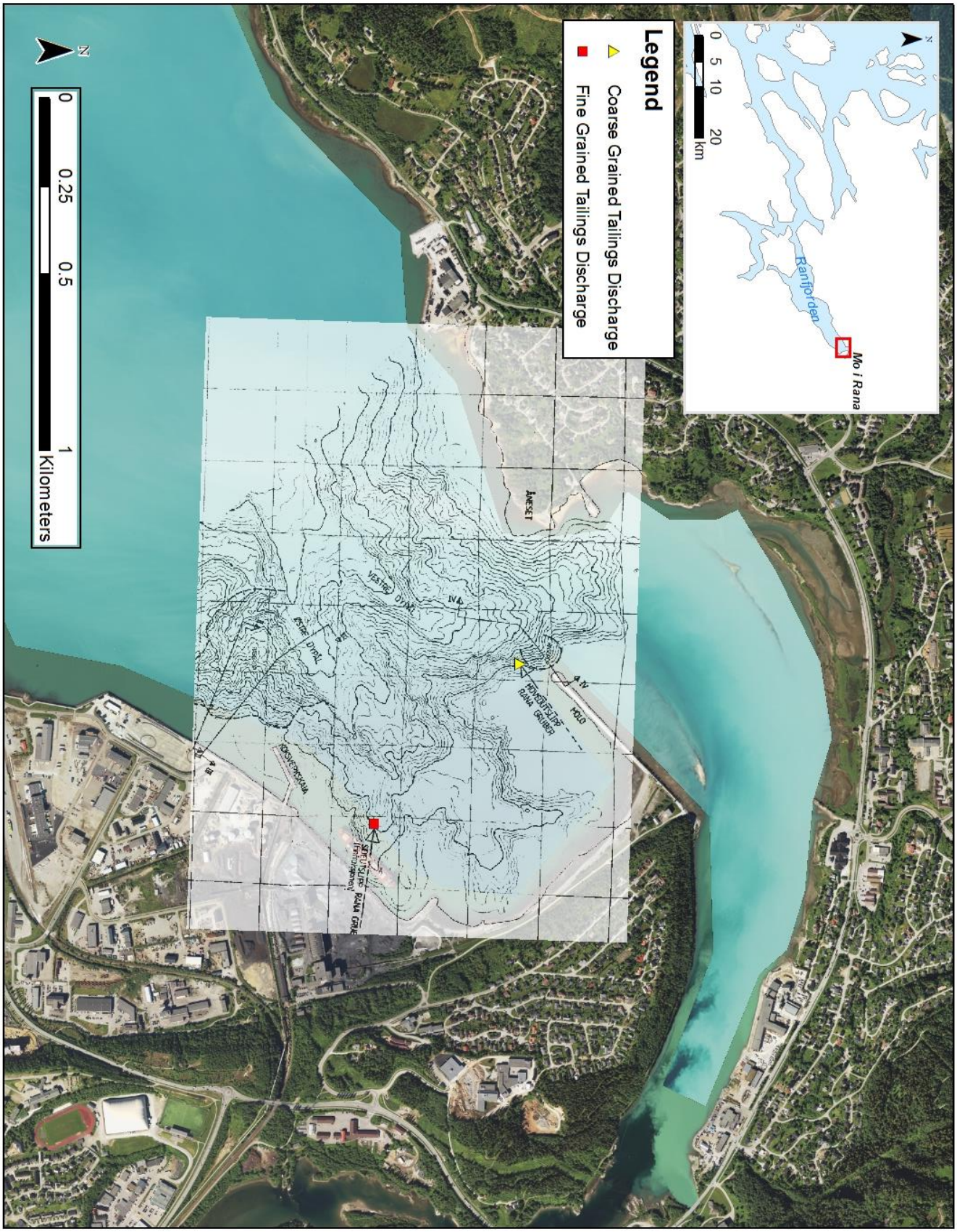

Figure 9. Tailing discharge points in Mo i Rana Harbor (Røe, 1994)

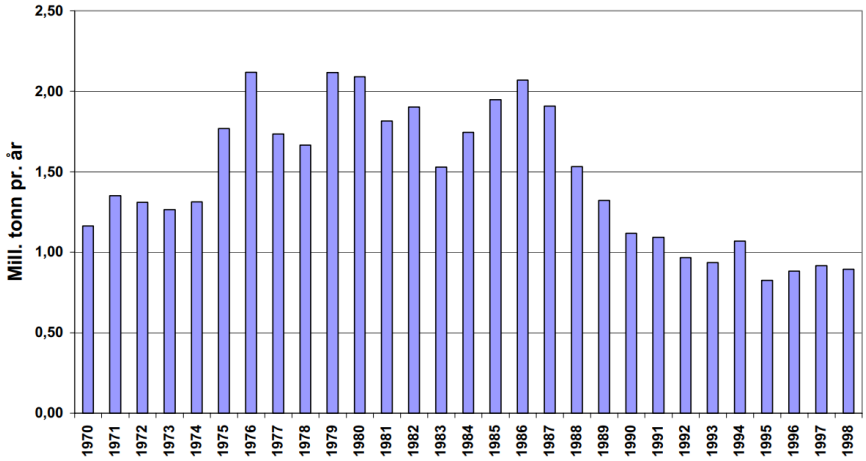

Figure 10. Rana Gruber yearly discharge 1970-1998 (Johnsen, 2004)

3 Fjord Hydrography and Sedimentary Processes

3.1 Fjord Hydrography

The fresh water input from Ranaelva has a profound effect on the hydrological structure of the inner Ranfjorden basin. As the freshwater runs into the fjord, it floats as a separate brackish surface layer above the more dense saline seawater creating a defined halocline. A thermocline is also present with this layer (Golmen and Norli 2013). The thickness and length of the brackish layer depends on the time of year and the amount of freshwater input from the Ranaelva, with periods of higher runoff creating a thicker, longer layer and the opposite for low runoff periods (Figure 11).

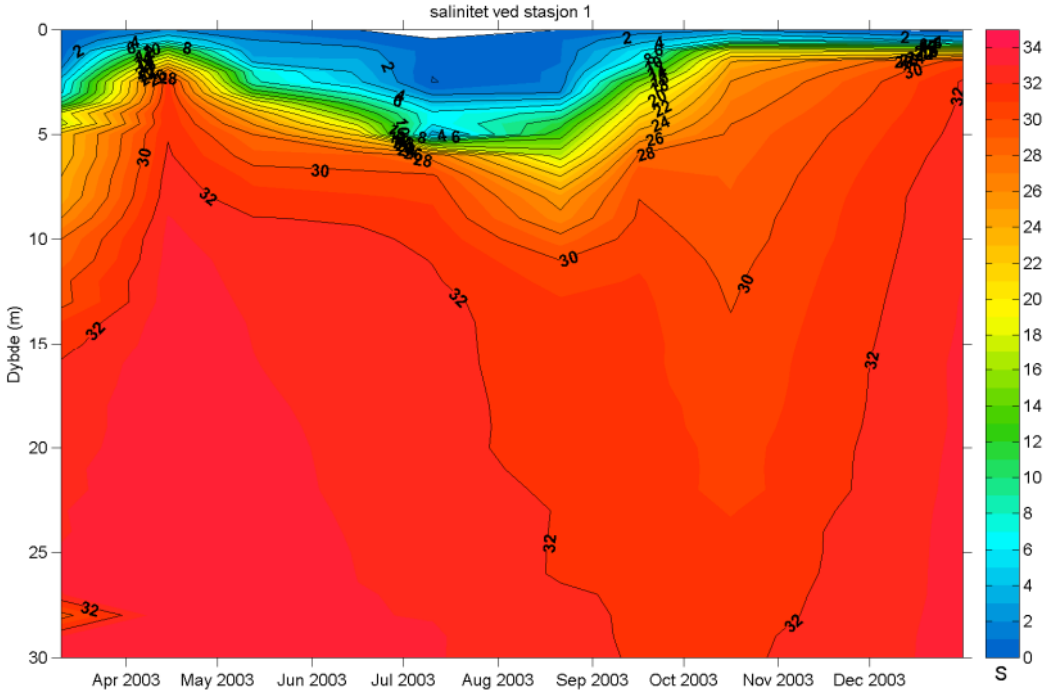

Figure 11. Salinity levels in Ranfjorden over the course of a year at the fine fraction tailings discharge location (Golmen, 2013)

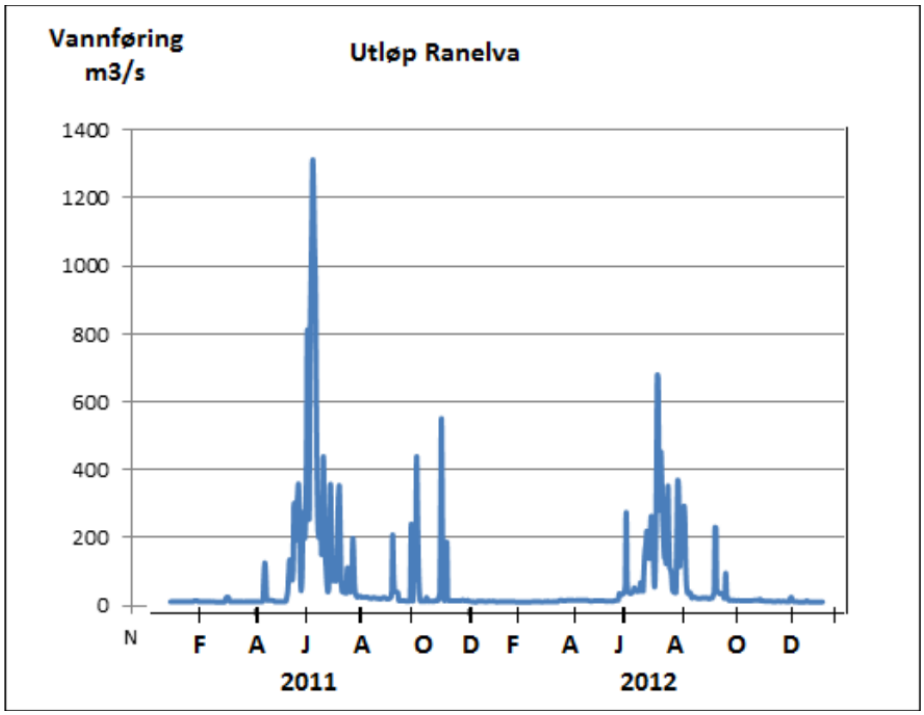

Figure 12. Ranaelva yearly average runoff 2011-2012 (Golmen, 2013)

Measurements of current direction and speed within the water column near the mouth of Ranaelva have shown that the stratified layers create a circular current pattern indicative of estuarine circulation. As the upper, less dense brackish layer floats outward into the fjord, a counter compensation current occurs. This denser, more saline current flows back toward the river mouth along the surface until it meets and drops below the brackish outflow current (Golmen and Norli 2013). The measurements taken from the inner fjord at the river mouth show that at a depth of 26 m there was a strong variable direction current (tidal influence) with a net direction back towards the river mouth. At a depth of 47 m and below there was another strong current with a net direction away from the river mouth and down through the channel present there. Overall, the inner fjord showed to have a net outward current at the surface and below 40 m with an inbound current in the depths between (Figure 13) (Leikvin 2009). Measurements taken near the tailings fine fraction discharge point slightly farther from the river mouth showed a net inbound current (Johnsen, Golmen et al. 2004, Leikvin 2009).

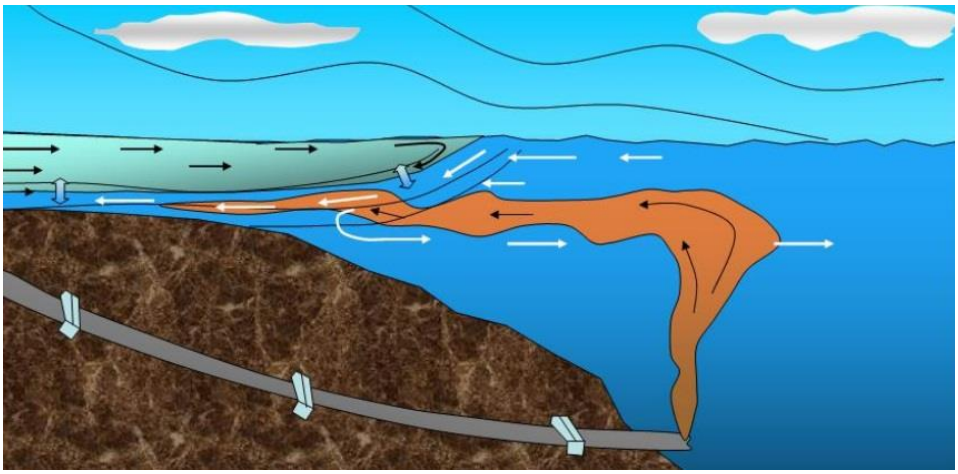

Figure 13. Estuarine circulation effect on fine fraction of tailings discharge (Golmen, 2013)

Since the mine tailings are mixed with freshwater before discharge, a portion of the finer fractions will rise up into the water column as they mix with the seawater (Figure 13) (Johnsen, Golmen et al. 2004). The inbound current at the point of the fine fraction discharge has shown to transport some sediments back toward the river mouth with the brackish surface layer halocline acting as a barrier for upward mobility (Golmen and Norli 2013). The minimum depths reached by the sediments in the water column depends on the thickness of the barrier layer. Heavy run-off during July 2013 showed sediment reaching up to only 28 m while during lower run-off in October 2012 showed sediments up to a depth of 8-10 m (Golmen and Norli 2013). It has also been shown that some fine fraction particles are stored at around 25 m in the water column farther out in the fjord (Helland, Rygg et al. 1994). For the coarser fraction of the tailings, the dispersal was shown to be more consistent, with spreading occurring up to 25 m depth and a maximum spreading around 30 m depth (Golmen and Norli 2013).

3.2 Fjord Sedimentation

Ranfjorden, like most fjords in northern Norway, receives its input of natural sediments primarily from riverine sources (Syvitski, Burrell et al. 1987) with Ranaelva being the major source to the inner basin (Johnsen, Golmen et al. 2004). The solid waste discharges from anthropogenic sources in the inner fjord are estimated to have been more than 100 times greater than the natural supply, dominating the sedimentation of the inner fjord over the last century (Syvitski, Burrell et al. 1987). Previous studies have shown that there have been periods of extremely high rates of sedimentation of up to 50 cm/yr in portions of the inner fjord (Helland, Rygg et al. 1994). The areas where the tailings are discharged and accumulate are near steep slopes where their build-up in large amounts can result in unstable conditions (Tesaker 1978). This is confirmed by the NOTEBY A/S study (Røe 1994) which described several parts of the inner fjord basin having experienced episodic mass movement events such as slides and slumping with large erosional features down to bare rock extending into the fjord basin. Figure 14 shows the discharge area in more detail with the documented older slides to the north and south.

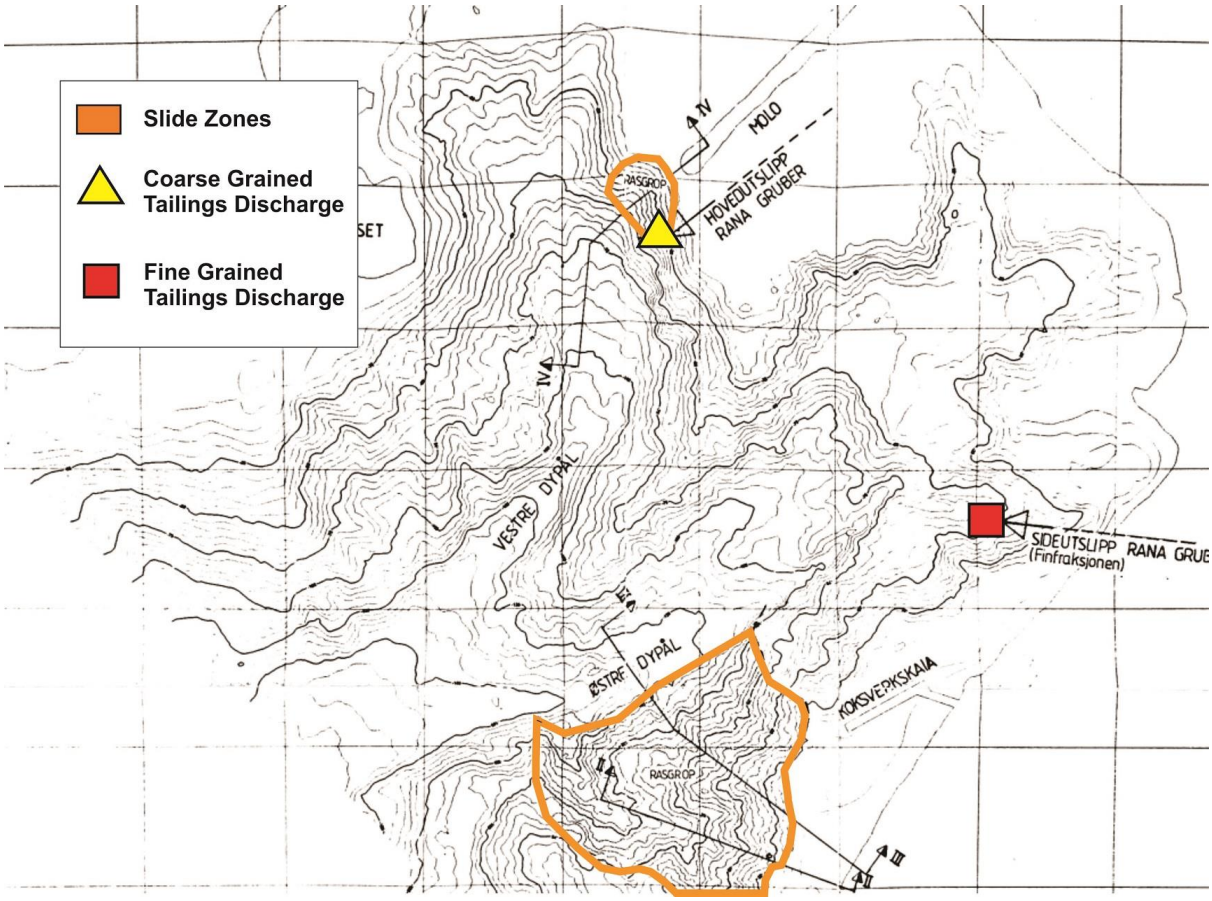

Figure 14. Tailings discharge points with surrounding bathymetry (Røe, 1994)

A 50 m deep submarine canyon at the fjord head has been confirmed to have eroded into loose deposits down to bare rock with the estimated volume of material removed over 7 years being 10^7 m^3 (Tesaker 1978). Below this canyon, in a channel at the bottom of the fjord, a suspension current has been measured with a velocity of 25 cm/s, 1 m above the bottom. Estimates made from this current indicate that up to 18% of the discharged tailings are transported by suspension currents into the fjord basin, with the remainder being moved as bed load (Tesaker 1978). An underwater plume has been measured below the halocline in the innermost 5 km of the fjord.

A confirmed slide on the inside of the breakwater at the mouth of Ranaelva and up fjord from the tailings discharge points has been attributed to tailing sediments that have been transported and accumulated to counter currents (Figure 14) (Røe 1994). This indicated that the bare rock at the discharge points was possibly a result of erosion from the discharged tailings (Røe 1994).

4 Materials and Methods

4.1 Sediment Collection

For this portion of the NYKOS project, 6 Niemistö cores (Table 2) and 10 sediment grabs (Table 3) provided the basis of the study. These samples were collected by the Geological Survey of Norway (NGU) research vessel FF Seisma on a cruise from April 19-22, 2015. Figure 15 shows the location of each sample within Ranfjorden. The Niemistö cores provided insight into the depositional record under sea floor while the sediment grabs showed a snapshot of the more recent depositional environment at each location.

4.1.1 Sediment Grab Documentation

All the sediment grabs were photographed and documented for color and grainsize at the time of their retrieval on board the FF Seisma on April 22, 2015. Geologist Nicole Jeanne Baeten from NGU performed all photography and documentation.

*Table 2. Sediment core lengths, sampling depths and positions (*Degrees Minutes Seconds)*

Core ID	Date of Sampling	Sampling Equipment	Water Depth (m)	Core Length (cm)	Longitude*	Latitude*
P1502-001	20.4.15	Niemistö Corer	100	37	13°46'42.29"	66°16'7.13"
P1502-004	21.4.15	Niemistö Corer	65	24	14°5'55.03"	66°19'28.02"
P1502-009	21.4.15	Niemistö Corer	230	19	14°6'28.78"	66°18'49.59"
P1502-013	21.4.15	Niemistö Corer	282	39	14°5'2.367"	66°18'33.90"
P1502-015	21.4.15	Niemistö Corer	180	35	14°4'27.30"	66°18'52.88"
P1502-016	21.4.15	Niemistö Corer	520	9.5	13°47'58.99"	66°15'37.33"

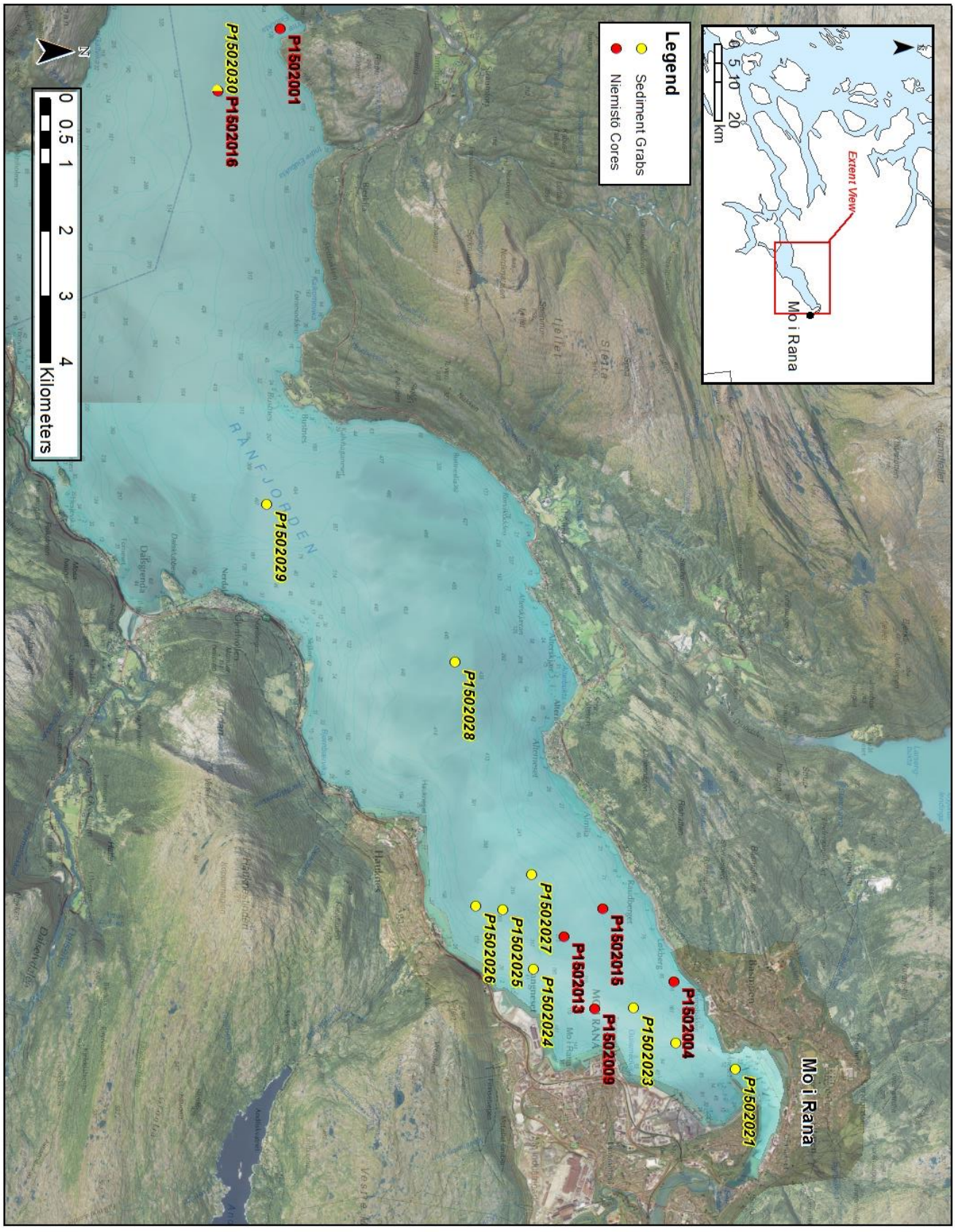

Figure 15. Niemistö and Sediment Grab Locations

Table 3. Sediment grab depth and location (Degrees Minutes Seconds)

ID	Date of Sampling	Sampling Equipment	Water Depth (m)	Latitude*	Longitude*
P1502-021	22.4.15	Grab	38	66° 19' 58.63"N	14° 7' 40.03"E
P1502-022	22.4.15	Grab	180	66° 19' 29.29"N	14° 7' 9.79"E
P1502-023	22.4.15	Grab	232	66° 19' 8.28"N	14° 6' 27.71"E
P1502-024	22.4.15	Grab	307	66° 18' 19.15"N	14° 5' 41.60"E
P1502-025	22.4.15	Grab	348	66° 18' 3.96"N	14° 4' 29.66"E
P1502-026	22.4.15	Grab	330	66° 17' 50.31"N	14° 4' 25.83"E
P1502-027	22.4.15	Grab	330	66° 18' 17.86"N	14° 3' 47.00"E
P1502-028	22.4.15	Grab	440	66° 17' 38.62"N	13° 59' 29.49"E
P1502-029	22.4.15	Grab	500	66° 16' 4.95"N	13° 56' 20.67"E
P1502-030	22.4.15	Grab	520	66° 15' 37.30"N	13° 47' 59.23"E

4.2 Swath Bathymetry

For this study, two different sets of bathymetry data were used. Each data set was collected at different time intervals with the first dataset being collected in 2012 by the NGU research vessel FF Seisma using WASSP multibeam sonar. The second dataset was collected in 2016 from the FF Seisma using Kongsberg EM2040 multibeam echo sounder. This data was post-processed using Caris data systems. Later editing and visualization of the data was performed using Esri ArcGIS software. The WASSP multibeam bathymetry dataset from 2012 covered a smaller area of the fjord and was of a lower quality than the 2016 EM2040 multibeam data. Due to this reason the 2016 data was primarily used to display the bathymetry features of the fjord. The 2012 and 2016 datasets were used in combination to create a layer displaying the changes between 2012 and 2016 to the bathymetry of the fjord. The 2016 data was also used to display the slope angles of the fjord bathymetry.

4.3 TOPAS Seismic

TOPAS parametric sub-bottom profile data was collected in 2015 from the NGU research vessel FF Seisma.

4.4 Laboratory Analysis

4.4.1 Opening, Photography and X-Ray of Cores

All the Niemistö cores used in this study were initially analyzed at the Geological Survey of Norway (NGU) lab in Trondheim between 2015-2016. There the analysis included a Multi Sensor Core Logger (MSCL) and X-ray imaging (XRI) before being opened and photographed. The MSCL scanned for X-ray fluorescence (XRF) and magnetic susceptibility. For this study only the photographs, X-ray imaging and magnetic susceptibility data were used.

The opened Niemistö cores arrived at the Department of Geosciences laboratory (IG) at UiT The Arctic University of Norway in the summer of 2017. Each core had an archive half and a working half. The archive half was to remain largely undisturbed and to be used for visual core-logging and XRF testing. The working half was to be used to for all physical testing of the sediments including shear strength and grainsize analysis. Some samples were removed from the working cores at NGU for physical testing prior to arriving at the IG lab. There would be very little remaining of the testing half of the core when the work was completed.

4.4.2 XRF Analysis

The archive half of the Niemistö cores were used for the XRF analysis at the IG lab during the summer and fall of 2017. The scanning was performed using an Avaatech XRF core scanner at 5 mm down core intervals with 30-second measuring times. The following settings were used on the XRF scanner (Figenschau 2018):

- 10 kV, 1000 µA, no filter, to measure light elements from Mg to Co
- 30 kV, 2000 µA, Pd-thick filter, to measure medium-heavy elements from Ni to “ca.” Mo
- 50 kV, 2000 µA, Cu-Filter, to measure heavy elements from “ca.” Mo to U.

The data retrieved from the XRF scanner is qualitative and for this study only the Fe values were used. This is due to Fe being associated with the mine tailings and an important distinguishing factor from more natural sediments (Skei and Paus 1979).

Karina Monsen performed the XRF scanning and data processing in the IG lab. For more information on the XRF scanning process, refer to the associated thesis of Nikolai Figenschau (Figenschau 2018).

4.4.3 Sedimentary Core Logging

The visual description of the sediment cores was performed on the archive half of the cores. Prior to the visual logging, the core surfaces were cleaned and smoothed. Lithological logs were created for each of the six cores showing the physical changes through their lengths. Color (Munsell Sediment Color Chart (MSCC)), relative grainsize, structures, clasts, bioturbation and shell fragments were logged.

4.4.4 Shear Strength Test

Shear strength tests were performed at different points along all six cores. Areas of transition in color and or grainsize were used to determine testing points. Undrained shear strength (S_u) and reworked shear strength (S_r) tests were performed at each testing point.

A GEONOR fall cone apparatus was used to perform the shear strength tests. The principle behind the test is that a cone of a certain weight and apex angle is hung touching the sediment surface and then dropped onto the sediment sample and the depth of penetration of the cone corresponds to a shear strength value in tables accompanying the apparatus (GEONOR). The shear strength of a soil (s) is proportional to the weight of the cone (Q) and inversely proportional to the square of the penetration (h) of the cone into the sample: $s=K(Q/h^2)$. The proportional constant (K) depends primarily on the angle of the cone and sensitivity of the clay (Hansbo 1957).

The tests for S_u were performed by dropping the cone directly onto the undisturbed sediment while it was still in the core. This was performed three times for each sample. For the S_r tests, sediment samples ~1cm in length were extracted from the core and placed into a small cup. The sample was thoroughly mixed and pressed into the cup to ensure no air pockets or original structures remained. The cone was then dropped onto the sediment in the cup. The test was repeated three times for each sample with the sample being reworked after each test. This reading provided a new shear strength reading with the same water content. Each S_r sample extracted from the core was bagged, sealed and frozen for later grainsize analysis.

Sensitivity of the sediments was calculated by taking the ratio of S_u/S_r , showing the sensitivity of the sediment to disturbance (Skempton and Northey 1952). Sediments with a higher sensitivity ratio when disturbed will have a greater chance of behaving as a viscous fluid and undergo flow (Reeves, Sims et al. 2006).

4.4.5 Grainsize Analysis

Grainsize analysis was performed on all six of the working cores but at different sampling intervals:

- P1502-001: Sampled every 1.0 cm (37 samples total)
- P1502-004: Sampled every 0.5 cm (46 samples total)
- P1502-009: Sampled every 1.0 cm (19 samples total)
- P1502-013: Sampled every 1.0 cm (39 samples total)
- P1502-015: Sampled every 1.0 cm (34 samples total)
- P1502-016: Sampled every 0.5 cm (19 samples total)

4.4.5.1 Acid Treatment (HCL) and Oxidation with Hydrogen Peroxide (H_2O_2)

All sediment samples underwent acid and oxidation treatment to remove calcium carbonate ($CaCO_3$) and organic matter before being analysed by a Particle Size Analyser (PSA). The following steps were made following procedural guidelines

developed by the Department of Geosciences (IG) lab at UiT The Arctic University of Norway (UiT-IG).

Approximately 2g of sediment was taken at each sampling interval and placed into a plastic test tube. Just enough 20% HCL was added to the test tubes to entirely cover the sediments. They were then left under a fume hood for 24hrs. After 24 hrs, each sample was centrifuged down for 4 minutes at 4000 rpm. Excess water was decanted and distilled water was added and the test tube was then placed on a test tube shaker before being re-centrifuged. This process was repeated 6 times. Enough 20% H_2O_2 was then added to each test tube to entirely cover the sample. A cap of aluminium foil with a small hole was then placed over each test tube and they were placed in a heated water bath of 85°C for 2 hrs. The water bath was performed under a fume hood due to the normally volatile reaction of samples to H_2O_2. The same centrifuge, decanting and rinsing process as described before was then repeated. A small amount of distilled water was then added to the test tubes before placing them on a shaker table and transferring them to plastic cups. The samples were then placed in a drying rack at 32°C until dry. Approximately 0.5 g of each dried sample was then placed in individual cups with lids and mixed with 20ml of distilled water. The remainder of each dried sample was individually bagged and sealed. These cups with the samples were then placed on a shaking table for 24hrs before being analysed by the PSA.

4.4.5.2 Laser Particle Size Analyser

The laser particle size analyser (PSA) machine in the IG lab at UiT is Beckman Coulter LS 13 320. This machine uses a technique based on the deflection of a laser beam when it hits a particle to determine its size. The angle of the deflection depends on the size of the particle. This can be used to determine the particle distribution in fine-grained sediments within a range of 0.04-2000 microns (IG-LPSA). A sieve allowing particles up to 2000 microns was used for this study.

Before each sample was placed in the PSA, two drops of Calgon to prevent clumping was added to the sample and it was then inserted into an ultrasonic bath for 5 minutes to help mixing. Each sample was analysed 3 times and the results were exported as Excel data spreadsheets. An average for each reading was then placed in a GRADISTATv8 Excel program (Blott and Pye 2010), which then processed the data into the desired grainsize parameters seen later in the study.

5 Swath Bathymetry

5.1 2012 WASSP and 2016 EM2040 Multibeam Bathymetry

The bathymetry data displayed in Figures 16, 17 and 18 shows the innermost ~10.5 km of the fjord bottom rising at a relatively low angle of between 0-5 degrees from the south-west towards the north-east. The deepest depths in the area covered by the bathymetry data are between ~531 m (2012 data) and ~490 m (2016 data) deep in the western basin and the shallowest depths are ~4 m along the shorelines. The bottom of the center of the fjord is relatively flat in the outer portion of the inner basin with a width of ~1.8 km and narrowing quickly towards the head of the fjord. Steep slopes with angles up to 87° rise up sharply from the fjord bottom on both sides of the fjord (Figures 16, 17 and 18). The northern edge of the fjord has abrupt steep slopes that continue until the innermost 5 km of the fjord where the slopes become longer and more gradual. The southern edge of the fjord has sharp steep slopes up until the inner most 2 km of the fjord where the slopes become slightly less steep and dominated by sharp gullies.

These defined gullies extend from close to the shoreline down into the fjord. They are located along the innermost 2 km of the southern fjord slope, beginning at the mouth of Ranaelva. The largest gullies are located in the innermost part of the fjord near the river mouth and the tailing discharge points. Most of the gullies join at a channel formation that extends along the bottom of the fjord. This channel is sinuous in shape with defined edges extending over 5 km out into the fjord. It has a width of ~250 m for over 5 km before widening and becoming less defined in the deeper waters to the west. The channel follows more along the southern part of the fjord closer to the steeply sloped southern fjord edge. At one point, the channel flows up against the steep southern fjord edge and almost appears to have eroded slightly into the slope (Figure 18).

To the north of the channel, slight ridges resembling smaller, potentially abandoned channels can be seen running parallel to the deeper, larger channel. These smaller channels are at shallower depths with less defined edges. Within both the larger and smaller channels are stepped crescent shaped ridges that run roughly perpendicular to the channel edges and point up-fjord (Figure 18).

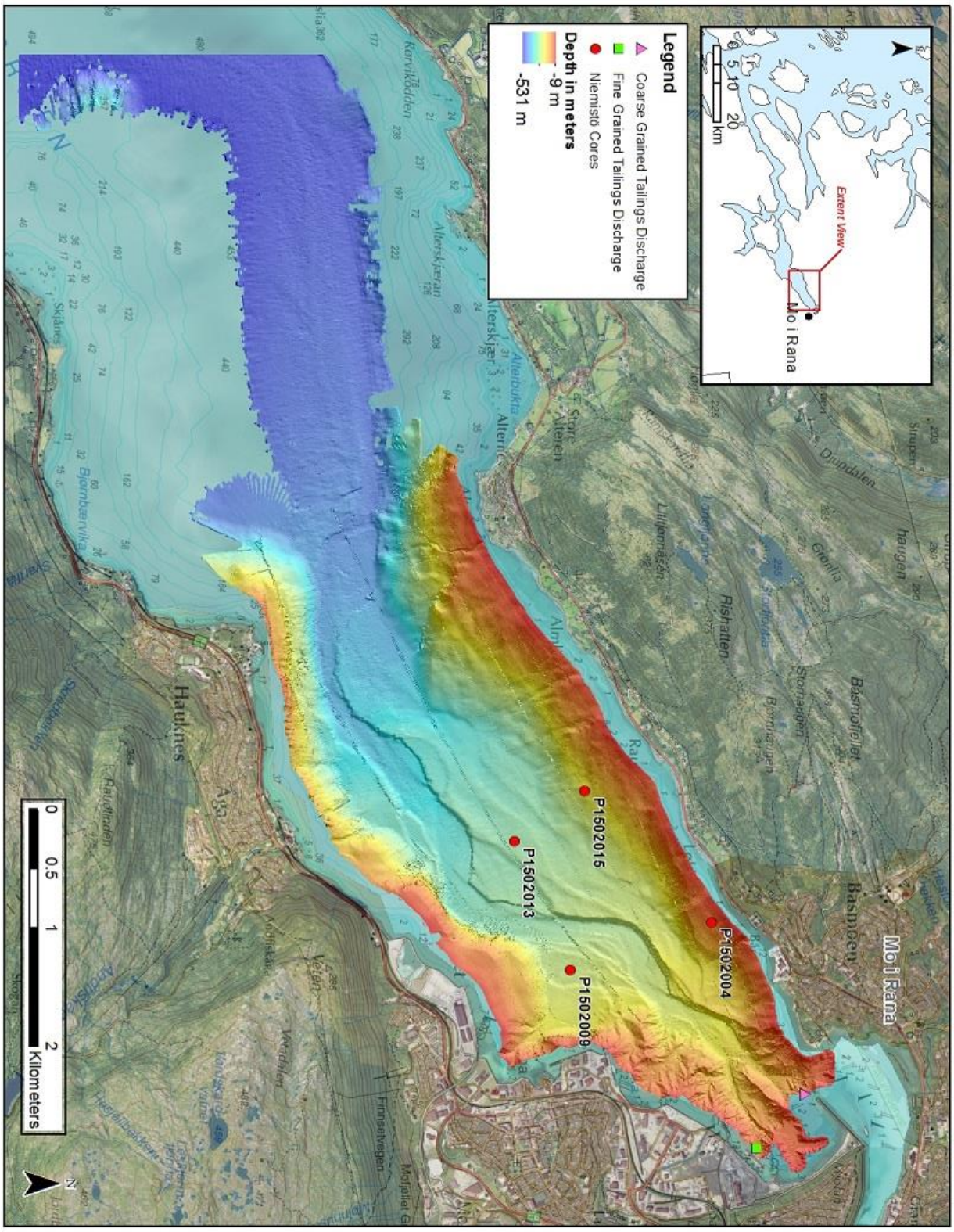

Figure 16. 2012 WASSP Multibeam Bathymetry

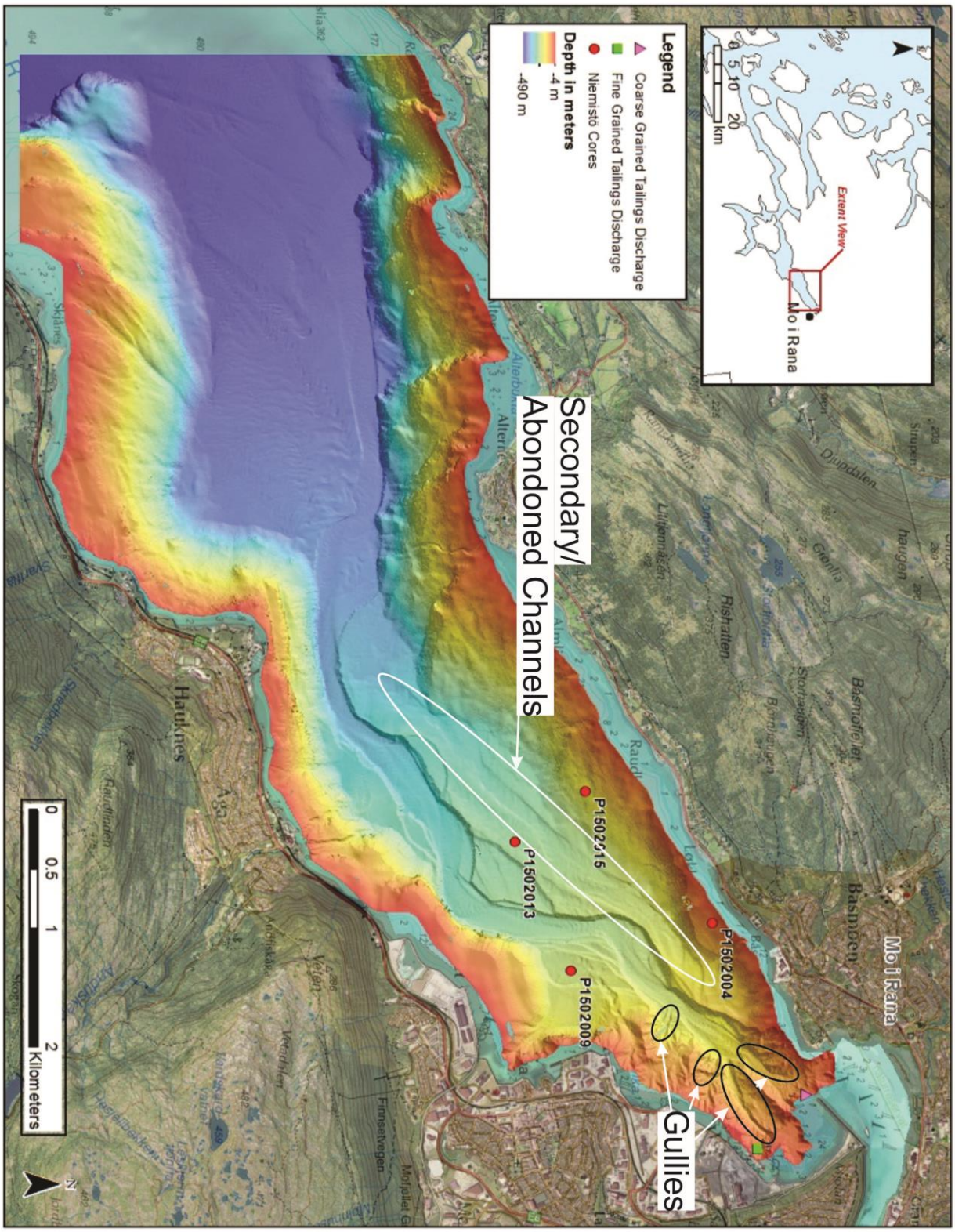

Figure 17. 2016 EM2040 Multibeam Bathymetry

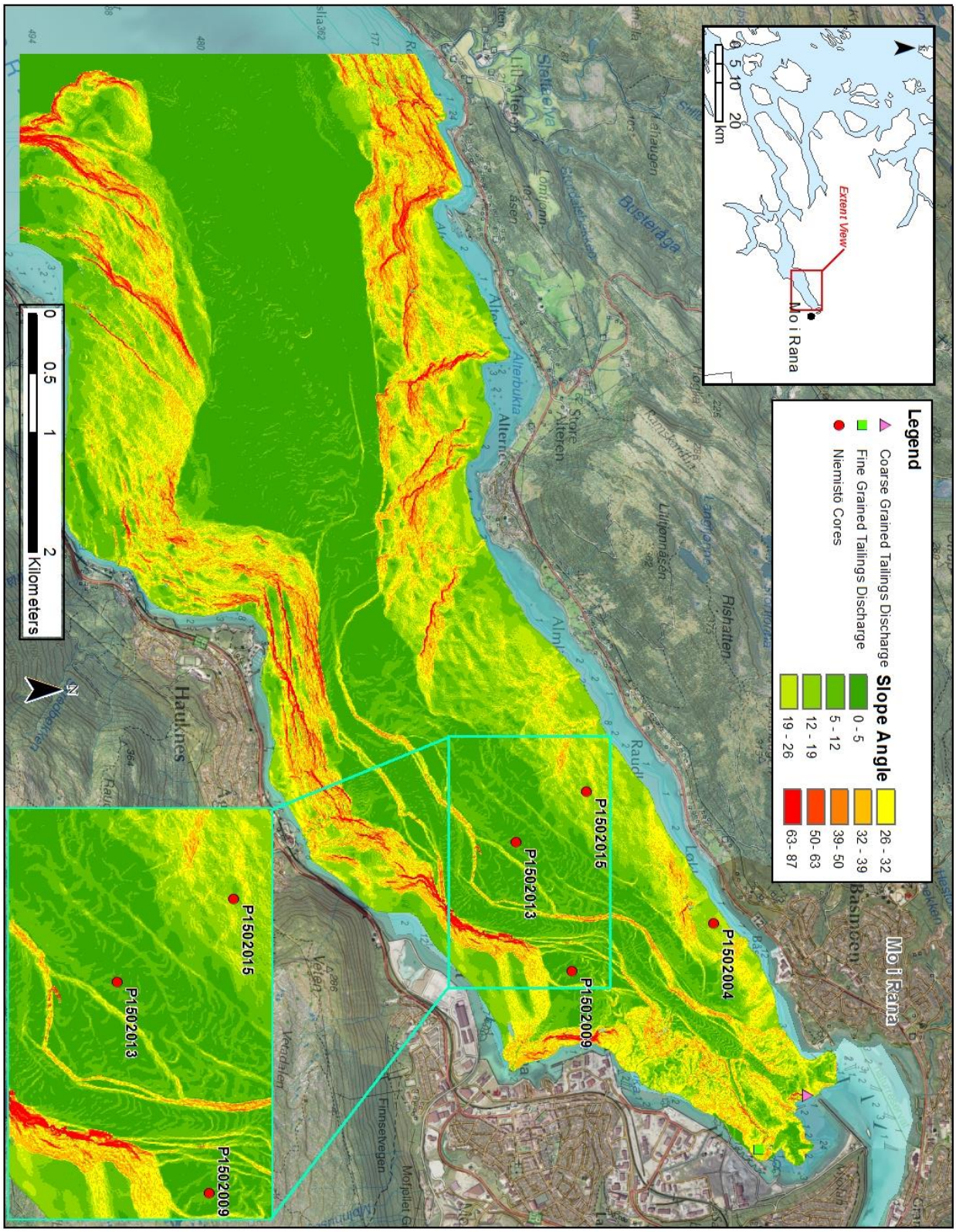

Figure 18. 2016 EM2040 Bathymetry Slopes

5.1.1 Interpretation:

The bathymetry data displayed here shows a fjord system that has a dominant channel system at its bottom. The gullies at the head of the fjord that lead down to the channel clearly indicate that these are pathways for sediments to flow down the slopes and into the channel (Figure 17). The sharp edges of the gullies indicate erosion has been recently occurring, eating into the slopes (Syvitski, Burrell et al. 1987). Since these gullies are located below the Ranaelva and mine tailings discharge points, it can be assumed that they are the sources for the sediments which cause of the erosion (Meiburg and Kneller 2010). This also indicates that these are most likely the sediment sources for the creation of the channel, which in turn is the main transport pathway for the sediments into the deeper fjord basin (Syvitski, Burrell et al. 1987). The smaller, shallower and less defined channels to the north of the main channel are possibly older abandoned channels and/or secondary channels that still occasionally continue to transport sediment (Figure 17 and 18). Several of the minor channels have somewhat defined edges indicating they could have transported sediment recently. Large outflow from Ranaelva or a sediment slide could have overflowed the main channel and fed into the smaller channels (Meiburg and Kneller 2010) . The crescent shaped features within the channels are most likely cyclic step formations created from surge/pulse turbidity currents flowing down the fjord (Figure 18) (Clarke 2016).

5.2 2014-2016 Changes in Bathymetry

The data displayed in Figure 19 shows the changes in bathymetry between 2012 and 2016. The greatest changes are seen in the form of erosion in the main channel along the fjord bottom. This erosion extends along ~5 km of the channel's north-northwestern edges with the largest amounts concentrated in the innermost ~2 km of the fjord. The same 2 km of the channel also sees large amounts of accretion occurring more to the center of the channels, directly to the south-southeast of the areas with high erosion.

The innermost parts of the fjord near the mouth of Ranaelva and the tailings discharge points shows narrow gullies of erosion extending down into the fjord channel. Several of these gullies seem to be the result of more recent mass movement events since they did not appear in the 2012 bathymetry dataset (Figure 20).

The northern slopes of the fjord at the western edge of the bathymetry data show high levels of change but due to the smaller coverage area of the 2012 data, a full display of the area is not available. As a result, an analysis of the area is not possible.

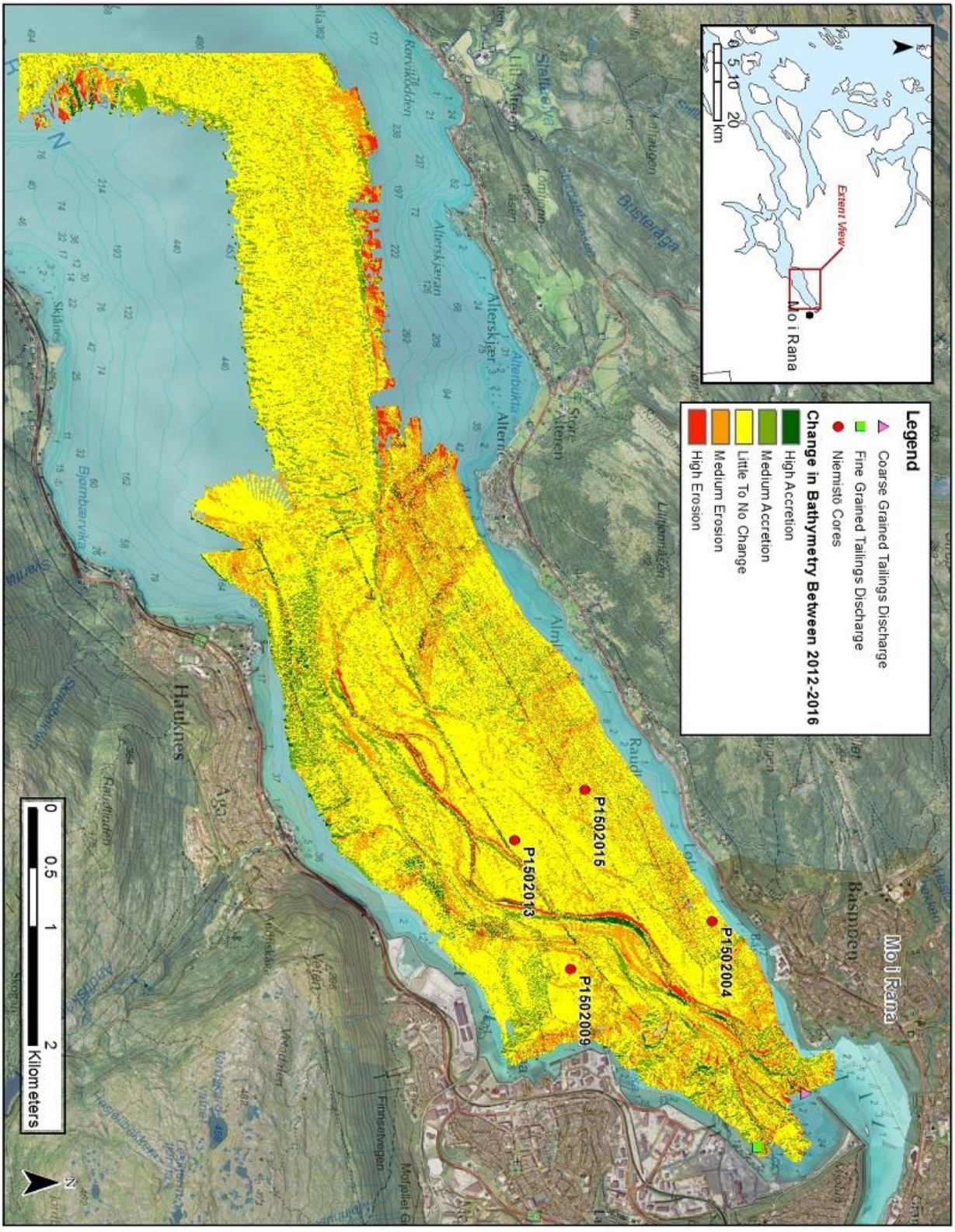

Figure 19. Change in bathymetry between 2012-2016

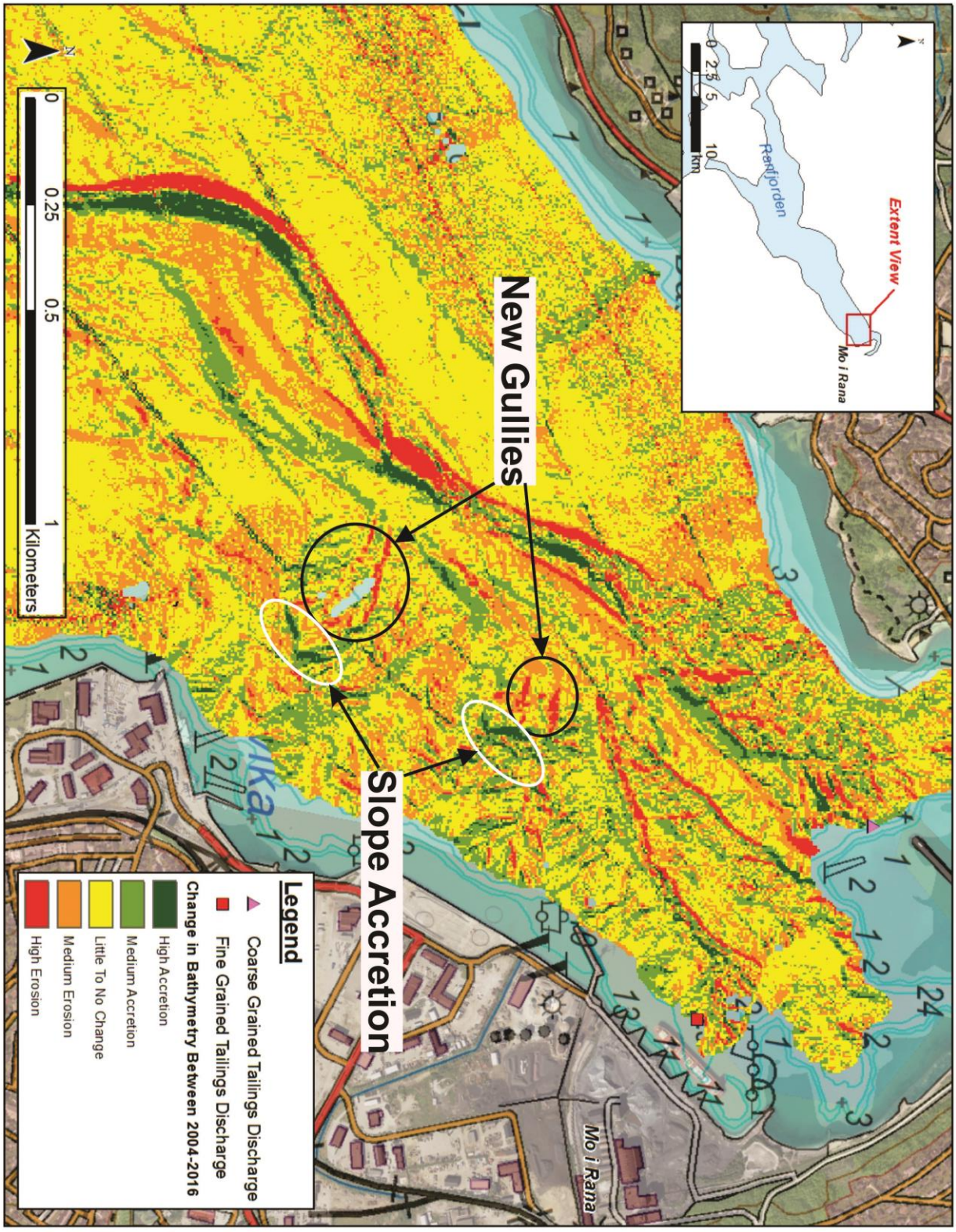

Figure 20. Close up of changes in Bathymetry

5.2.1 Interpretation

The high amount of erosion along the fjord's main channel and slopes in the inner fjord indicates that large amounts of sediment have been transported from these areas down into the fjord by sediment gravity flows (Syvitski, Burrell et al. 1987). The gullies occurring near the mouth of the Ranaelva and the tailings discharge points could possibly be from a combination of slides/slumps. This is shown by the areas directly above these gullies having accretion from possible nearby mass movements (Figure 20). These mass movements would have resulted in debris flow/turbidity currents due to the steep slopes and would have carried with them the majority of the sediment eroded (Tesaker 1978, Meiburg and Kneller 2010). These gullies would have then funneled the gravity flow down into the channel and the high amounts of erosion directly below them confirms this (Meiburg and Kneller 2010). The accretion also seen in these areas indicates that portions of the sediment load is being deposited as well. The erosion occurring farther out in the channel indicates that the gravity flows continue to flow out into the fjord basin most likely as a turbidity current (Pratson, Imran et al. 2000, Meiburg and Kneller 2010, Clarke 2016). The erosion occurring in the channel appears to be concentrated on its western sides which could be due to the Coriolis effect forcing the outflowing current to the right (Syvitski, Burrell et al. 1987). This would cause the erosion seen and could help account for the accretion towards the middle of the channel. The areas outside the main channel see relatively little change perhaps due to the channel being the main sediment transport pathway in the fjord.

6 Sediment Cores and Grabs

6.1 Sediment Cores

The 6 sediment cores used in this study were analysed in conjunction with Nikolai Figenschau and 4 of the same cores were used in his thesis (P1502-001, P1502-004, P1502-013, P1502-015) (Figenschau 2018). Much of the same data was used for both of these studies but the interpretation for each of the 6 cores provided here was made independently from his thesis.

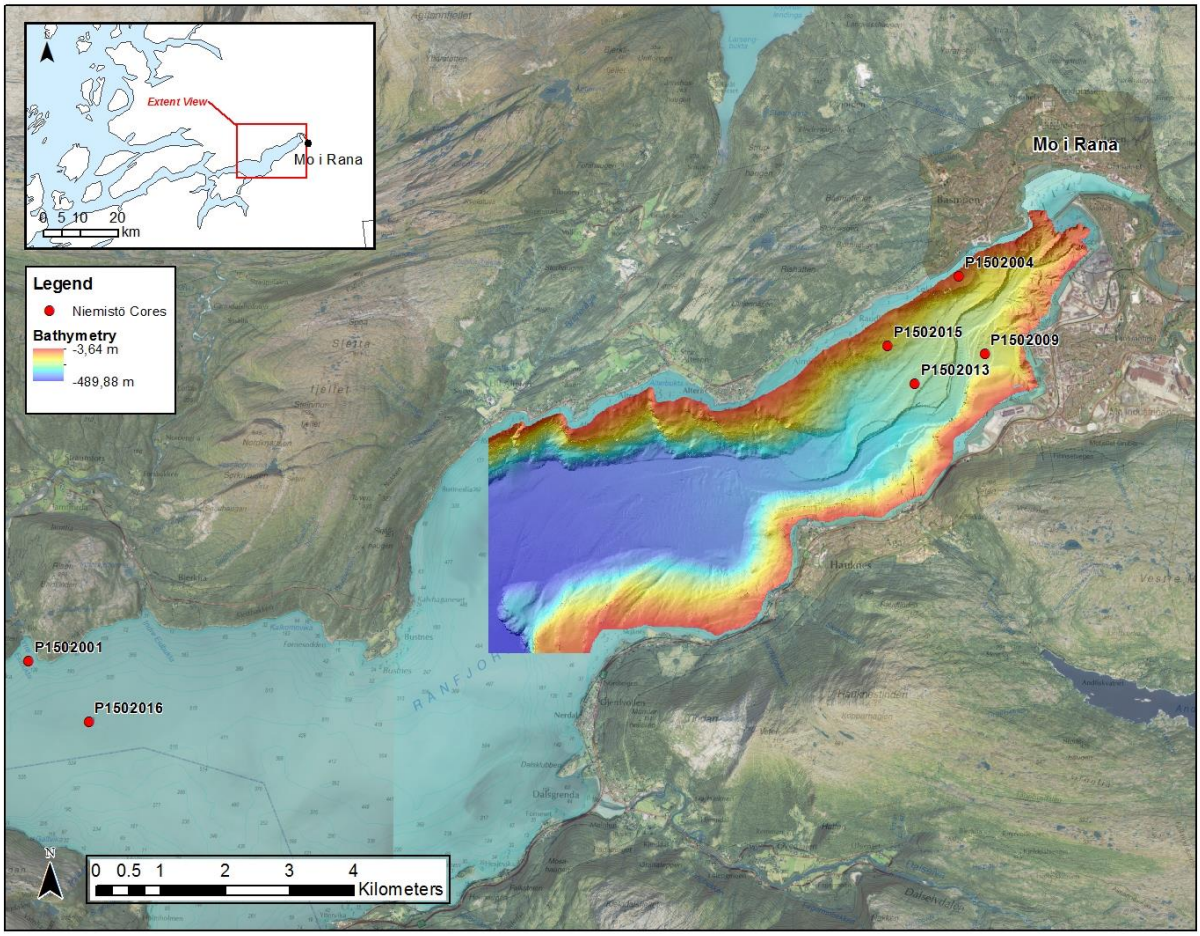

Figure 21. Niemistö core locations

6.1.1 Core P1502-001

Niemistö core P1502-001 was retrieved from the central part of Ranfjorden close to the northern shoreline approximately 17.3 km from the mine tailings point of deposition (Figure 21). Water depth at the core location was 100m and the core is 37 cm long. The core is divided into 3 units: P1502-001A, P1502-001B and P1502-001C (Figure 22).

6.1.1.1 Unit P1502-001A (37-25 cm)

Unit A consists of a uniformly gray color (5Y 4/1 MSCC) from 37-29 cm that becomes slightly more brown from 29-25cm. Very little internal structure is observed within the

unit. There are sporadic lenses of black sediment observed throughout the unit. The unit consists primarily of fine silt with a mean grainsize of approximately 10 µm for the entirety of the unit with very little fluctuation. The upper boundary is a gradual transition to unit B.

The one shear strength test performed in this unit shows an undrained shear strength (S_u) value of ~12 kPa and a remolded (S_r) value of ~2 kPa resulting in a sensitivity (S_u/S_r) of ~6. Magnetic susceptibility for the unit is relatively stable at ~25 10^{-5}SI with very few small changes. The XRF element ratio data shows that Fe and Si have an almost directly inverse relationship with several peaks and dips throughout the unit.

6.1.1.2 Unit P1502-001B (25-5 cm)

Unit B is a predominantly massive unit with a brown-gray color (5Y 4/2 MSCC) that shows some slight chaotic internal structure between 14-11 cm. Shell fragments are also observed. The unit consists primarily of fine to medium silt with a mean grainsize of ~10 µm at the base of the unit increasing gradually to ~17 µm towards the top. A gradual increase in the total percentage of sand is seen upward through the unit. Both the lower and upper boundaries are gradual.

The shear strength tests performed in this unit show a decrease in S_u and in sensitivity upward through the unit with a sensitivity of ~8 at 24 cm and ~4 from 19-8 cm. Very little change in S_r is seen.

Between 25-14 cm magnetic susceptibility decreases slightly from ~25 to ~10 10^{-5} SI. However a distinct spike occurs at 21 cm. From 12-5 cm the magnetic susceptibility increases gradually towards unit C with a spike at 8 cm and then increasing rapidly from ~15 10^{-5}SI to ~60 10^{-5} SI just below the boundary with unit C.

The XRF element ratio data for this unit is very similar to that in unit A with Fe and Si ratios having an almost direct inverse relationship. There are several spikes and dips for both Fe and Si throughout the unit with the largest interval for Fe and dip for Si occurring between ~15-11cm. Over the whole of the unit Fe and Si show a relatively stable trend with both having a similar value at the base of the unit as at the top.

6.1.1.3 Unit P1502-001C (5-0 cm)

Unit C is comprised of 3 different color zones with the bottom portion from 5-3 cm being a brown-gray color (5Y 4/2 MSCC) similar to unit B. From 3-2 cm the color abruptly changes to a gray color (5Y 4/1 MSCC) similar to that seen in unit A. The final 2 cm are a reddish brown color (2.5Y 3/2). Some lenses are seen in the lower layers along with some bioturbation in the upper portion of the unit. From 5-3 cm the unit is made up of mainly medium silt with mean grainsize staying relatively level at ~17 µm. From 3-1 cm the unit is composed of a more coarse silt with a mean grainsize of 30 µm. From 1-0 cm the unit is composed of more a more coarse silt/very fine sand mixture with the mean grainsize increasing to closer to 50 µm. The gradual increase in mean grainsize upward in the unit can be partially attributed to a gradual increase in the percentage of sand.

No shear strength tests were performed in this unit. Magnetic susceptibility is around ~50 10^{-5} SI from 5-3 cm before dipping to ~40 10^{-5} SI from 3-2cm. From 2-0cm the magnetic susceptibility increases steeply to closer to 90 10^{-5} SI. The XRF element sum-ratio data for Fe and Si again shows the same inverse relationship seen in the other units of the core. The ratios for both elements remain relatively stable for the unit with a peak for Si and a dip for Fe between 3-2 cm and again between 0.5-0 cm.

6.1.1.4 Interpretation

Core P1502-001 shows generally gradual changes in both its physical and geochemical properties upward throughout the core. These factors indicate that the sediments were likely deposited in in a more open marine environment with alternating natural sediment sources (Syvitski, Burrell et al. 1987). No sharp boundaries are seen between facies and very little structure is seen throughout the core. The chaotic structure seen in unit B from 14-11 cm could possibly be from a small mass-movement event that brought in more Si dominated sediment as shown by the XRF data. Shear strength values initially show an increase in S_u from unit A to B, coinciding as expected with a slight increase in sand content (Cabalar and Mustafa 2015). From ~24-17 cm the S_u value drops even as sand content increases, potentially due to having been reworked by the aforementioned episodic event (Perret, Locat et al. 1995). Grainsize increases subtly upward through the core with the color changing accordingly. The shift from a grayer to a more brown color correlates with the increasing percentage of sand at 25 cm. Magnetic susceptibility for the majority of the core is extremely low decreasing slightly as the percentage of sand increases towards the upper portion of the core. The upper 5 cm sees a shift to an even more sand dominated source potentially comprised of magnetite due to the higher magnetic susceptibility readings.

The low magnetic susceptibility and lower Fe/Sum values along with the stable Fe/Si relationship seen throughout the core, supports that the sediment sources were primarily natural, from similar sources and did not originate from mine tailings. Even though for the core as a whole, the Fe and Si/Sum values do not alter greatly, they do fluctuate rapidly and continuously through its entire length. This would indicate slight shifts between similar sources. Shell fragments and evidence of bioturbation at the top of the core further supports that the core is comprised of natural sediments though the final 5 cm with its higher magnetic susceptibility readings could indicate the presence of some mine tailings.

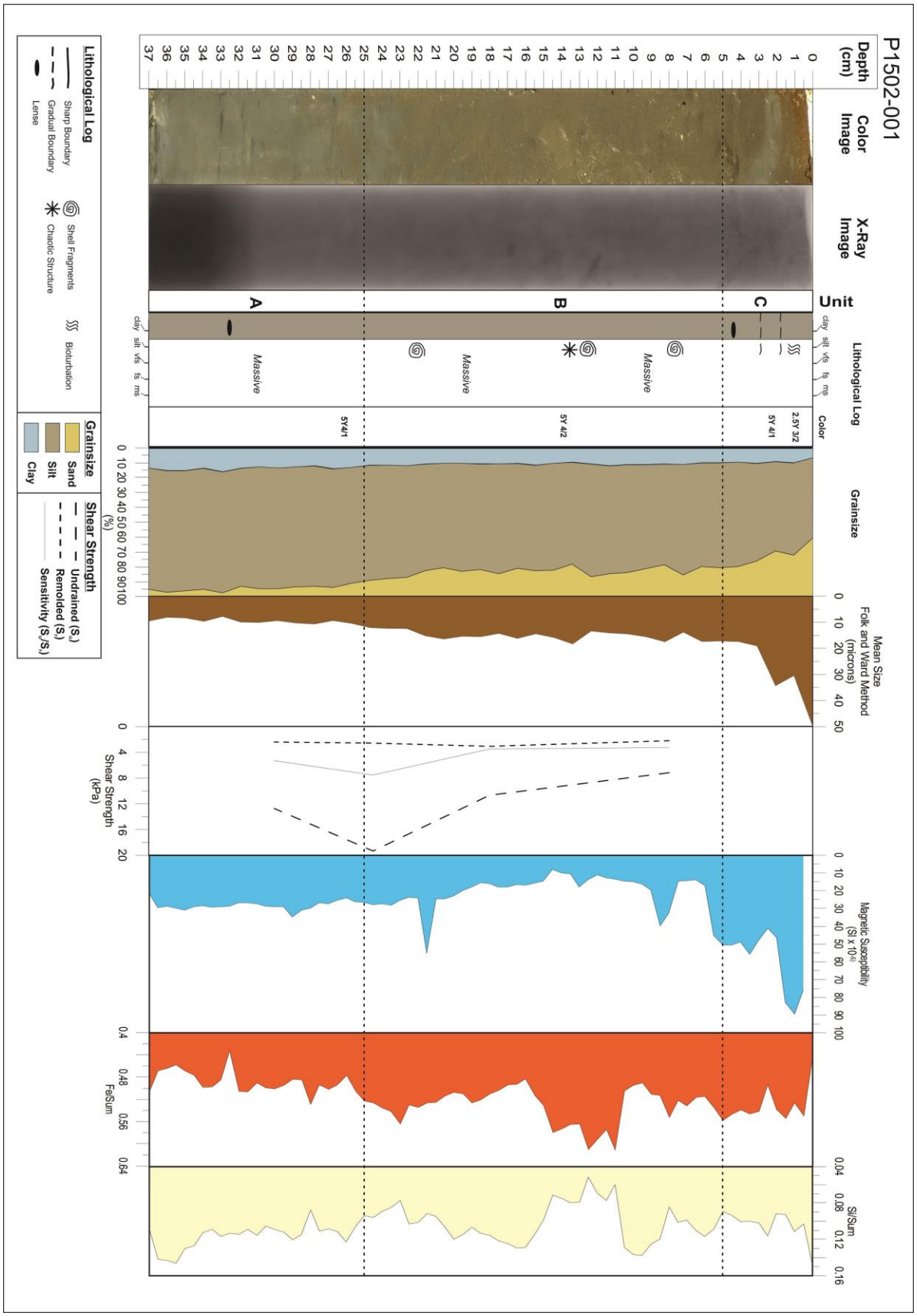

Figure 22. Core P1502-001 Analysis Results. .

6.1.2 Core P1502-016

Niemistö core P1502-016 was retrieved from the central portion of Ranfjorden approximately 16.9 km from the mine tailings point of deposition (Figure 21). Water depth at the core location was 520m and the core is 9.5cm long. The core is divided into 4 units: P1502-016A, P1502-016B, P1502-016C and P1502-016D (Figure 23).

6.1.2.1 Unit P1502-016A (9.5-9cm)

Unit A is a darker red color (10YR 3/2 MSCC). The lithological log shows that the unit consists mainly of sandy silt coarsening slightly upward with no observed structure until it is truncated at the upper portion by a coarser sandy unit. This boundary is sharp and curved in shape. No grainsize analysis or shear strength tests were obtained for this unit.

Magnetic susceptibility is low for this unit but gradually increases upward. The XRF element sum ratios for Fe and Si are relatively low with both increase upward through the unit.

6.1.2.2 Unit P1502-16B (9.5-6cm)

Unit B is gray color (2.5YR 3/2 MSCC). It has a curved shape with some darker layering within. The majority of the layer consists of very fine sand and coarse silt with the mean grainsize increasing steeply from 40 µm to 70 µm toward the middle before decreasing toward the upper portion of the unit. The upper boundary of the unit is an abrupt transition to a silt layer. This boundary is similar to the lower boundary with having a deformed curved shape.

Shear strength tests were performed in this layer but due to a high sand content, the results were determined to be unreliable (compared with (Hansbo 1957)) and therefore not used in the later discussions. Magnetic susceptibility mirrors the steep increase in grainsize toward the middle of the unit and also drops towards the upper portion from a peak of near ~2000 10^{-5}SI. The XRF element ratios for Fe and Si in this unit fluctuate only slightly and there is a slight inverse relationship between the two. The Si ratio increases slightly as the mean grainsize and magnetic susceptibility increase. The Fe ratio drops slightly with these increases and rises as they decrease. The trend for both Fe and Si are very smooth without large changes or fluctuations through the unit.

6.1.2.3 Unit P1502-16C (6-2.5cm)

Unit C has a darker reddish color (10YR 3/2 MSCC) that is dominant throughout the unit and is very similar to Unit A. The lower boundary is an abrupt shift from a sandier lower layer to a more massive sandy silt layer. From 6 cm to 5.5 cm, the mean grainsize decreases quickly from 50 µm to approximately 30 µm and remains there throughout the rest of the unit.

Shear strength tests were performed here but due to the sand content the results were found to be unreliable and not taken into consideration (compare with (Hansbo 1957)). Magnetic susceptibility follows the same decreasing trend as the mean grainsize from 6 cm to 5.5 cm and stays relatively stable at around 500 10^{-5}SI for the rest of the unit. The element ratio for Fe follows a very slight inverse trend compared to mean grainsize and

magnetic susceptibility. Both Fe and Si show generally very little change throughout the unit.

6.1.2.4 Unit P1502-16D (2.5-0cm)

Unit D is very similar to unit B with a gray color (2.5YR 3/2 MSCC) but with no internal structure. The layer primarily consists of very fine sand and silt with the mean grainsize increasing steeply from approximately 25 µm at 2.0 cm to nearly 70 µm at 0.5 cm. The lower boundary is an abrupt shift from the lower red silt layer. This boundary is irregular with tendrils of the upper sandy layer extending downward into the lower silt layer and vice versa. The upper portion of the unit from 0.5 to 0 cm sees a shift to a darker reddish color (10YR 3/2 MSCC) and a higher silt content.

Shear strength tests were again performed here but due to the high sand content in the unit were not considered reliable (compare with (Hansbo 1957)). Magnetic susceptibility increases steeply upward through the unit with a peak close to approximately 2000 10^{-5}SI at 1 cm, before it decreases toward the end of the unit and top of the core. This mirrors the trend seen with the mean grainsize. The XRF element ratio data shows a slight inverse relationship between Fe and Si but with very little change throughout the unit.

6.1.2.5 Interpretation

The physical properties of core P1502-016 show two types of deposits that are distinctly different from each other. Two very different depositional environments are shown by the one type consisting of gray sand and the other consisting of reddish silt. A probable explanation is that the sediments have been transported and deposited by two successive mass-transport events with units B and D being at their bases (Syvitski, Burrell et al. 1987). This is supported by units B and D both consisting mostly of fine sand while units A and B mostly of silt. In addition, the boundaries between all the units are sharp with the boundary between C and D showing distinct load casts. A distinct color change is also seen between the units, shifting from a dark red in units A and C to a gray in B and D. Since the deposits in units B and D are reasonably well-sorted, consist of fine sand and above them there is a general fining upward, they are most likely distal turbidites (Pickering, Stow et al. 1986, Pratson, Imran et al. 2000, Collinson, Mountney et al. 2006).

The sharp deformed boundaries above and below units B and D indicate that these units were deposited rapidly and their coarser grainsize correlate with a higher energy depositional environment seen in mass-transport events. The deformed boundary between units C and D with tendrils of sandier unit D sediment extending down into the more silty unit C are consistent with load casts (Collinson, Mountney et al. 2006). This also supports them having been rapidly deposited by conditions seen in turbidity currents (Collinson, Mountney et al. 2006).

Units A and C both consist of red, fine to medium silt and could have been deposited by a combination of the turbidity currents finer fraction dropping out of suspension and other

finer sediments settling after being transported by other currents in the fjord. Almost no clay is seen in the core which also supports a higher energy depositional environment.

The origin of the large majority of the sediment in the core is most likely from the mine tailings due to the successive red colors observed and the very high magnetic susceptibility values seen throughout the core. A minimum of ~400 10^{-5}SI is seen at 2.5 cm while the more natural sediments seen in core P1502-001 never go above ~90 10^{-5}SI. The peaks in magnetic susceptibility and the gray color seen in units B and D are most likely due to a concentration of magnetite. Fe values do not alter greatly with the increase in magnetic susceptibility, which can support that magnetite is being concentrated in units B and D. This is due to only a slight increase in highly magnetic magnetite would have a large increase in magnetic susceptibility readings. The magnetite sediments also seem to be a coarser grainsize relative to other tailings sediments since their location in the core corresponds to where the sediments were deposited from higher energy transport mechanisms.

The relative lack of any large shifts or changes in the XRF data throughout the core indicates that the sediments very likely all came from a similar source. The high Fe readings along with the high magnetic susceptibility values support the source being mine tailings.

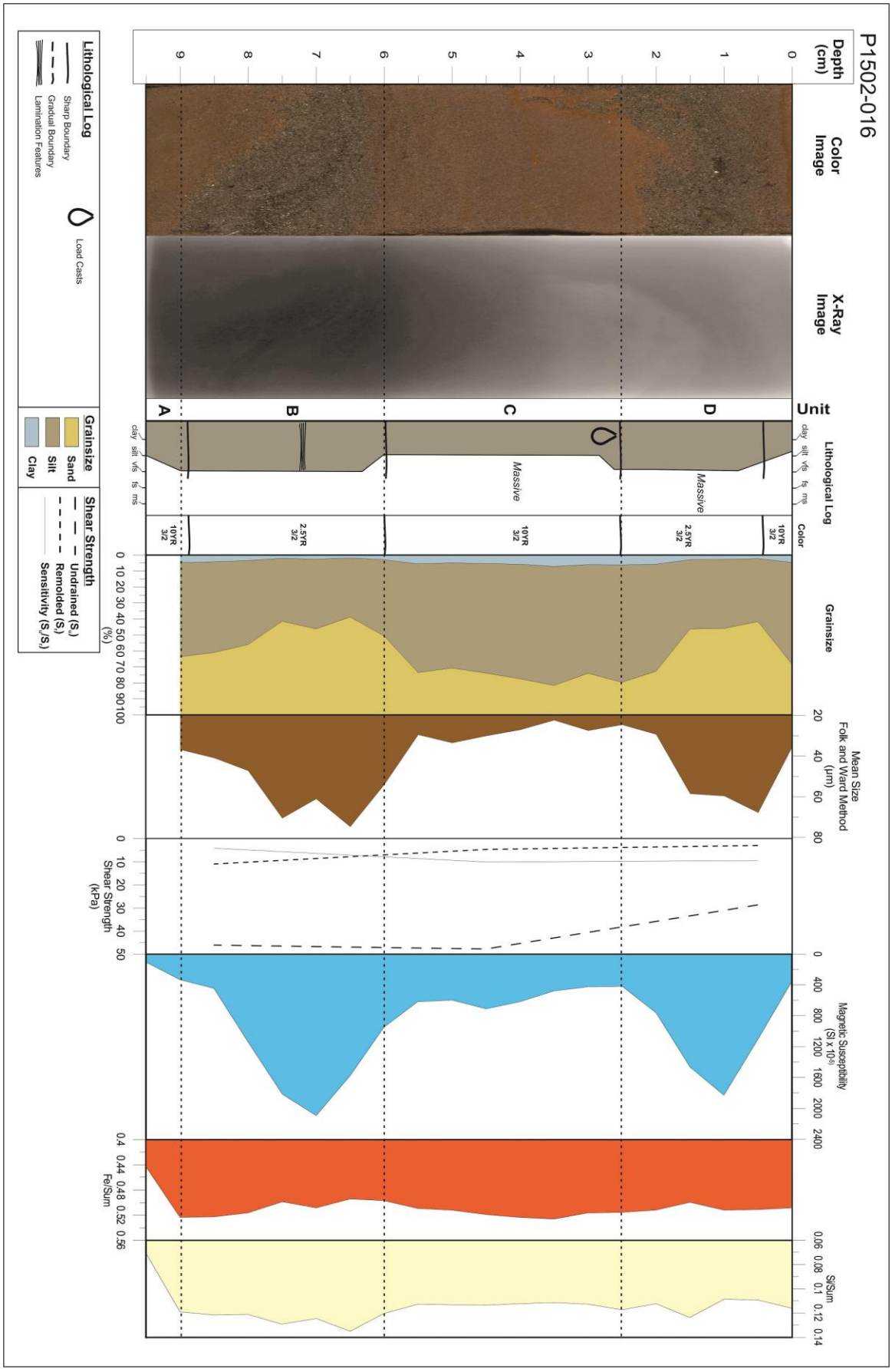

Figure 23. Core P1502-016 Analysis Results

6.1.3 Core P1502-013

Niemistö core P1502-013 was retrieved from the center of the inner portion of Ranfjorden approximately 3.4 km from the mine tailings point of deposition (Figure 21). Water depth at the core location was 282 m and the core is 39 cm long. The core is divided into 4 units: P1502-013A, P1502-013B, P1502-013C and P1502-013D (Figure 24).

6.1.3.1 Unit P1502-013A (39-29 cm)

Unit A is a brownish black (7.5YR 3/2 MSCC) colored massive medium silt layer with a gradual upper border. Mean grainsize fluctuates slightly up through the unit with variations in sand input. The mean grainsize increases slightly upward through the unit with undrained shear strength (S_u) decreasing upcore.

Magnetic susceptibility is relatively low and gradually increases up through the unit with a slight dip at 30 cm. The Fe/Sum values closely following the same trend. The Si/Sum values follow a nearly inverse relationship to magnetic susceptibility and Fe/Sum and shows a slight decrease through the unit. Fe and Si values show fluctuating values up through the core.

6.1.3.2 Unit P1502-013B (29-19 cm)

Unit B is made up of alternating layers of dark (10YR 3/2 MSCC) and darker brownish black (10YR 3/1 MSCC) medium silt with some thin, darker lamination structures. Mean grainsize fluctuates greatly from 29-22 cm with each darker lamination, corresponding to an increase in the percentage sand. An increase in Si/Sum values occurs at each lamination and with the Fe/Sum values following an inverse trend. Magnetic susceptibility follows a slightly similar trend to the mean grainsize, fluctuating between ~400 10^{-5}SI at the lower mean grainsize and ~600 10^{-5}SI at the points of higher mean grainsize. Fe and Si/Sum values fluctuate continuously up through the core.

From 22-19 cm the mean grainsize decreases slightly. A darker laminate layer at 20 cm corresponds to a steep spike in magnetic susceptibility and a decrease in mean grainsize. A slight increase in Fe/Sum values is seen at the same time. The upper boundary is sharp with the conclusion of the darker laminate layer. Undrained shear strength (S_u) for the unit is much lower than in unit A overall but shows a gradual increase upward through the unit.

6.1.3.3 Unit P1502-13C (19-12.5 cm)

Unit C is composed of dark brown (10YR 3/2 MSCC) massive medium to fine sandy silt with almost no internal structure. The mean grainsize overall decreases up through the unit with some fluctuations. Each increase in percentage sand correlates to an increase in the Si/Sum values and a decrease in the Fe/Sum values. Magnetic susceptibility and Fe/Sum values increase upward through the unit as mean grainsize decreases. Shear strength values vary little from the lower unit and continue to stay low.

6.1.3.4 Unit P1502-013D (12.5-0 cm)

Unit C consists of dark brown (10YR 3/2 MSCC) massive fine silt with little internal structure. The color is a slightly darker brown from 12.5 to 5 cm. The mean grainsize gradually decreases upward through the unit with a slight percent increase in silt and a decrease in sand. From 12.5-5 cm magnetic susceptibility increases and stays relatively high, Fe/Sum values also hold relatively high while Si/Sum values are low over this length. From 4-0 cm magnetic susceptibility and Fe/Sum values decrease rapidly while Si/Sum values increase.

Undrained shear strength (S_u) generally decreases over the length of the unit with the remolded shear strength (S_r) staying very low for the whole unit.

6.1.3.5 Interpretation

The whole length of core P1502-013 displays a continuously shifting depositional environment with altering sediment sources. The dominant red coloration throughout the core and the relatively high magnetic susceptibility and Fe/Sum values indicate that the predominant sediment type throughout the core is likely mine tailing derived. The mean grainsize generally decreasing and the Fe/Sum values increasing up through the core show a continuous trend towards more mine tailings dominated sources. Units A, C and D due to their massive structure were most likely deposited by low energy suspension fallout from a more continuous source.

The several brief abrupt increases in mean grainsize that correspond to the darker laminations between 29-22 cm indicate brief shifts in the depositional environment and sediment source. These color changes also correspond with increases in magnetic susceptibility. Since these laminations are relatively thin, predominantly fine grained and not continuous indicates that they were likely deposited during short pulse events due possibly to brief, strong seasonal discharges or other episodic event (Syvitski, Burrell et al. 1987, Collinson, Mountney et al. 2006). A heavy seasonal fluvial runoff or the overflow of the channel from a nearby mass-movement event could all be causes (Pickering, Stow et al. 1986, Syvitski, Burrell et al. 1987). The high magnetic susceptibility and dark color with no spike in Fe/Sum values could indicate these laminations contain higher levels of magnetite. The darker brown sediment seen from 12.5 to 5 cm corresponding to higher magnetic susceptibility and Fe/Sum values could also be related to higher magnetite levels within that section.

The upper portion of the core from 4-0 cm sees a sharp increase in the Si/Sum values and a slight increase in the silt percentage as there is a sharp decrease in magnetic susceptibility and Fe/Sum values. This would indicate an alternate source consisting of more Si rich silt gradually beginning to become more dominant.

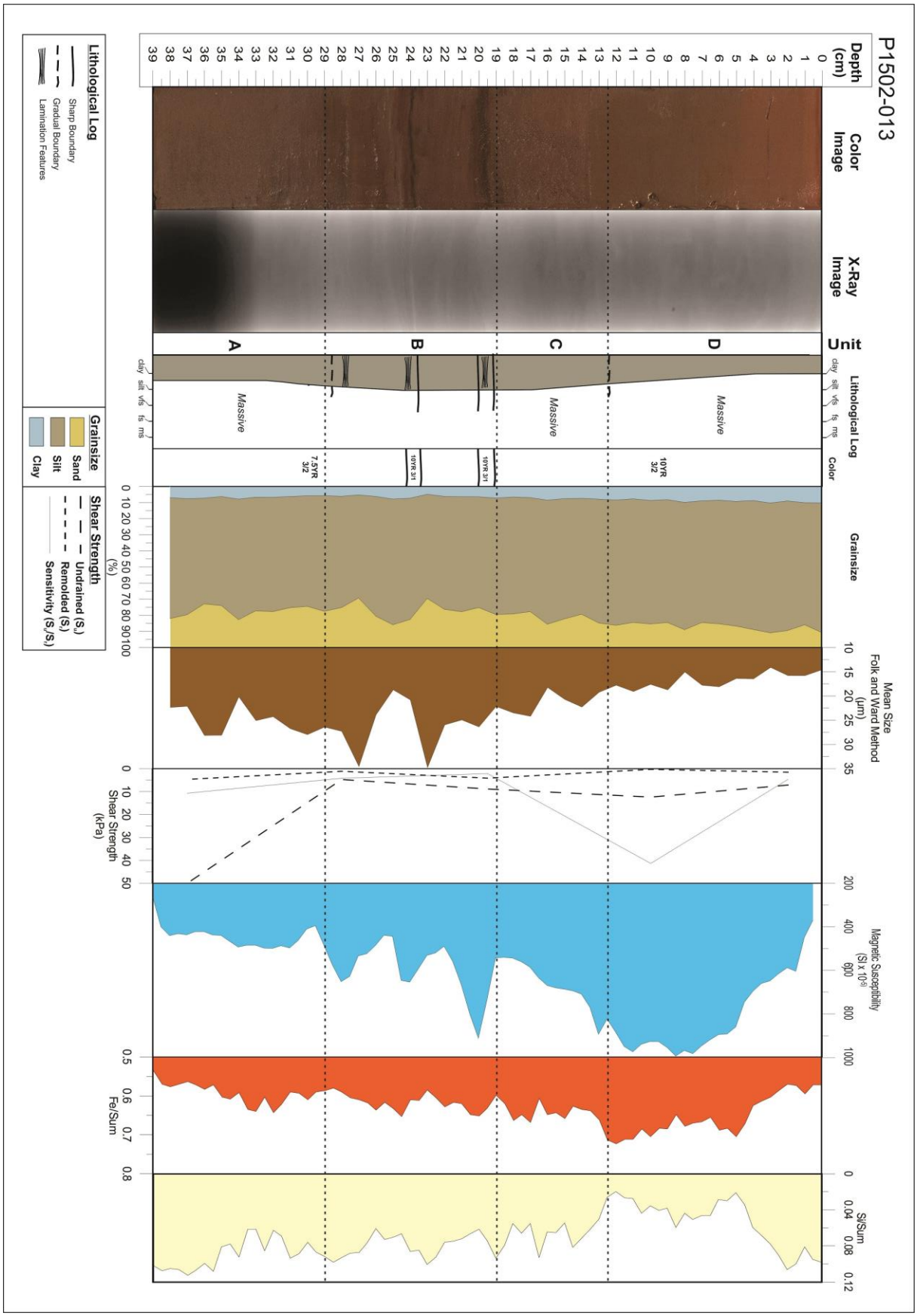

Figure 24. Core P1502-013 Analysis Results

6.1.4 Core P1502-015

Niemistö core P1502-015 was retrieved from inner Ranfjorden close to the northern shoreline approximately 3.2 km from the mine tailings point of deposition (Figure 21). Water depth at the core location was 180 m and the core is 35 cm long. The core is divided into 3 units: P1502-015A, P1502-015B and P1502-015C (Figure 25).

6.1.4.1 Unit P1502-015A (35-17.5 cm)

Unit A is a reddish gray color (2.5YR 4/1 MSCC) and consists of massive medium to fine silt with no internal structure and a gradual upper border. Some red fine-grained clasts are seen from 33-29 cm. The mean grainsize remains relatively steady at ~18 µm from ~34-20 cm before fluctuating to a high of ~22 µm and ending at ~14 µm at 17.5 cm. The magnetic susceptibility values are very low between 35-20 cm before rapidly increasing from 20-17.5 cm. The XRF element ratio data shows a direct inverse relationship between Fe and Si with Fe/Sum values increasing from 34-32cm and Si/Sum values dropping. For the rest of the unit Fe and Si/Sum values fluctuate continuously but hold a mostly stable trend with Fe slightly increasing and Si decreasing.

6.1.4.2 Unit P1502-015B (17.5-9.5 cm)

Unit B consists of dark brown(10YR 3/2 MSCC) massive medium to fine silt and gradual upper and lower boundaries. Some slight streaks of fine black sediment are seen along with a larger lighter colored lense of finer sediment at ~12cm. The mean grainsize has an initial spike at ~16 cm before gradually decreasing up through the rest of the unit as the percentage silt increases slightly and the sand percentage decreases. The undrained shear strength (S_u) of ~11 kPa at ~17.5cm increases to ~16 kPa at ~15 cm following the spike in mean grainsize. The S_u then gradually decreases upward through the unit.

Magnetic susceptibility progressively increases upwards throughout the unit. Fe/Sum and Si/Sum values again have an largely inverse relationship with Fe/Sum values increasing slightly up through the unit and Si/Sum slightly decreasing. Slight fluctuations in values are seen in both elements up throughout the unit.

6.1.4.3 Unit P1502-015C (9.5-0 cm)

Unit C is comprised of a brownish black (7.5YR 3/2 MSCC) massive fine silt with no internal structure and a gradual lower boundary. Mean grainsize is relatively stable for the length of the unit with only a few slight variations related to changes in the percentage sand. The undrained shear strength (S_u) for the lower portion from the bottom portion of the unit shows a value lower than that measured in unit B.

Magnetic susceptibility increases steadily up through the unit until ~4 cm where it reaches a core high of ~800 10^{-5}SI. From 4-0 cm it drops to ~350 10^{-5}SI. Fe/Sum and Si/Sum values again have an inverse relationship with Fe gradually decreasing through the unit and Si increasing.

6.1.4.4 Interpretation

Core P1502-015 shows a clear shift in the sediment sources up through its core while the transport method that deposited them seems constant. The dramatic color change from the lighter-gray medium silt to the darker-brown fine silt is a clear indication of a change in origin for the sediments. Other changes in physical and geochemical characteristics indicate the dominant sediment source shifted from a more natural to a more mine tailings dominated origin. From 35-19 cm the core resembles the more natural sediments seen in core P1502-001 with low magnetic susceptibility, lower Fe/Sum values and more dominated by medium-grained silt. From 19-9.5 cm there is a gradual transition with mixing between the sources as indicated by the steadily increasing magnetic susceptibility and Fe/Sum values and the decreasing mean grainsize. From 9.5-4.5 cm the high magnetic susceptibility and Fe/Sum values indicate the sediments are dominated by mine tailing. The last 4 cm of the core show a large decrease in magnetic susceptibility, which could be attributed to testing error since the Fe/Sum values remain stable and the color does not change.

Each boundary transition is gradual and the sediment is fine grained with almost no internal structure indicating that the depositional environment throughout the core was low energy without any large changes, as seen with slow suspension fallout (Syvitski, Burrell et al. 1987, Collinson, Mountney et al. 2006).

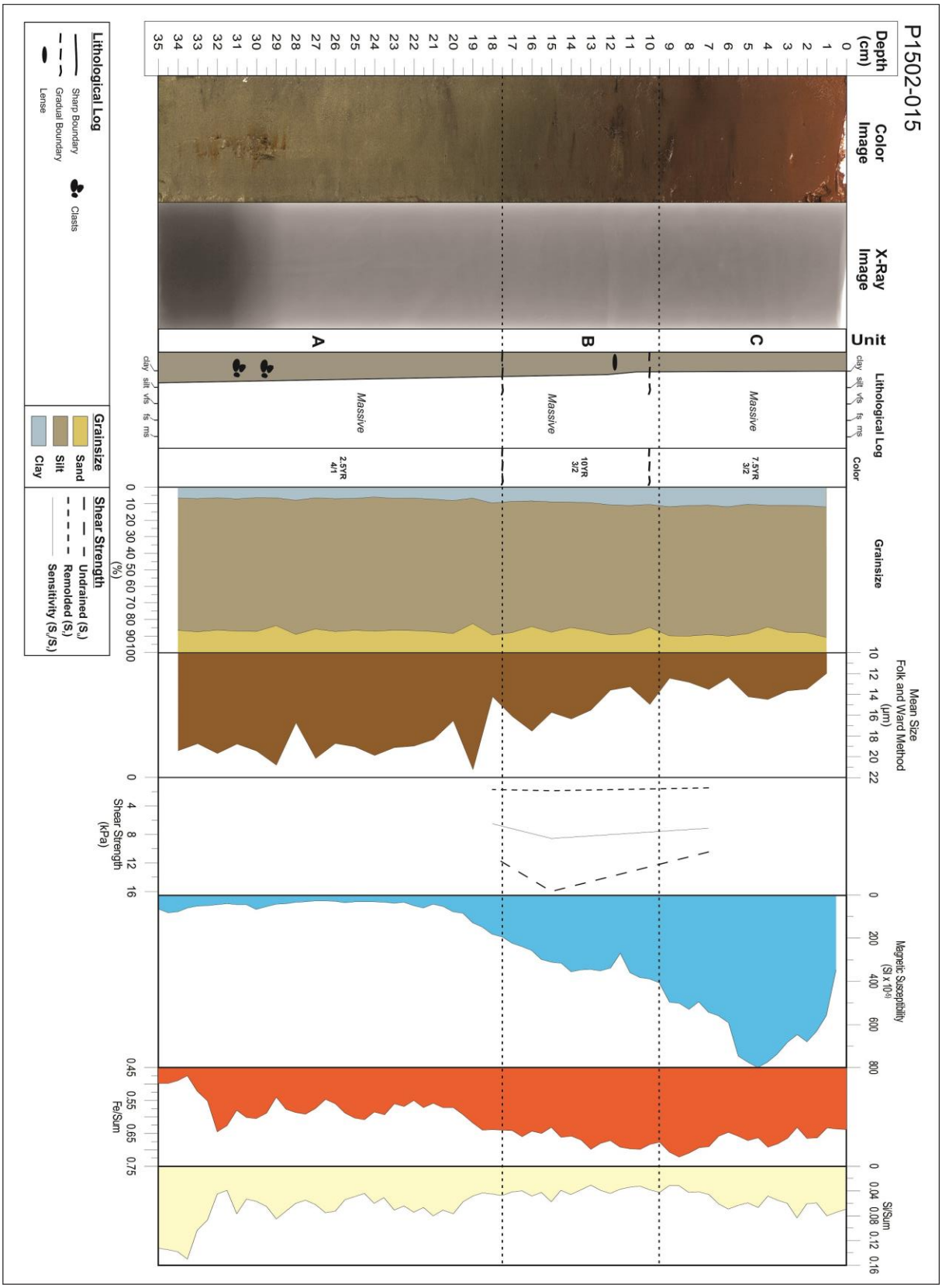

Figure 25. Core P1502-015 Analysis Results

6.1.5 Core P1502-009

Niemistö core P1502-009 was retrieved from the inner portion of Ranfjorden close to the southern shoreline approximately 2.4 km from the mine tailings point of deposition (Figure 21). Water depth at the core location was 230m and the core is 19 cm long. The core is divided into 3 units: P1502-009A, P1502-009B and P1502-009C (Figure 26).

6.1.5.1 Unit P1502-009A (19-17 cm)

Unit A consists of brownish black (7.5YR 3/2 MSCC) massive sandy silt with no internal structure and a sharp upper boundary. Grainsize does not change much through the unit and no shear strength tests were completed.

Magnetic susceptibility shows an increase to ~400 10^{-5}SI that holds for the majority of the unit. The XRF element sum-ratio data for Fe shows a slight decrease to ~0.54 for the unit. Si/Sum data has several fluctuations with the majority of the unit showing values of ~0.1 to ~0.09 near the upper boundary. Both Fe and Se have a generally inverse relationship.

6.1.5.2 Unit P1502-009B (17-12 cm)

Unit B consists of predominantly gray (2.5YR 3/2 MSCC) partly sorted silty sand with little internal structure. The upper and lower boundaries are relatively abrupt with slightly irregular transitions between the darker silt layers above and below. Some dark clasts and shell fragments are seen within the unit. From 17 cm the mean grainsize increases due to the sand percentage increasing abruptly to over 65 µm at ~14 cm and then decreasing rapidly to ~30 µm at 12 cm. Due to the higher sand content shear strength readings were not found to be reliable (Hansbo 1957) and not used later in the discussions.

Magnetic susceptibility values drop between 17 and 15 cm before rapidly peaking alongside mean grainsize and percentage sand at ~14 cm. From 14-12 cm the magnetic susceptibility drops from a high of ~1400 10^{-5}SI to ~750 10^{-5}SI before increasing gradually to the end of the unit. The XRF element sum-ratio data for Fe shows it following a similar trend to magnetic susceptibility from 17-14 cm but instead of spiking between 14-12 cm it gradually continues increases up to 12 cm. Si/Sum values follow an almost exact inverse trend to Fe/Sum for the entirety of the unit. Both elements show very little fluctuations up through the unit.

6.1.5.3 Unit P1502-009C (12-0 cm)

Unit C consists of predominantly massive silt that shifts from a darker brown (7.5YR 3/2 MSCC) to a more reddish brown (5YR 3/2 MSCC) color as the sand content decreases up through the unit. There is no structure in the unit and the lower boundary is somewhat irregular but generally showing a sharp transition from a gray to a brown color. Undrained shear strength (S_u) values show a decreasing trend upward through the unit that mirrors the decrease in the mean grainsize.

Magnetic susceptibility gradually decreases throughout the whole unit and closely mirrors the trend shown by the mean grainsize. The XRF element sum ratio data shows

Fe and Si having the same inverse relationship seen in the lower units. Fe values initially increase but decrease from ~10 cm to ~1cm before gradually increasing the last cm of the core.

6.1.5.4 Interpretation

The sediments displayed in core P1502-009 clearly show an abrupt change between two very different depositional environments. While units A and C show many similarities in color, mean grainsize and Fe/Sum values, unit B differs in all these characteristics indicating that it was very likely deposited by a more abrupt episodic deposition event from an alternate source. The higher, stable Fe/Sum values in units A and C indicate that they are dominated by mine tailings sediments as described in P1502-015C and their massive structure show they were deposited in a more calm and constant environment (Collinson, Mountney et al. 2006). Unit B has a sharper upper and lower border with a large increase in the percentage sand indicating it was very likely deposited by an episodic gravity flow event. Since the unit is predominantly sand and has no real internal structure and fines slightly upward, it has most likely been deposited by a turbidity current/surge (Pratson, Imran et al. 2000, Collinson, Mountney et al. 2006). Initially in unit B from 17-15 cm, the magnetic susceptibility and Fe/Sum values drop and Si/Sum values rise indicating a shift from mine tailings sediments to more natural sediments. Shell fragments seen here also support this. Due to the close proximity to the mouth of the Ranaelva River (and the submarine channel), a surge of sediment from the river could be a potential source. From 15-14 cm there is sharp increase in magnetic susceptibility coinciding with the few clasts seen, indicating a potentially greater composition of magnetite. This could show a mixing of more mine tailings sediments into the turbidity current. Fe/Sum values from 15-12 cm gradually increase indicating a mixing upward of natural and mine tailing sediments. The final 12 cm of the core show a gradual transition back to mine tailings dominated sediments as the sand content and mean grainsize drops.

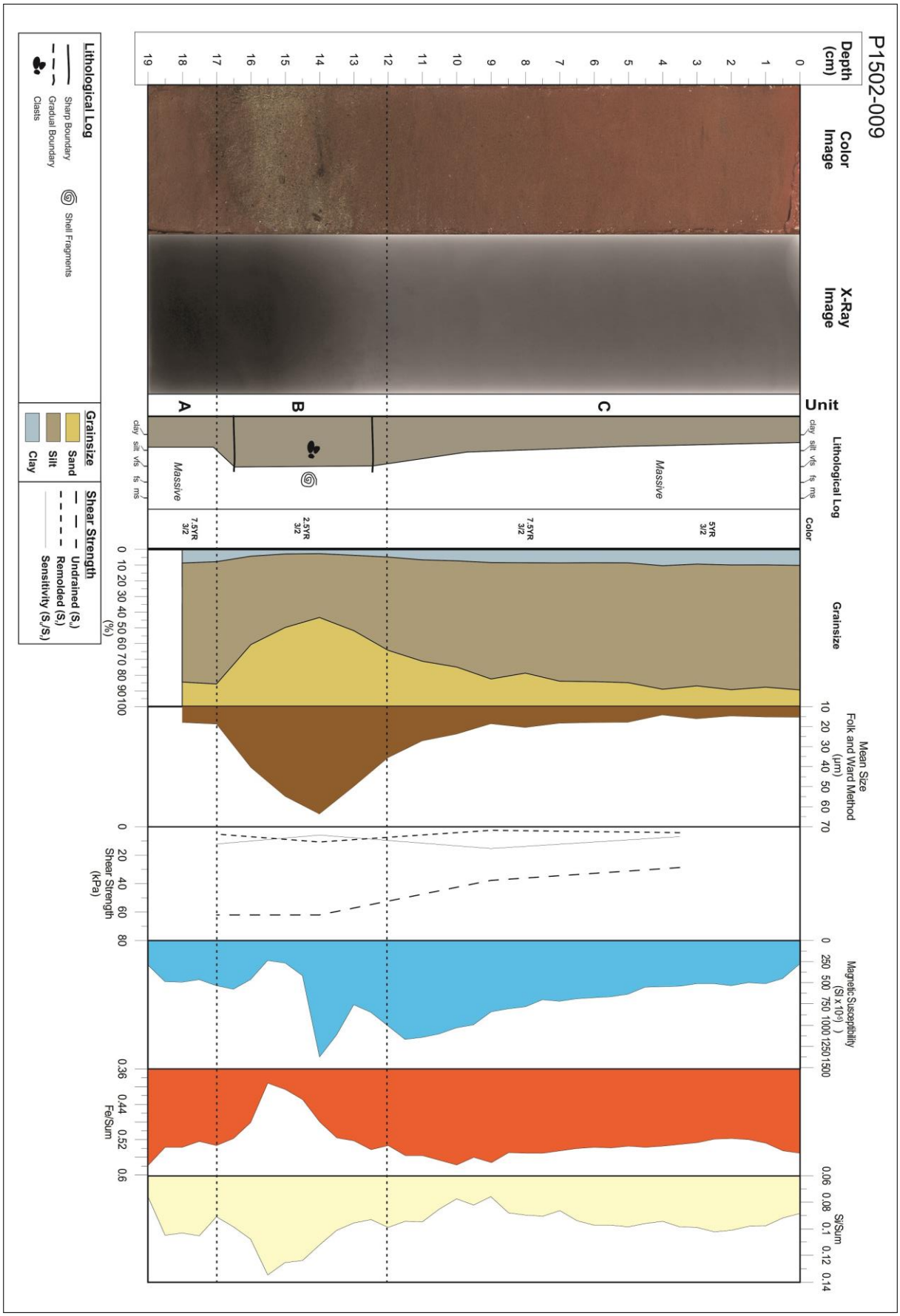

Figure 26. Core P1502-009 Analysis Results

6.1.6 Core P1502-004

Niemistö core P1502-004 was retrieved from the inner portion of Ranfjorden close to the northern shoreline approximately 1.7 km from the mine tailings point of deposition (Figure 21). Water depth at the core location was 65m and the core is 24 cm long. The core is divided into 3 units: P1502-004A, P1502-004B and P1502-004C (Figure 27).

6.1.6.1 Unit P1502-004A (24-15 cm)

The lower part of unit A from 24 to 21 cm is made up of gray (5Y4/1 MSCC) medium sandy silt transitioning upward to darker reddish-gray (2.5YR 3/2 MSCC) massive sandy medium silt from 21 to 15 cm. This lower portion from 24-21 cm resembles the color and other physical and geochemical characteristics seen in the more natural sediments of core P1502-001. Sporadic lenses of red and black sediment become more prominent from 19-15 cm. Grainsize fluctuates slightly from 24-17 cm between ~20-28 µm before dropping to between ~18-22 µm from 17-15 cm. Shear strength values for S_u also decrease from 24-15 cm following the drop in grainsize.

Magnetic susceptibility has one slight fluctuation from 23.5-17 cm before increasing from 17-15 cm. This upward trend inversely follows the trend seen for grainsize. The XRF element ratio data shows an inverse relationship between the Fe and Si sum ratios with several fluctuations up through the unit. From 24-21 cm Si sees a general decrease from ~0.15 to ~0.04 while Fe increases from ~0.45 to ~0.65. For the rest of the unit the two element ratios remain relatively stable and close to these values. Any following increase or decrease in an element results in a decrease or increase in the other.

6.1.6.2 Unit P1502-004B (15-6 cm)

Unit B is made up of dark brown (7.5YR 3/2 MSCC) massive medium to fine silt. Some black lenses of sediment are seen from 15-12 cm shifting to darker and lighter interspersed red layers from 12-6 cm. No internal structure is seen with gradual borders between the upper and lower units. Mean grainsize shows a slight decrease upward through the unit from ~20 µm at 15 cm to ~15 µm at 6 cm with a dip at 10 cm and a peak at 7 cm. Shear strength values for S_u follow the same decreasing trend upward through the unit as seen with grainsize.

Magnetic susceptibility increases abruptly from ~300 10^{-5}SI to ~700 10^{-5}SI between 15-14cm. From 14-6 cm it gradually increases to ~750 10^{-5}SI with a small peak at 7 cm. The XRF element ratio data for Fe sum shows that it follows the same increasing trend as magnetic susceptibility. The sum ratio for Si is relatively stable with a slight decreasing trend. Both elements show fluctuating values up through the unit.

6.1.6.3 Unit P1502-004C (6-0 cm)

Unit C consists of dark reddish-brown (5YR 3/2 MSCC) massive fine silt with the final 2 cm of the unit becoming a slightly lighter red color. No structure is seen in the unit and it has a gradual lower boundary. Mean grainsize stays stable at close to ~15 µm for the

majority of the unit with a drop to ~13 µm at 2-0 cm. Shear strength values for S_u follow the same decreasing trend as seen in unit B.

Magnetic susceptibility increases steeply from 6-3 cm to a high of ~1500 10^{-5}SI before dropping slightly from 3-0 cm. The XRF element sum ratio data for Fe shows a slightly decreasing trend and an increasing trend for Si throughout the unit, with very few small fluctuations for both elements throughout the unit.

6.1.6.4 Interpretation

Core P1502-004 shares many of the same characteristics seen in core P1502-015. It shows a clear gradual transitional change in color from gray to red upward through its length indicating a shift between two different sediment sources. The overall lack of structure and gradual boundaries indicate that the sediments were deposited by a more gradual, lower energy sedimentation process (Collinson, Mountney et al. 2006). The lower portion of the core below 21 cm appears to be a more natural sediment as described in core unit P1502-001A due to the lower Fe and higher Si sum values and the low magnetic susceptibility. The upper 6 cm of the core most likely originated predominantly from mine tailings as seen in core unit P1502-015C due to the increased Fe/Sum values, large increase in magnetic susceptibility and decrease in mean grainsize. This shift begins as early as 22cm and is evident by the sudden increase in the Fe/Sum and decrease in the Si/Sum ratios. The zone between 22-15 cm appears to be an early transition zone with considerable mixing between the natural and tailings sediments since the mean grainsize fluctuates but overall holds constant, as does the magnetic susceptibility. At 15 cm there is a sharp increase in magnetic susceptibility indicating a transition to more tailings dominated sediments that continues to 6 cm. From 6-0 cm the sediments are tailings dominated as mentioned earlier.

Undrained shear strength (S_u) decreases upward through the core as the sediment becomes more tailings dominated and the mean grainsize decreases. This would indicate that the tailing sediments are more prone to mass-movements when compared to the natural sediments in the fjord.

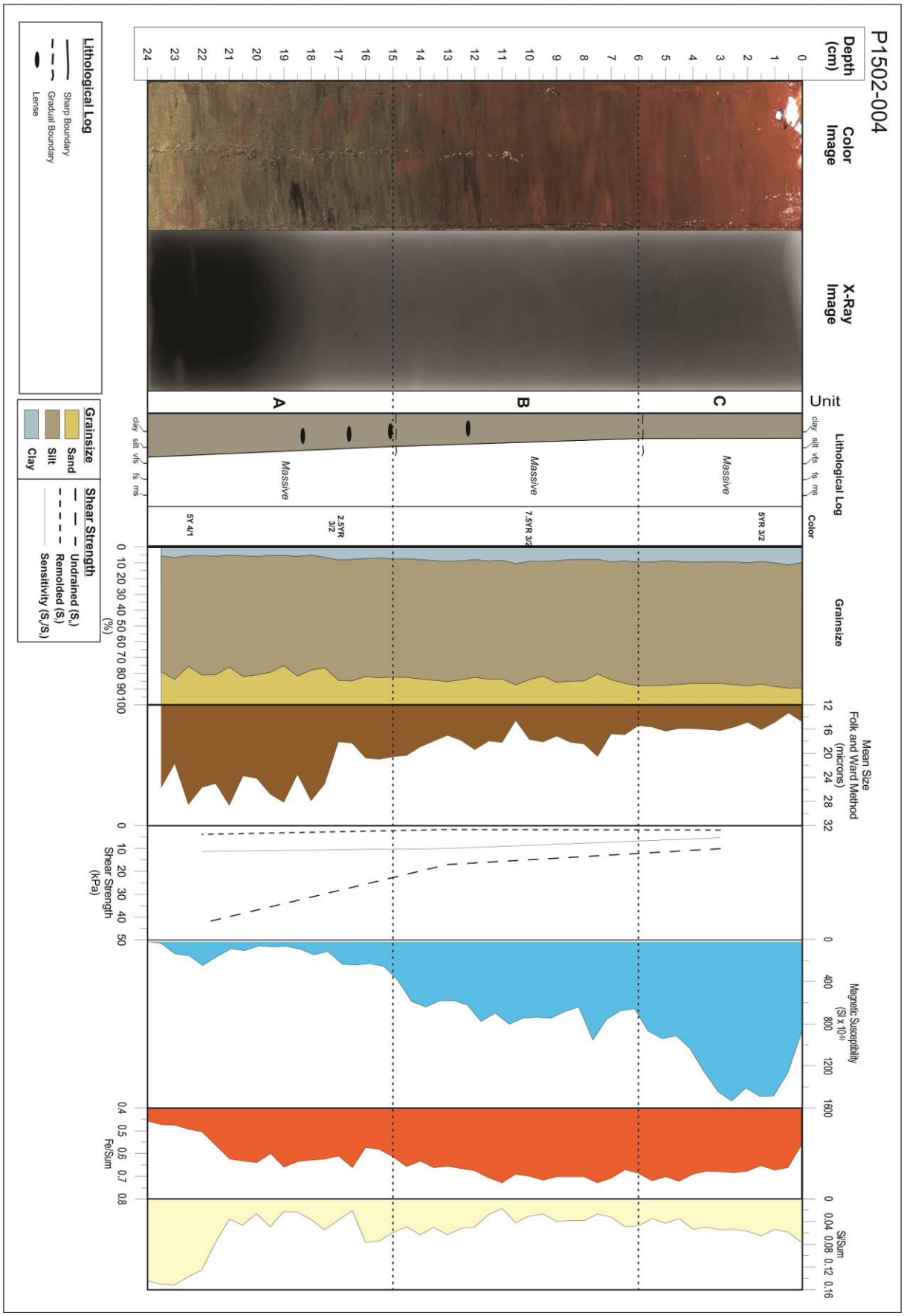

Figure 27. Core P1502-004 Analysis Results

6.2 Sediment Grabs

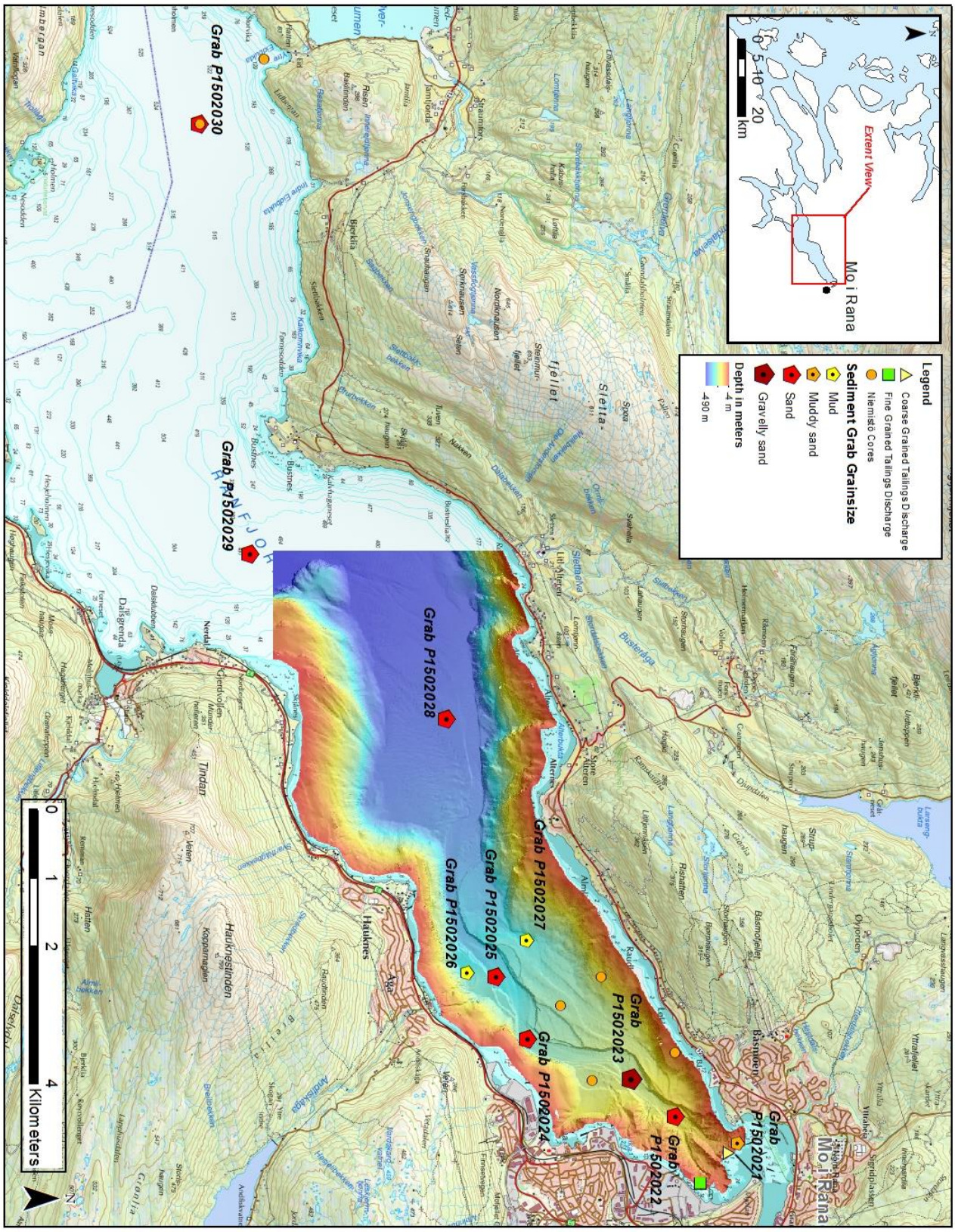

Figure 28. Sediment Core Locations and Grainsize

6.2.1 Sediment Grab P1502-030

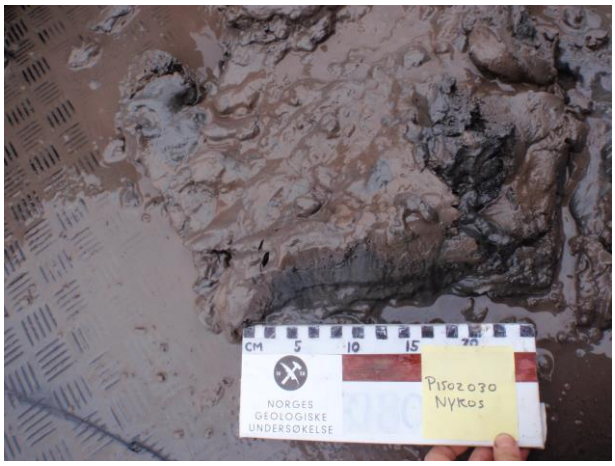

Figure 29: Sediment grab P1502-030

6.2.1.1 Description

Red, very fine sand with some mud at the top. Gray fine sand with large amounts of mica flakes below upper layer.

6.2.2 Sediment Grab P1502-029

Figure 30. Sediment grab P1502-029

6.2.2.1 Description

Red, very fine sand with some mud at the top. Layer below consisting of gray fine sand with large amounts of mica flakes. Bottom layer consisting of gray medium to course sand with large amounts of mica flakes.

6.2.3 Sediment Grab P1502-028

Figure 31. Sediment grab P1502-028

6.2.3.1 Description

Red, very fine sand with some mud at the top. Layer below consisting of gray fine sand with large amounts of mica flakes.

6.2.4 Sediment Grab P1502-027

Figure 32. Sediment grab P1502-027

6.2.4.1 Description

Red mud at the top layer. Gray mud/silt with mica flakes in the layer below. No sand in sample but large amounts of silt.

6.2.5 Sediment Grab P1502-026

Figure 33. Sediment grab P1502-026

6.2.5.1 Description

Red mud at the top with dark gray mud with mica flakes right below. No sand with a large amount of silt.

6.2.6 Sediment Grab P1502-025

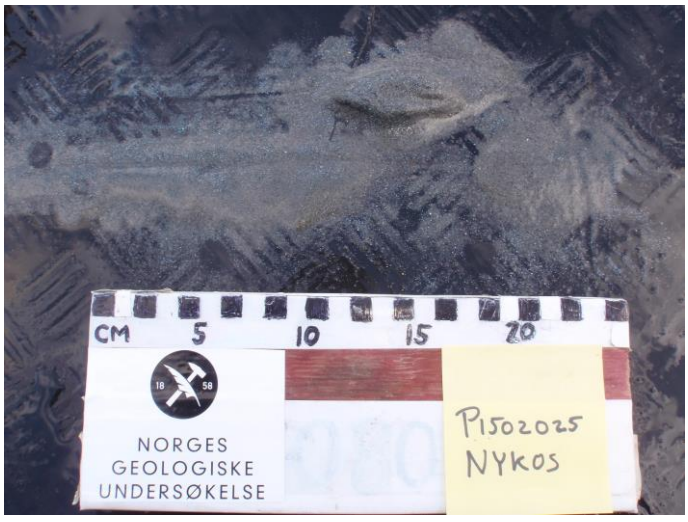

Figure 34. Sediment grab P1502-026

6.2.6.1 Description

Reddish brown medium/coarse sand at the top and gray medium/coarse sand below. Very small recovery on sample.

6.2.7 Sediment Grab P1502-024

6.2.7.1 Description

Red, very fine sand with some mud at the top. Gray medium to coarse sand with large amounts of mica flakes in the layer below.

6.2.8 Sediment Grab P1502-023

Figure 35: Sediment grab P1502-023

6.2.8.1 Description

Fine red gravely sand at the top, with potentially a slight amount of mud. Gray medium gravely sand farther down with large amounts of mica flakes. Gravel of all sizes throughout.

6.2.9 Sediment Grab P1502-022

Figure 36: Sediment grab P1502-022

6.2.9.1 Description

Coarse gray sand with a large amount of mica flakes.

6.2.10 Sediment Grab P1502-021

Figure 37: Sediment grab P1502-021

6.2.10.1 Description

Red sand at the top with darker, black-red muddy sand farther down. Lots of roots and plants.

6.2.11 Interpretation

All the sediment grabs taken show a fine layer of red sediments varying from sands to muds potentially indicating mine tailings deposits. Sediment grabs P1502027, P1502026 and P1502021 are the only samples collected outside of the main channel in the fjord and contain muddy sediments. The rest of the samples are all collected from the fjord channel or along the centerline of the fjord, and all consist of sandy sediments. This indicates that the channel is potentially experiencing sediment transport from turbidity currents (Syvitski, Burrell et al. 1987, Pratson, Imran et al. 2000). The other areas of the fjord are experiencing sedimentation potentially from suspension fallout. Grab P1502021 is located up fjord from the mine tailings discharge point and the mine tailing sediments found in the sample could have potentially been transported there by estuarine circulation currents (Leikvin 2009, Golmen and Norli 2013).

7 TOPAS Seismic

Two TOPAS seismic profiles displaying different locations in the fjord are analyzed for this study (Figure 38). These profiles cover the approximate center length of the inner fjord (Profile 1502006) (Figure 39) and the deeper inner fjord basin (Profile 1502006) (Figure 40). Each profile is broken into 2 distinct units (A and B) with the acoustic basement being categorized as either bedrock or moraine deposits. This is due to the difficulty of distinguishing between bedrock and morainal deposits in TOPAS profiles (Hjelstuen, Kjennbakken et al. 2013)

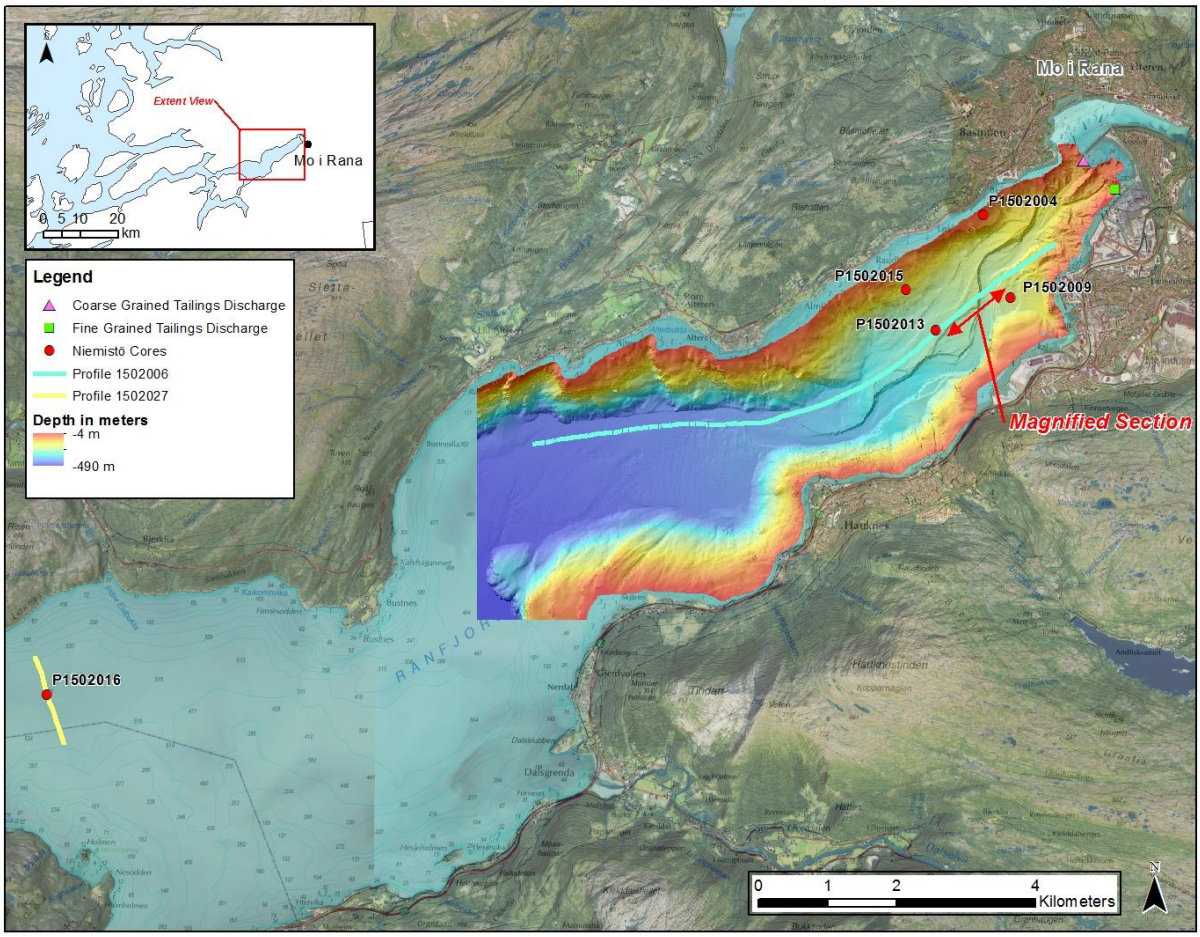

Figure 38. TOPAS Profile Locations

7.1 Profile 1502006

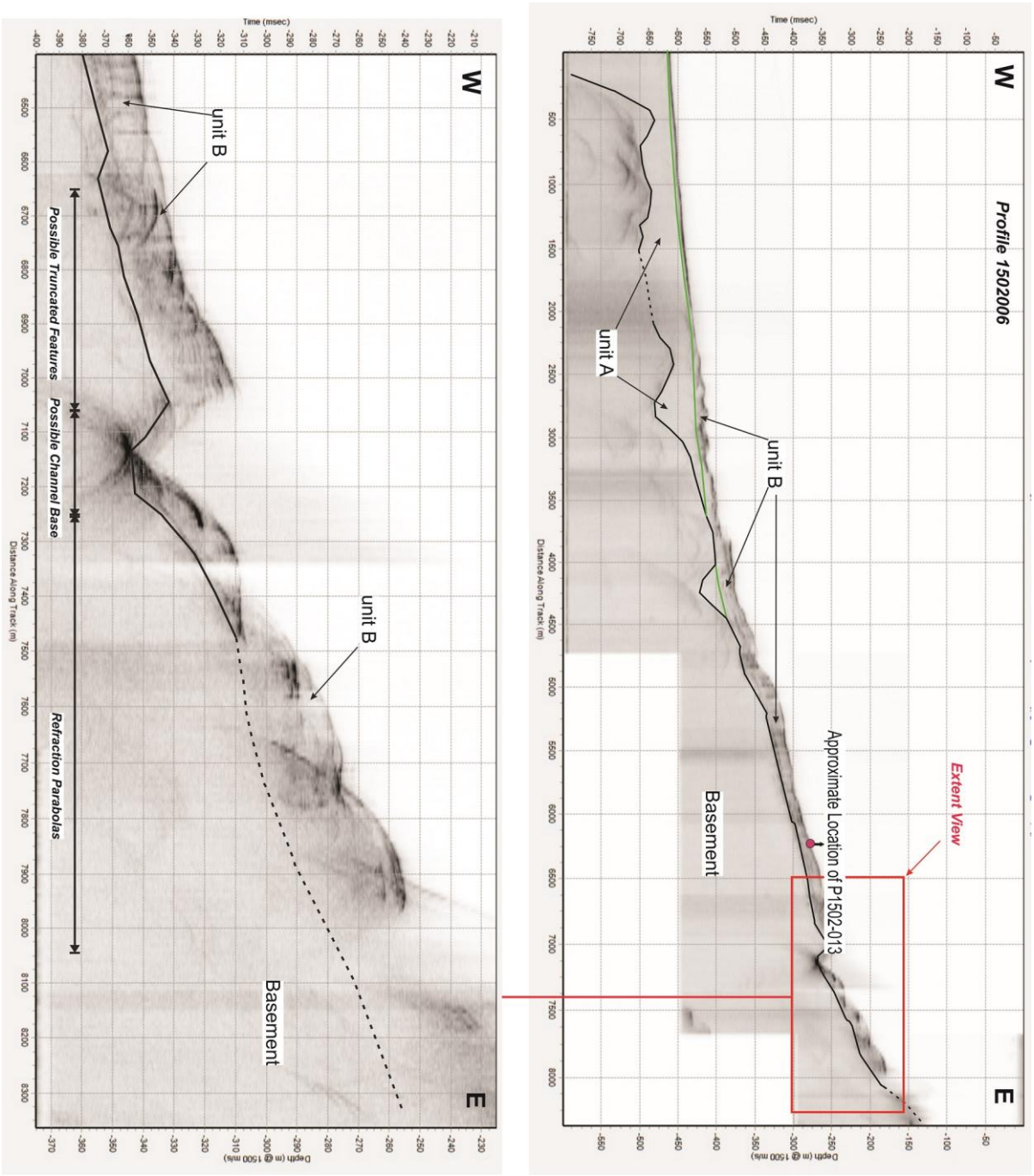

Figure 39. TOPAS Profile 1502006

Profile 1502006 (Figure 39) extends over 9km from the west to the east following close to the center of the fjord and crosses the sampling point of sediment core P1502-013 (Figure 38). Unit A begins at the west edge of the profile and extends approximately 4.5 km towards the east. As described by Lysså (2004), it is distinguished by internal patterns of weakly inclined reflections with low amplitude. It extends down to the basement and is over 150 m at it's thickest point and thins greatly towards the east. The upper boundary is sharp. Unit B extends along the majority of the profile, varies in thickness between 10 to 20 m in the east, and thins to less than 1 m to the west. It is characterized by repeating parallel reflections of moderate to high amplitude (Lysså, Seirup et al. 2004). In the inset in Figure 39, features closer to the inner fjord are seen in more detail. Moving from the western edge towards the east, unit B appears to gain thickness and shows truncated, blocky features. Directly to the east of this, the unit is truncated and an over 20 m deep depression is formed down to the bedrock/moraine basement layer. Further to the east are apparent refraction parabolas.

7.2 Profile 1502027

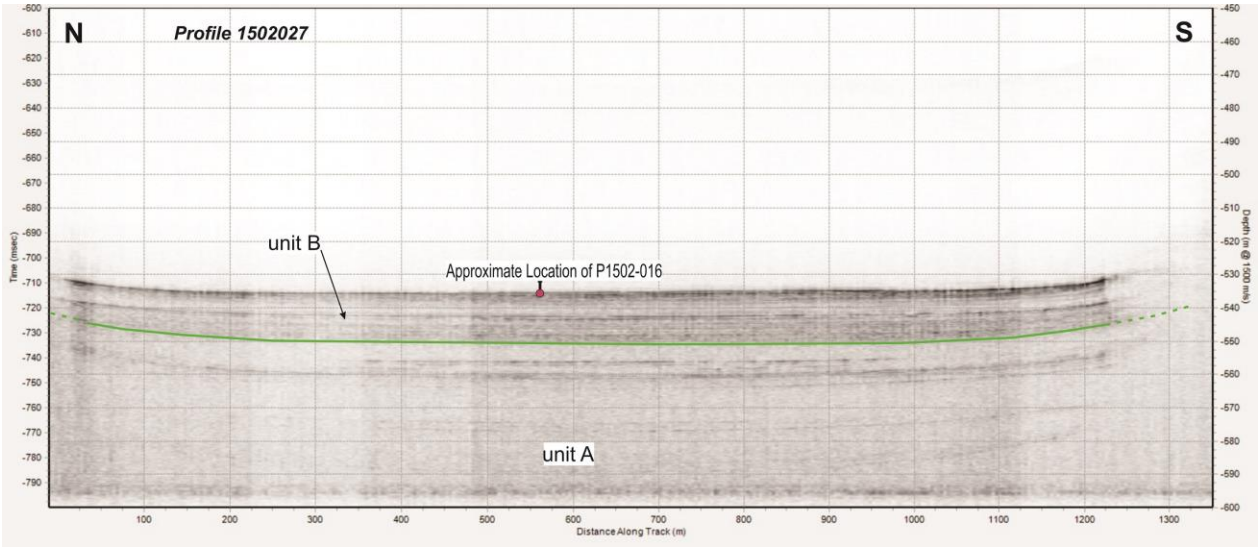

Figure 40. TOPAS Profile 1502027

Profile 1502027 (Figure 40) extends over 7 km across the inner fjord basin from the north-northwest to the south-southeast and crosses the sampling location of sediment core P1502-016 (Figure 38). Unit A extends across the whole profile and has parallel reflections with low amplitude (Lysså, Seirup et al. 2004) and a few faint discontinuous reflections of low acoustic quality at its center. The upper boundary is sharp and defined. Unit B extends across the whole profile and is ~15 m thick for the entire length. The unit shows parallel medium to high amplitude reflectors with a more transparent center layer. All the units hold approximately the same thickness across the profile with all layers parallel. At each edge, the units begin to angle slightly upward, giving the profile a very subtle U-shape.

7.3 Interpretation

Unit A appears to be submarine ice-contact fan deposits as described in (Lysså, Seirup et al. 2004). The thin, low-resolution layer seen in profile 1502027 could possibly be from an influx of coarser sediment. The acoustic lamination pattern apparent in Unit B indicates that it was likely deposited in an alternating depositional environment often seen in basin fill (Lysså, Seirup et al. 2004) The layers alternate between clay/silt from hemipelagic sedimentation and coarser sand layers most likely from turbidity currents (Lysså, Seirup et al. 2004). The more acoustically transparent layer in the unit seen in profile 1502027 could possibly be from higher density turbidity currents (Lysså, Seirup et al. 2004).

The depression feature seen in profile 1502006 (Figure 39 inset) is most likely the main channel with possible truncated features on its western bank. The thickening of unit B along the western side of the channel could indicate a partial levee (Meiburg and Kneller 2010). The truncated features of unit B along the western bank could indicate that this side of the channel is experiencing erosion.

8 Discussion

The main goal of this study is to distinguish and identify the natural and anthropogenic deposits within Ranfjorden and to gain a better understanding of the spreading and impact of the submarine tailings placement on the fjord's seafloor. Combining swath bathymetry, TOPAS seismic profiles and the lithological analysis of the fjord sediments, the following chapter will describe the depositional environment within the fjord and how it is affected by the submarine tailings disposal.

8.1 Depositional Environment

The majority of the data collected and described in sections 5, 6 and 7 covers the most recent history of the depositional environment of the fjord. This is mainly due to the short lengths of the sediment cores combined with the high rate of sedimentation in the fjord (Syvitski, Burrell et al. 1987, Helland, Rygg et al. 1994). The TOPAS seismic profiles in section 7 provide a deeper look into the history of the fjord but will only be used to help describe the youngest, uppermost unit of the fjord's sediments. The portions of the sediment cores that contain mine tailings are estimated to be no older than 100 years since no considerable anthropologic influences existed in the fjord before that time (Berg 1996, Lyså, Seirup et al. 2004). The longest core, P1502-013 (Figure 24) is 39 cm long and mine tailings dominate its entire length. Cores P1502-004 (Figure 27) and P1502-015 (Figure 25) show a transitional boundary from more natural sediments to mine tailings but are no longer than 35 cm and with no more than half being natural sediments. Core P1502-001 (Figure 22) was collected in a more distant portion of the fjord very close to shore as a reference core for natural sediments and is 36 cm long. Its uppermost 2 cm potentially contain some mine tailings. Even though sedimentation rates have been shown to be higher in the inner fjord (Helland, Rygg et al. 1994), high sedimentation rates throughout the fjord (Syvitski, Burrell et al. 1987, Lyså, Seirup et al. 2004) indicate that core P1502-001 can potentially represent a similar though somewhat longer time-period compared to the other more mine tailings dominated cores.

8.1.1 Sediment Distribution

All the sediment cores analyzed in the study show some evidence of mine tailings (Section 6) indicating spreading of the tailings throughout the inner fjord. The mine tailings are predominantly characterized by a reddish color, higher Fe/Sum values and have much higher magnetic susceptibility when compared to the more natural sediments. Fe/Sum values can also help distinguish mine tailings from more natural sediments by showing a high or low presence of fluctuations in values. Core P1502-001 shows a largely level overall trend for Fe/Sum but its values continuously fluctuate sharply up through the core (Figure 22 and 41). This is indicative of a continuous uniform source such as the Ranaelva, seasonally fluctuating its sediment input into the fjord (Syvitski, Burrell et al. 1987, Helland, Rygg et al. 1994, Johnsen, Golmen et al. 2004, Golmen and Norli 2013). The cores more dominated by mine tailings show much smoother Fe/Sum trends, as seen in core P1502-009 unit A and C (Figure 26 and 41) and P1502-016 (Figure 23), due to the uniform source of sediment from the tailings. Cores P1502-004 (Figure 27), P1502-013 (Figure 24) and P1502-015 (Figure 25 and 41)

shows trends that are smoother than those seen in P1502-001 but still contain fluctuations, indicating possible mixing between natural and mine tailings sediments.

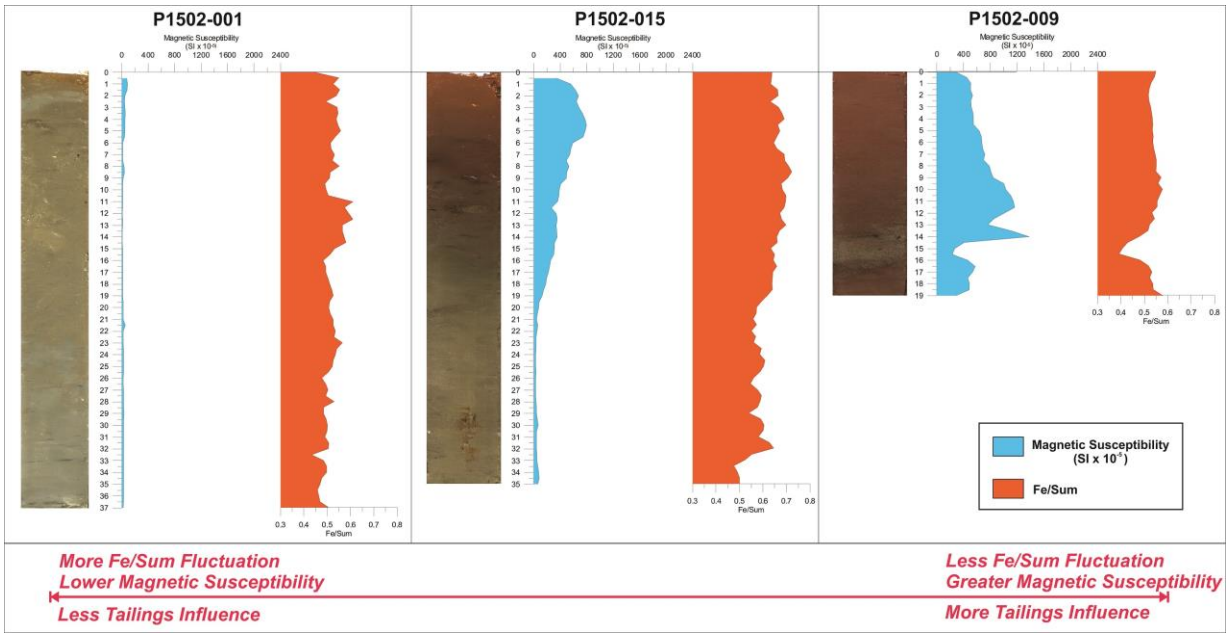

Figure 41. Representative core comparison of the 3 different Fe/Sum characteristics in sediment cores

Figure 42 shows each sediment core location, magnetic susceptibility and Fe/Sum values. Core P1502-001 clearly shows the low magnetic susceptibility of the natural sediments. Cores P1502-004 and P1502-015 located along the northern slopes of the fjord also show low magnetic susceptibility values towards the bottoms of their lengths coinciding with the lighter sediment color (Figures 27 and 25). Up core they both show a shift through color, magnetic susceptibility and Fe/Sum value changes towards more mining dominated sediments. Cores P1502-009 and P1502-013 (Figures 26 and 24), located more towards the inner fjord centerline, all have red coloration and higher magnetic susceptibility values throughout their lengths potentially indicating higher sedimentation from mine tailings occurred in these areas. Unit B in core P1502-009 (Figure 26) shows a sharp drop in magnetic susceptibility and Fe/Sum values and is attributed to turbidity current transported sediments originating from a surge from Ranaelva. This current then mixes with more mine tailing dominated sediments up core as shown by the rise in magnetic susceptibility. Core P1502-009 is located close to the center channel in the fjord and only 2.4 km from the tailings discharge point. When it is compared to cores P1502-004, P1502-013 and P1502-015 that are located more to the north and on the opposite side of the channel, it becomes clear that it has much fewer fluctuations in its Fe/Sum values. This would indicate that more mixing with natural sediments is occurring on the northern side of the channel while areas closer to the southern side of the fjord are seeing a more dominant input of mine tailings.

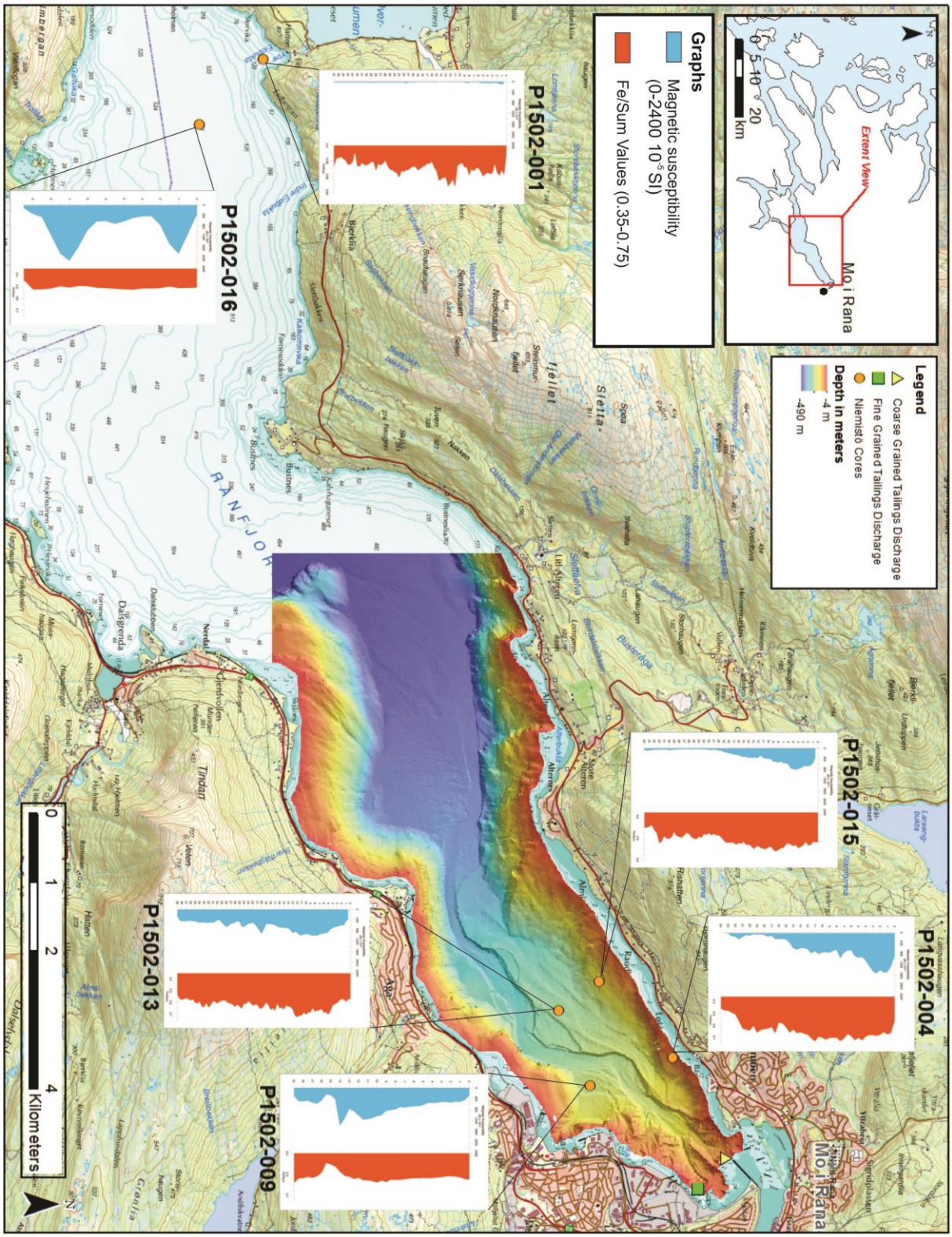

Figure 42. Magnetic susceptibility and Fe/Sum values for each sediment core location. (The same scale is used for each data type to better show relative differences. Core lengths are not to scale.)

Core P1502-016 (Figure 23) is primarily a red color, has very little fluctuation in Fe/Sum values, the highest magnetic susceptibility of all the cores and is almost 17 km from the tailings discharge points. This indicates that the mine tailings are being transported long distances and becoming somewhat concentrated in the process.

The mine tailings themselves are reported to vary in size from below 10 µm to above 800 µm (Johnsen, Golmen et al. 2004, Skei 2014)) and how they are distributed within the cores and sediment grabs varies greatly depending on the sample's location in the fjord (Figure 43). Reference sediment core P1502-001 (Figure 22) shows natural sediments outside of the deeper, center portions of the fjord have a mean grainsize below ~20 µm. As described in Section 5, the fjord bathymetry shows a distinctive main channel running down the center length of the inner fjord with smaller, potentially abandoned parallel channels to its north. The southern slope of the inner portion of the fjord also shows deep gullies cutting into the slopes and merging with the deeper larger channel. As seen in Figure 43, all the sediment cores (P1502-013, 015, 009 and 004) and sediment grabs (Grabs P1502026 and P1502027) from the inner fjord collected outside of the center fjord channel consist predominantly of silt and finer sediments. Sediment cores P1502-015 and P1502-004 are both located on the northern slope of the fjord and show a gradual fining upward as they become more dominated by mine tailings (Figure 43). Sediment core P1502-013 is located along the centerline of the fjord to the north of the main channel and it generally fines upward but shows several small spikes in grainsize indicating slightly higher energy depositional environments. Sediment core P1502009 is the closest core to the inner channel and the only sediment core on its southern side (Figure 43). It contains a sandy unit B (Figure 26), indicating an earlier higher energy depositional environment. The remaining sediment core P15020-016 and sediment grabs (P15020030, P1502029, P1502028, P1502025, P1502024, P1502023, P1502022 and P1502021) all consist mainly of sand and are collected from either within the inner fjord channel or along the centerline of the fjord (Figure 43). The sand unit seen in core P1502-009 is very similar in color and grainsize as the sand layers seen in core P1502-016 (Figure 23) indicating a similar source and transport mechanism.

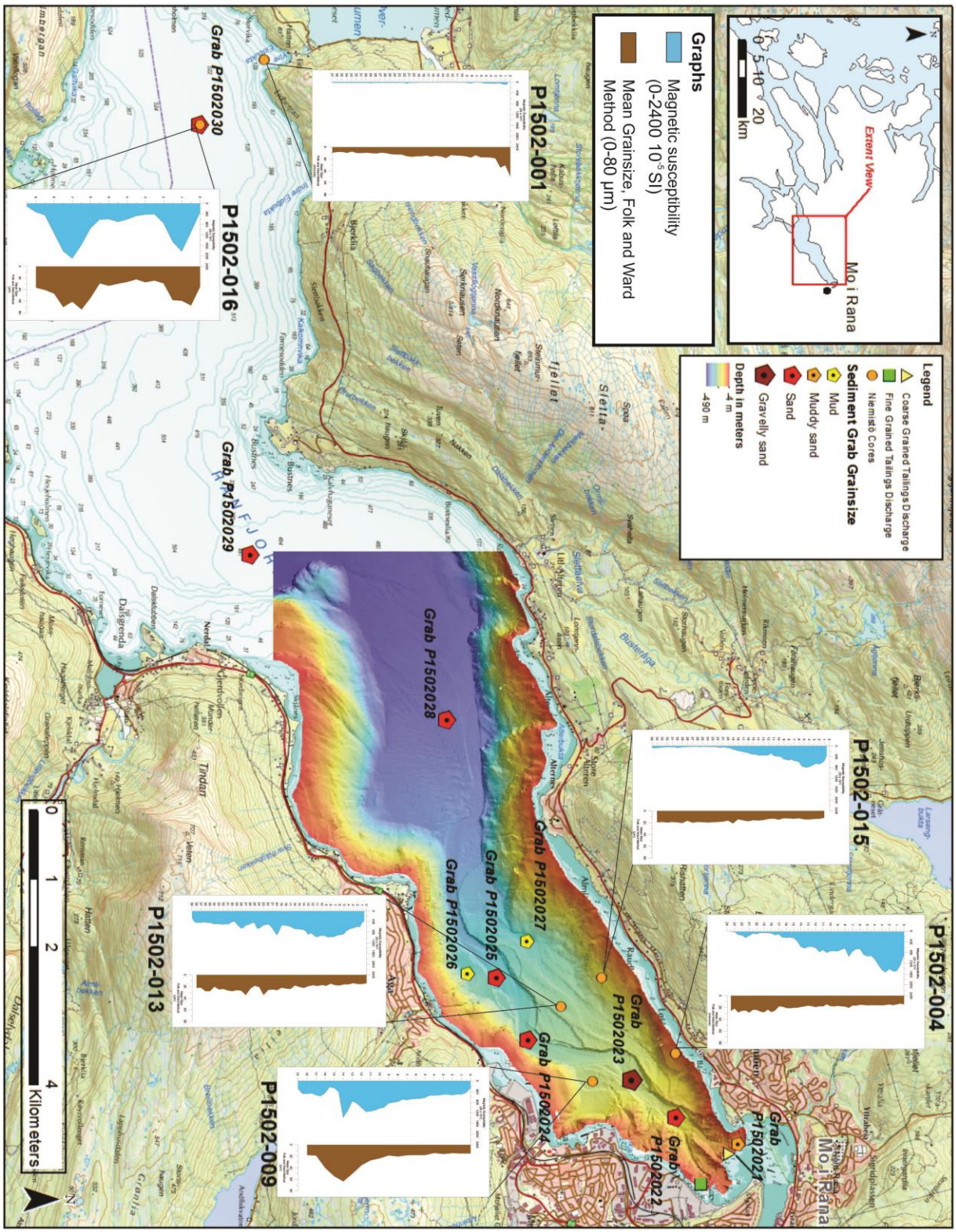

Figure 43. Magnetic susceptibility and Mean Grainsize for each sediment core location. (The same scale is used for each data type to better show relative differences. Core lengths are not to scale.)

8.1.2 Sedimentary Processes

The sedimentary processes of Ranfjorden are greatly influenced by the influx of fresh river water and natural sediments from Ranaelva and the resulting estuarine circulation that occurs within the water column of the fjord (Syvitski, Burrell et al. 1987, Leikvin 2009, Golmen and Norli 2013). The more recent discharge of mine tailings at the head of the fjord has begun to play a more dominating role in these processes since it began over 100 years ago (Tesaker 1978). The estuarine circulation that occurs in the inner fjord has been shown to play a large role in the transport and spreading of all the these discharged sediments (Helland, Rygg et al. 1994, Leikvin 2009, Golmen and Norli 2013). The distinct layering within the water column causes a net outward current along the surface and below 47 m away from the mouth of the river. At around 26 m a current with a net flow back towards the river mouth has been measured. The area around the tailings discharge point has also recorded a net inward flowing current, greatly impacting how these sediments are dispersed.

As recorded by Tesaker (1978), because of the submarine tailings placement discharge into the fjord, gravity flows and their effects have become the fjord's dominating sedimentary processes. The sediment samples collected throughout the fjord potentially confirm this by all showing traces of tailings at varying levels of both concentration and grainsize. Swath bathymetry data shows that the area around the tailings discharge points at the head of the fjord have experienced extensive mass movement and gravity flows (Figure 17 and 20). These gravity flows are strengthened by the deeper outflowing current from Ranaelva (Tesaker 1978, Lysså, Seirup et al. 2004). All the samples collected down fjord from this point and near the channel show evidence of an influx of sandy sediments from a potential turbidity current (Figure 43) (Pratson, Imran et al. 2000). The unit B in core P1502-009 (Figure 26) is potentially deposited by turbidity currents since it contains finer sands that fine slightly upward (Pratson, Imran et al. 2000). The finer sediment layers above and below unit B indicates the core location only experiences periodic turbidity current events. The crescent shaped bedforms seen in the large and smaller channels support surge/pulse turbidity currents traveling down the channels of the fjord (Figure 17 and 18) (Meiburg and Kneller 2010, Clarke 2016). Core sample P1502-016 (Figure 23), with its closely spaced sandy units B and D, combined with the parallel reflector layers seen in the TOPAS data (Figure 40) (Lysså, Seirup et al. 2004) from the same location (Figure 38), potentially show successive turbidity currents transporting mine tailings deep out into the fjord. These sandy units within cores P1502-009 and P1502-016 show a large increase in magnetic susceptibility with little increase in Fe/Sum values (Figure 42 and 43). This is potentially due to magnetite in the mine tailings being coarser and becoming concentrated in the fjord channel by turbidity currents. Since magnetic susceptibility is very sensitive to magnetite, a minor amount would influence readings. The units directly above the sandy units (Figure 23, 26 and 43) fine upward, a characteristic of turbidites (Syvitski, Burrell et al. 1987, Pratson, Imran et al. 2000, Meiburg and Kneller 2010), and show a gradual upward decrease in magnetic susceptibility. This indicates a decrease in the energy of the depositional environment and as a result, a potential decrease in the amount of coarser magnetite being

deposited. Cores P1502-013, P15602-015 and P1502-004 all show a fining upward and an upward increase in magnetic susceptibility and Fe/Sum values (Figure 42 and 43). This is potentially due to the hematite fraction of the mine tailings being finer and as a result is transported by sediment plumes to areas outside of the main channel.

Unit B in core P1502-013 (Figure 24), taken from the center of the fjord (Figure 43), shows alternating grainsizes that could indicate sedimentation from overflow from the channel bringing coarser sediments (Meiburg and Kneller 2010). The TOPAS data from the center of the fjord near the location of core P1502-013 (Figures 38 and 39) shows a potential levee (Amundsen, Laberg et al. 2014) and laminated layers west of the channel indicating potential overflows having occurred. The potential truncation of these laminated layers on the western side of the channel indicate possible erosion occurring in this area, as is also seen in the change in bathymetry Figure 19. The reason for the higher erosion and the levee being on the western side could be due to the influence of the Coriolis Effect forcing the outflowing turbidity currents to the right and into the western edge of the channel (Syvitski, Burrell et al. 1987).

Cores P1502-015 (Figure 25) and P1502-004 (Figure 27) show an overall finer sediment content that gradually shifts up core from more natural to mine tailings dominated. They are located farther up the northern slopes of the fjord (Figure 43) and their massive layers indicate gradual sedimentation from fallout (Syvitski, Burrell et al. 1987). The suspension plumes at the discharge points caused by rising lower density tailings and debris flow movement would have raised a large percentage of the finer fraction into the water column (Helland, Rygg et al. 1994). Due to the estuarine currents and halocline in the fjord (Leikvin 2009, Golmen and Norli 2013), a portion of these finer sediments would have been carried up and back into the inner fjord before settling out, increasing both the area and rate at which the inner fjord is affect by tailings sedimentation. The relative shallow discharge depths of both the coarse (30 m depth) and especially the fine fraction (45 m depth) mine tailings potentially increased the spreading potential of the suspension plume. Their close proximity to the halocline would have allowed the rising sediments to be more easily captured and entrained in currents below the halocline (Golmen and Norli 2013). The fining upward within cores P1502-015 and P1502-004 shows this shift from the coarser natural sediments to the finer mine tailings as the finer mine tailings fell out of suspension. A portion of this sediment plume can even be seen in the uppermost layer of core P1502-001 (Figure 22), possibly indicating resuspension of sediments from turbidity currents. Sediment grab P1502021 (Figure 37) shows potential traces of mine tailings having been carried up fjord by back flowing currents and deposited at the mouth of Ranaelva, but with no detailed analysis this cannot be confirmed.

8.2 Impact of Tailings on the seafloor of the fjord

As has been shown in the previous sections, the majority of the inner Ranfjorden is impacted by the mine tailings through either erosion, sedimentation or a combination of both. Mine tailings appear even at the western edges of the study area, farthest from the tailings discharge points.

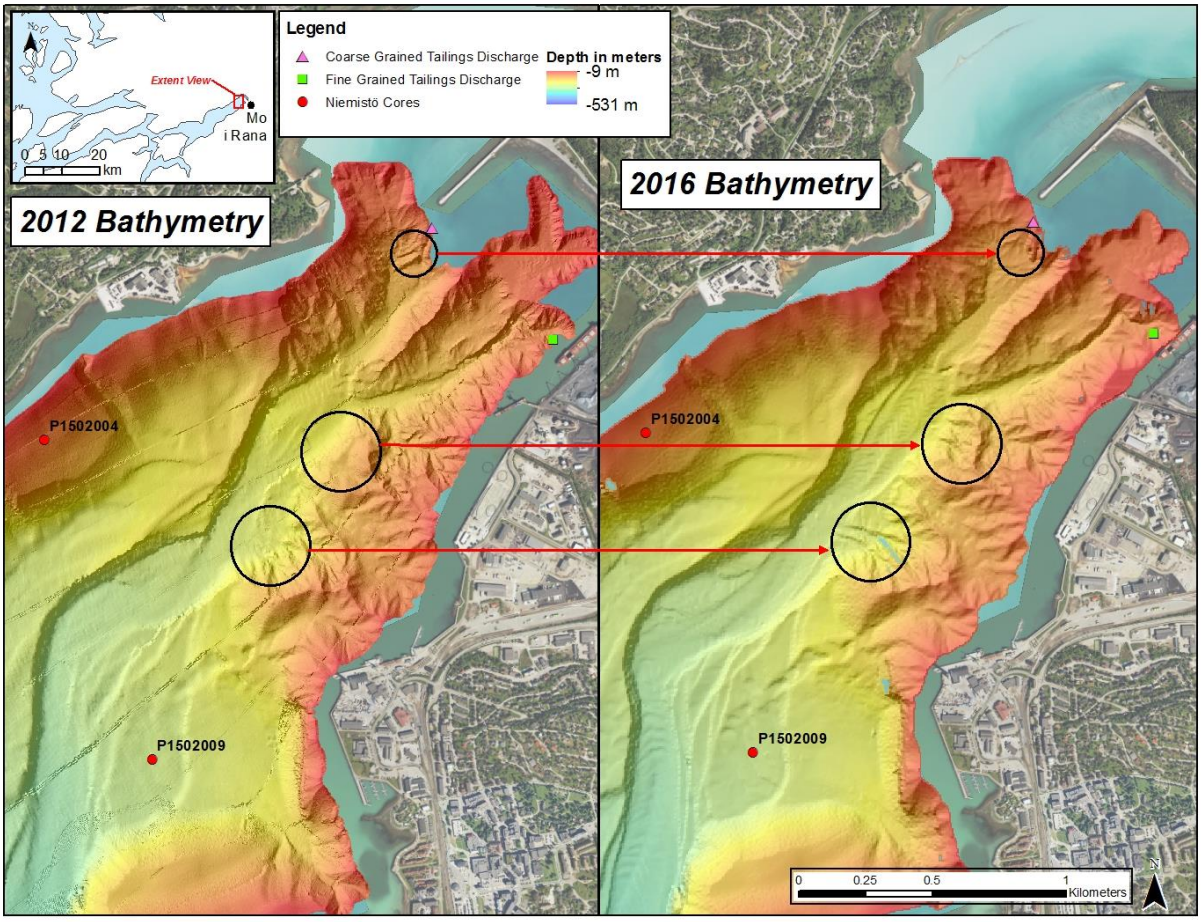

Figure 44. Areas of potential mass movement/gravity flows.

The areas that have seen the most impact from erosion and sedimentation are the innermost portions of the fjord and channel (Figure 19 and 20), particularly the areas immediately around the mine tailings discharge points and the slopes to their south (Figure 44). The mine tailings discharge and the resulting erosion shown in Figure 44 has led to potentially greater erosion and sedimentation throughout the fjord in the form of turbidity currents and suspensions plumes (Tesaker 1978).

The accumulation of mine tailings sediments along the steeper southern slopes has also apparently led to numerous mass movement events as seen in Figure 44. These events are possibly resulting from suspended fine fraction tailings being carried within the water column back into the fjord and deposited in this area in larger quantities than other parts of the fjord. When comparing the undrained shear strength (S_u) properties of the sediment cores closest to the tailings discharge point, cores P1502-009 and P1502-004, they both show a decrease in S_u and sensitivity (S_u / S_r) up through the core as the mean

grainsize decreases (Figure 45). Core P1502-004 also shows a large drop in S_u as the sediments transition from natural to mine tailings. Both of these cores show mine tailing sediments fining upward in their upper cores, typical of suspension fallout (Syvitski, Burrell et al. 1987). This could indicate that the steep slopes along the shoreline become more prone to sliding as the finer fraction tailings accumulate and the S_u decreases (Syvitski, Burrell et al. 1987). This potentially explains the reason for the excessive erosion occurring in that area. The lower S_u values of the mine tailings versus the more natural sediments could also show that more erosion is occurring along the fjord slopes now than in the past due to the fine fraction tailings accumulation.

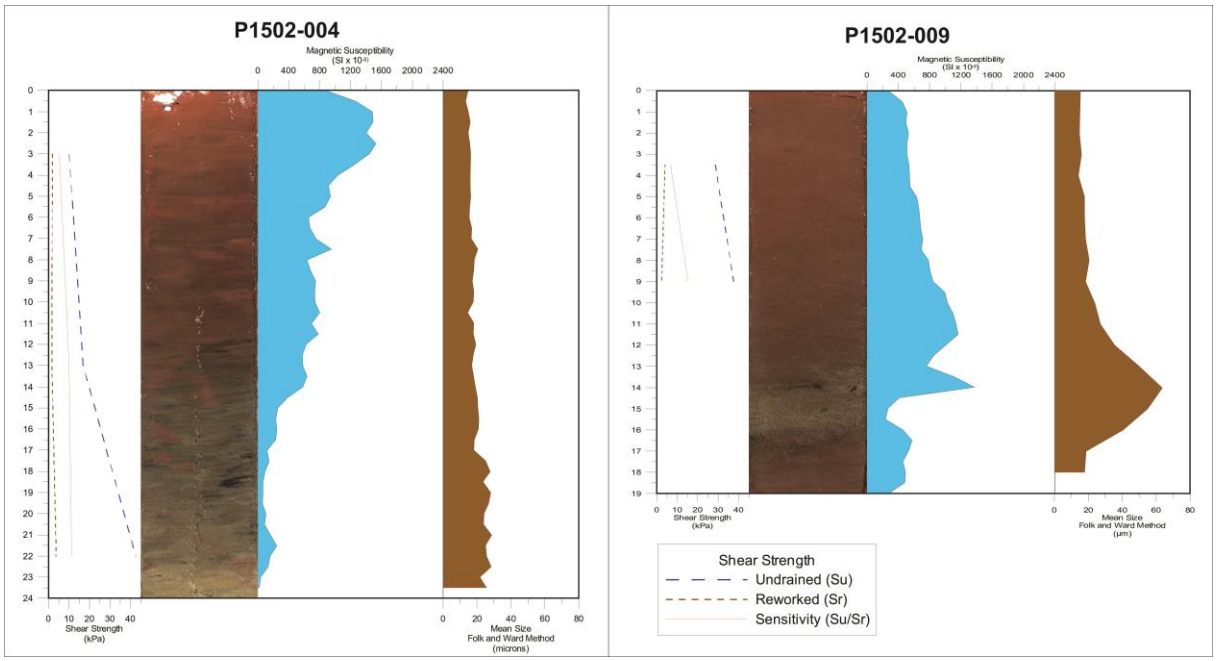

Figure 45. Shear Strength Comparison of Cores P1502-004 and P1502-009

9 Conclusion

The goal of this study was to gain a better understanding of both the natural and anthropologic sediments within Ranfjorden in northern Norway and how their interaction and distribution has been influenced by, and in turn affected the dynamics of the fjord. Using a combination of 6 Niemestö cores, 10 sediment grabs, swath bathymetry and TOPAS seismic data, a deeper understanding of the hydrological and sedimentary processes of the fjord's relationship with the submarine tailings placement was gained. The following conclusions can be drawn:

- The mine tailings sediments are characterized by a darker red color, higher magnetic susceptibility and Fe/Sum readings with low fluctuations in Fe/Sum values. The more natural fjord sediments are characterized by gray colors, low magnetic susceptibility and Fe/Sum values with higher fluctuations in Fe/Sum values. The sediment samples collected from Ranfjorden indicate that mine tailings sediments have spread throughout the majority of the inner 18 km of the Ranfjorden study area, with all the sediment cores showing evidence of mine tailings.

- The bathymetry from the inner Ranfjorden shows a low angle outer basin with a seafloor rising gradually at an angle of between 0-5° towards the head of the fjord to the northeast. The inner fjord basin narrows from ~1.8km at the outer basin down to ~500m in the inner fjord. Both sides of the fjord show steep slopes rising up at angles of up to 87° from the fjord bottom. The innermost 2 km of the fjord shows steep, sharp gullies cutting into the slopes below the mouth of the Ranaelva and the slopes near the mine tailings discharge. The centerline of the fjord shows a large, sinuous channel starting at the slopes below the mouth of the Ranaelva and running out into the deeper basin. Smaller secondary/abandoned channels are also seen to the north of the larger channel in the inner 5 km of the fjord. Horizontal step features are seen within all the channels and are interpreted to be cyclic step features from turbidity currents. Bathymetry data collected between 2012 and 2016 show large amounts of erosion and accretion having occurred in this channel and along the innermost 2 km of the fjord's southern slopes and fjord head.

- The TOPAS profiles show the uppermost unit of the fjord to consist of acoustically laminated parallel layers of medium to high reflectors. This indicates repeated changes in the depositional environment consistent with turbidity currents. The truncation of the upper unit's lamination features and a thickening of the unit surrounding the main channel indicate a potential levee and overflow deposits.

- The mine tailings are reported to range in grainsize from 800 µm to 10 µm (Johnsen, Golmen et al. 2004, Skei 2014). How they are dispersed within the fjord displays the sedimentary processes of turbidity currents and suspension plume fallouts that dominate the fjord's depositional environment. Samples collected from the fjord channel all contained high amounts of sandy mine tailings transported by turbidity currents. Samples were recorded showing turbidity current transported sediments 17 km out into the fjord. Samples taken from the centerline of the fjord but outside the main channel show evidence of coarser

channel overflow sediments. These coarser layers are preceded and followed by thicker units of finer suspension fallout sediments indicating surge/pulse turbidity current events. Samples taken in shallower waters farther up the fjord slopes show continuous sedimentation of finer mine tailings sediments from suspension fallout. Evidence of the mixing of natural sediments was found in these areas.

- The southern slopes and gullies within 2 km of the mouth of the Ranaelva and the mine tailings discharge points experience greater fine tailings sediments accumulation than other slopes in the fjord. This accumulation is due to recently discharged and also re-suspended fine fraction tailings rising in the water column and becoming contained and transported by the net inflowing estuarine circulation current in the area. These steep fjord slopes then experience higher levels of erosion due to mass movements and gravity flows as a result from this accumulation of the potentially less stable finer fraction mine tailings.

Works Cited

Amundsen, H. B., et al. (2014). "Late Weichselian-Holocene evolution of the high-latitude Andøya submarine Canyon, North-Norwegian continental margin." Marine Geology **363**: 1-14.

Arnesen, R. T., et al. (1997). Comparison of model predicted and measured copper and zinc concentrations at three Norwegian underwater tailings disposal sites. Proceedings of the Fouth International Conference on Acid Rock Drainage. Vancourver, B.C. Canada.

Berg, A. E. (1996). "Dunderland Iron Ore, Limited i Rana. Forspillet of første drifsperiode. ." Mo i Rana-Prosjektet **12**.

Blott, S. J. and K. Pye (2010). GRADISTAT Version 8.0.

Cabalar, A. F. and W. S. Mustafa (2015). "Fall cone tests on clay-sand mixtures." Engineering Geology **192**: 154-165.

Clarke, J. E. H. (2016). "First wide-angle view of channelized turbidity currents links migrating cyclic steps to flow characteristics." Nature Communications **7**(11896): 1-13.

Collinson, J., et al. (2006). Structures created by deformation and disturbance. Sedimentary Structures**:** 182-230.

Cornwall, N. (2013). Submarine tailings disposal in Norway's fjords. Is it the best option? Lund, Sweden, IIIEE. **MSc Thesis**.

Davis, R. A., et al. (2000). "Rio Tinto estuary (Spain): 5000 years of pollution." Environmental Geology **39**(10): 1107-1116.

Figenschau, N. (2018). Interaction of submarine tailings with natural sediments in three northern Norwegian coastal areas: Sedimentological, minieralogical and geochemical constraints. Institute of Geosciences. Tromso, UiT.

Franks, D. M., et al. (2011). "Sustainable development principles for the disposal of mining and mineral processing wastes." Resources Policy **36**: 114-122.

GEONOR, I. Fall Cone Apparatus Manual. Augusta, NJ**:** 2.

GEOTEAM (1983). Dypvannskai Rana. Seismiske Målinger og Fjellkontrollboringer. Trondheim, Rana Kommune/Norsk Jernverk A/S Rapport 8871.01.

Golmen, L. G. and M. Norli (2013). Sporstoff-forsøk i Ranfjorden 2012-2013, NIVA Rapport L.NR. 6576-2013**:** 33.

Green, N. W., et al. (1995). Ranfjorden 1992-93 - Grunvannssamfunn (Statlig program for forurensningsovervåkning. Overvåkningsrapport nr.625/95. TA-nr. 1267/1995), NIVA Rapport.

Gustavson, M. and S. T. Gjelle (1991). Geologisk kart over Norge. Berggrunnskart MO I RANA, M 1:250 000, Norges geologiske undersøkelse.

Hansbo, S. (1957). A new approach to the determination of the shear strength of clay by the fall cone test. . Stockholm, Royal Swedish Geotechnical Institute

Helland, A., et al. (1994). Ranfjorden 1992-1993. Hydrografi, sedimenterende materiale, bunnsedimenter and bløtbunnsfauna, Statens forurensningstilsyn (Statlig program for forurensingsovervåkning) (NIVA Rapport 551/94)**:** 84.

Hicks, E. C., et al. (2000). "Seismic activity, inferred crustal stresses and seismotectonics in the Rana region, Northern Norway." Quaternary Science Reviews **19**: 1423-1436.

Hjelstuen, B. O., et al. (2013). "Fjord stratigraphy and processes-evidence from the NE Atlantic Fensfjorden system." Journal of Quaternary Science **28**(4): 421-432.

IG-LPSA. "Laser Particle Size Analyser." from https://uit.no/om/enhet/artikkel?p_document_id=390304&p_dimension_id=88137.

Johnsen, T. M., et al. (2004). Miljøundersøkelser i Ranfjorden 1994-96, NIVA Rapport LNR 4366-2001**:** 94.

Kirkerud, L., et al. (1985). Basisundersøkelse i Ranafjroden - en marin industriresipient., Samlerapport. Statlig program for forurensningsovervåkning. Rapport 207/86 (NIVA rapport. 1/1800)**:** 76.

Kirkerud, L. A. (1977). Resipientundersøkelse i Ranafjorden. Rapport nr. 2. Innledende hydrografiske, geokjemiske og biologiske undersøkelser. Oslo, NIVA 0-31/75.

Leikvin, Ø. (2009). Vurdering av nytt utslippspunkt for Mjølanodden renseanlegg i Rana kommune. Rapport nr. 44601-412, Akvaplan-niva**:** 45.

Lyndersen, E., et al. (2002). "Metals in Scandivanvian Surface Waters: Effects of Acidification, Liming, and Potential Reacidification." Critical Reviews in Environmental Science and Technology **32**(2-3): 73-295.

Lyså, A., et al. (2004). "The late glacial-Holocene seismic stratigraphy and sedimentary environment in Ranafjorden, northern Norway." Marine Geology **211**: 45-78.

Meiburg, E. and B. Kneller (2010). "Turbidity Currents and Their Deposits." Annual Review of Fluid Mechanics **January**.

Neira, C., et al. (2011). "Macrobenthic community response to copper in Shelter Island Yacht Basin, San Diego Bay, California." Marine Pollution Bulletin **62**(4): 701-717.

Olesen, O., et al. (1994). Neotectonic studies in the Ranafjorden area, northern Norway. NGU report no. 94.073, Geological Surveey of Norway, Nordland Programme.

Olsgard, F. and J. R. Hasle (1993). "Impact of waste from titanium mining on benthic fauna." Journal of Experimental Marine Biology and Ecology **172**(1-2): 185-213.

Perret, D., et al. (1995). "Strength development with burial in fine-grained sediments from Saguenay Fjord, Quebec." Canadian Geotechnical Journal **32**: 247-262.

Pickering, K. T., et al. (1986). "Deep-water facies, processes and models: a review and classification scheme for modern and ancient sediments." Earth-Science Reviews **23**(2): 75-174.

Pratson, L. F., et al. (2000). Debris Flows vs. Turbidity Currents: a Modeling Comparison of Their Dynamics and Deposits. Fine-grained Turbidite Systems. A. H. Bouma and C. G. Stone**:** 55-72.

Ramberg, I. B., et al. (2013). Landet blir til - Norges geologi (2. ed.). Trondheim, Norsk Geologisk Forening.

Ramirez-Llodra, E., et al. (2015). "Submarine and deep-sea mine tailing placements: A review of current practices, environmental issues, natural analogs and knowledge gaps in Norway and internationally." Marine Pollution Bulletin **97**: 13-35.

Reeves, G. M., et al. (2006). Properties of Clay Materials, Soils and Mudrocks. Clay Materials Used in Construction**:** 110-116.

Røe, Ø. (1994). Stabilitet Ranafjorden/Videre Rasutvikling Utenfra Geofysiske Målinger/Geotekniske Vurderinger., Rana Kommune. Rapport 1. Oppdragsnr: 37960.

Skei, J. (2014). Methodologies for Environmental Impact Assessment of Deep Sea Tailings Disposal (DTSP) Projects. 34th Annual Converence of the International Association for Impact Assessment. 'IAIA14 Conference Proceedings' Impact Assessment for Social and Economic Development. Vina del Mar, Chile**:** 5.

Skei, J. (2014). Norwegian Experiences with Sea Disposal of Mine Tailings. Report Number 1 In a Series About Sea Disposal of Mine Tailings, Norwegian Bergindustry/Norwegian Mineral Industry.

Skei, J. and P. E. Paus (1979). "Surface metal enrichment and partitioning of metals in a dated sediment core from a Norwegian fjrod." Gechimica et Cosmochimica Acta **43**(2): 239-246.

Skempton, A. W. and R. D. Northey (1952). "The Sensitivity of Clays." Géotechnique **3**(1): 30-53.

Smit, M. G. D., et al. (2008). "Species sensitivity distributions for suspended clays, sediment burial, and grain size chagne in the marine environment." Environmental Toxicology and Chemistry **27**(4): 1006-1012.

Syvitski, J. P. M., et al. (1987). Fjords - Processes and Products, Springer Verlag New York.

Tesaker, E. (1978). Sedimentation in recipients. Disposal of particulate mine waste. VHL-Report No. STF Go A78105**:** 72.

UiT-IG Acid treatment (HCL) and oxidation with hydrogen peroxide (H_2O_2) - procedure of perparation of marine sediments. UiT The Arctic University of Norway.

Vogt, C. (2013). International Assessment of Marine and Riverine Disposal of Mine Tailings. Final Report Adopted by the International Maritime Organization, London Convention/Protocol.